Characterization of the ammonium transporter family AMF1 in maize

A thesis submitted in fulfillment of the

requirements for the Degree of

Doctor of Philosophy

By

Wenjing Li

School of Life and Environmental Science

Faculty of Science

The University of Sydney

December 2017

Statement of Originality

I certify that to the best of my knowledge, this thesis is my own work and contains no material that has been accepted for the award of any other degree or diploma in any university or other tertiary institution. In addition, I certify that this work contains no material previously published or written by another person, except where due reference and due acknowledgment have been made in the text.

Wenjing Li

December 2017

Acknowledgements

First and foremost, I would like to express my deep gratitude to Prof. Brent Kaiser, my supervisor, for his guidance, encouragement, and support both in my research and in my life during my PhD. I am grateful for his support for me to apply for the CSC scholarship to get the opportunity to start my PhD study in the University of Adelaide in 2013. I am very appreciative for his generous patience and enthusiastic encouragement on me, a student who has no research background about molecular biology. The transfer of Kaiser lab and my PhD study in 2015 to the University of Sydney made my research progress on schedule difficultly, especially the last year of my PhD is also the year of my pregnancy. I am profoundly grateful to Brent's support and help to get my research move on, and especially the last year for his help to secure the Completion Scholarship to make this thesis possible. Thank you Brent for the mental support to make me believe I can be a strong mum and can get my PhD finished. Now I will have time to read the book " The Good Earth" which you suggest me.

My sincere thanks also go to Dr. Julie Dechorgnat. I am really appreciated for her patience to teach me how to do experiment in molecular biology from scratch, and being a good friend to me to give me her kind and warm care in my life. I would also like to recognize Karen Francis, who helped me with maize planting, and also gives me valuable suggestions to cultivate maize in my research. I would like to extend my thanks to Dr. Zhengyu Wen, Dr. Danielle Mazurkiewicz and Yue Qu for sharing experience and giving me suggestions in my research, especially

Dr. Danielle Mazurkiewicz for her help in my yeast work.

My study cannot finish without the financial aid from China Scholarship Council, the University of Adelaide and the University of Sydney. Thanks for China Scholarship Council to support me to study in Australia, the University of Adelaide to offer me the tuition fee scholarship, and the University of Sydney for the Faculty of Science tuition fee scholarship and Completion Scholarship. I also would like to thank Dupont Pioneer Company for the materials of TUSC lines, and I also would like to thank Dr Claudia Keitel from the University of Sydney for the help of isotope analysis.

I cannot make my PhD finished without my friends' help and support. Many thanks to Jiao, Limin, Qiaoqi and Zhouhan. I cannot forget our "PhD super star team". We are all Chinese students who are far away from home to pursue PhD in Australia. I really enjoyed every gathering together during the weekends, where we explore Adelaide and also share our happiness, sorrows and troubles with each other in our life and research, making me feel I have a home in Adelaide. I would also like to thank my friends in Sydney, who are Arjina, Shahanoosh, Julie, Lisa, Zhengyu, Die, Hongbin, Shengwei…. Thank you all to give me a wonderful life outside of lab.

Nobody has been more important to me in pursuit of my PhD than my family. I cannot be more grateful to my beloved husband Teng Zhang. Thank you for coming to Australia to support me, and thank you for your selfless support, understanding and patience in the last year of my PhD. We did it. Our baby Philo arrived to this world safely and is happily and healthily growing, and I also get my thesis done. Last but not least, I would like to thank my dear baby Philo.

Thank you for choosing me to be your mum, and you are the best gift ever for me. You have been my motivation and companion to finish my PhD.

I dedicate this thesis to my dear

baby Philo and my dear

husband Teng.

Thesis summary

Nitrogen is one of the most important macronutrients required for plant growth. In most situations, the availability of nitrogen is important to a growing plant requiring sufficient supplies in the soil solution and plant-based mechanisms to access it. The uptake of ammonium by plant roots involves two types of ammonium transport pathways, the high-affinity ammonium transporters (HATS), which operate at low ammonium concentrations and the low-affinity ammonium transporters (LATS), which operate at high ammonium concentrations (typically > 0.5 mM). Genes encoding HATS proteins belong to the AMT/MEP/Rhesus superfamily. Many of these AMT family genes have been studied in plants where location, expression, activity and regulation have been investigated. However, the genetic identity of transport proteins responsible for the LATS pathway is not sufficiently understood. Recently, through a transcriptional linkage to a membrane bound transcription factor, bHLHm1, a novel family of ammonium transporters, AMF1 (ammonium facilitator 1) were discovered. Heterologous expression of yeast and soybean AMF1 orthologs in *Xenopus laevis* oocytes, indicates AMF1 proteins increase the level of low-affinity ammonium transport. AMF1 candidate genes have been identified in many plants including soybean, Arabidopsis and maize.

In this study the functional activity of two orthologs of ScAMF1 in maize (ZmAMF1;1 and ZmAMF1;2) were investigated using a yeast heterologous expression system, gene expression analysis and functional studies using loss of function mutants to characterize their net contribution to ammonium transport

into and within maize plants. This study has provided an initial understanding of AMF1's function in maize through the following outcomes:

1) In yeast, both ZmAMF1;1 and ZmAMF1;2 were capable to rescue growth of a K^+-transport mutant CY162 when external ammonium concentration was high but potassium supply was limiting. It is predicted that ZmAMF1;1 and ZmAMF1;2 act as putative NH_4^+/ H^+ antiporters in yeast to facilitate ammonium efflux in the vacuole to the cytoplasm, but the mechanism behind this remains unclear.
2) In maize, loss of ZmAMF1;1 and ZmAMF1;2 activity resulted in a significant increase in short-term ammonium uptake, increased shoot development and root nitrogen content.
3) *ZmAMF1;1* and *ZmAMF1;2* were both localized in the vascular cylinder in maize roots starved of nitrogen. Both genes were significantly upregulated (around 3.3 to 3.7-fold) in shoot tissues under nitrogen starvation but not downregulated with nitrogen resupply (4 hrs).
4) *ZmAMF1;1* and *ZmAMF1;2* had different expression profiles in maize where *ZmAMF1;1* was more expressed in shoot tissues especially during the reproductive stage, while *ZmAMF1;2* expression was primarily in the roots.

Overall, this project has established a better understanding of the role maize AMF1 proteins have in ammonium transport, their potential role as a NH_4^+/ H^+ antiporter and their role in influencing maize growth and development in response to external nitrogen supply.

Table of Contents

List of Figures

List of tables

Chapter 1 Introduction

Nitrogen is one of the most important macronutrients required for plant growth. It is an essential structural component of proteins, nucleic acids, pigments, chlorophyll, secondary metabolites and many other important metabolic molecules found in plant cells. Therefore, it is important to a growing plant that there are both sufficient supplies of available nitrogen in the soil and mechanisms by the plant to access it.

In agricultural plant production, inorganic nitrogen has been widely used as a nitrogen fertilizer to improve crop yield. This has resulted in the global use of $\sim 10^{11}$ kg/annum nitrogen fertilizers (Glass, 2003). Unfortunately in cereal production, a staple component of human nutrition, only about 30-50% of the total nitrogen applied to the crop is actually used for the production of the final grain yield (Raun and Johnson, 1999; Tilman et al., 2002). Nitrogen use efficiency (NUE) is a term to help describe the efficient utilization of applied nitrogen for the development, growth and eventual yield of agricultural plants. With nitrogen being a major component of plants, the definition of NUE can vary depending on the measured outcome (yield, growth, competition). NUE has been described as nitrogen uptake efficiency, nitrogen utilization efficiency and combinations of these two which may be linked to harvest index or plant biomass. Ultimately, all NUE measures are linked to supply and access of soil nitrogen and how the plant effectively uses that nitrogen and what other competing factors may play limiting nitrogen uptake, utilization and capture into harvested products. Poor nitrogen use

efficiencies can result in the loss of nitrogen into the environment, which causes water and soil pollution as well as greenhouse gas production (Masclaux-Daubresse et al., 2010). In addition, the waste of nitrogen fertilizers also gives rise to financial losses to the farmers, a significant cost in the production cycle. Therefore, improving plant NUE is an important strategy to overcome many of these constraints. One direction in enhancing NUE in plants is to increase the efficiency of root nitrogen transport processes. This includes, the proteins involved in the uptake of nitrogen from the soil as well as the internal storage and redistribution of nitrogen required to support growth and final seed yields (Garnett et al., 2009). Improved nitrogen use efficiencies will ultimately reduce excess nitrogen application, decrease nitrogen pollution and improve plant sustainability.

In most soils and agricultural contexts, nitrate and ammonium are the predominant inorganic sources of nitrogen utilized by plants. Since the uptake and assimilation of ammonium requires less energy than nitrate, some plants prefer to use ammonium when both forms are present, even if the concentration of ammonium is lower than that of nitrate (von Wirén et al., 2000). Ammonium availability is influenced by several soil properties including, pH, aeration, temperature, and the activity of nitrifying bacteria. Soils that are acidic, anaerobic and or cool, favour ammonium as the predominant ion present in the soil solution. In contrast with temperate, well-aerated, microbiologically active soils, nitrate is often the predominant ion. Although ammonium acts as an important nitrogen source and intermediate in many metabolic reactions, excessive ammonium supply can be toxic to many plants, resulting in poor shoot and root growth and yield depression.

The mechanisms contributing to ammonium toxicity in plants varies from the disruption of membrane potentials and charge balance that influence other cellular transport processes to energy loss through futile cycling of ammonium across the plasma membrane (Britto et al., 2001; Britto and Kronzucker, 2002, 2006; Balkos et al., 2010; Bittsánszky et al., 2015). Therefore, it is important to understand how plants regulate ammonium uptake and the mechanisms used to manage this important resource.

Plants transport ammonium through two kinds of ammonium transport pathways, which include the high-affinity ammonium transporters (HATS), which operate at low ammonium concentrations and low-affinity ammonium transporters (LATS), which operate at high ammonium concentrations (typically > 0.5 mM) (Nacry et al., 2013). Genes encoding HATS proteins belong to the AMT/MEP/Rhesus superfamily. Many of these genes have been studied in plants where location, expression, activity and regulation have been investigated (Ludewig et al., 2007; Yuan et al., 2007b; Masclaux-Daubresse et al., 2010; Gu et al., 2013). However, the genetic identity of transport proteins responsible for the LATS pathway is not sufficiently understood. Some potassium channels have been found to be permeable to ammonium (Schachtman et al., 1992; White, 1996; Hoopen et al., 2010), and the non-selective cation channels (NSCCs) are also found to conduct low affinity ammonium transport (Demidchik et al., 2002; Balkos et al., 2010). Besides, aquaporins are also found to be permeable to ammonia (Jahn et al., 2004). Recently, through a transcriptional linkage to a membrane bound transcription factor, bHLHm1, a novel family of ammonium transporters, AMF1 has been discovered (Chiasson et al., 2014). Heterologous expression of yeast and soybean

AMF1 orthologs in *Xenopus laevis* oocytes, indicates AMF1 proteins increase the level of low-affinity ammonium transport (Chiasson et al., 2014). AMF1 candidate genes have been identified in many plants including soybean, Arabidopsis and maize.

Maize, is one of the most important agricultural crops in the world, where yield and quality are strongly linked with nitrogen nutrition. In maize, two AMF1 candidate genes (*ZmAMF1;1* an *ZmAMF1;2*) have been identified, however, their activities remain to be characterized. In this study the functional activity of ZmAMF1;1 and ZmAMF1;2 proteins were determined using a yeast heterologous expression system, and *ZmAMF1;1* and *ZmAMF1;2* expression pattern and specific tissue localization were also studied in maize. In addition, this study also developed loss of function mutants to characterize their net contribution to ammonium transport into and within maize plant lines. Overall, this projects aim is to contribute to a better understanding of the role AMF1 proteins to plant nitrogen transport and metabolism, their role as low-affinity ammonium transporters and their ability to influence maize growth and development. It is intended this research will lead to strategies that improve nitrogen use efficiency and agricultural plant production.

Chapter 2 Literature Review

2.1 Nitrogen assimilation

Nitrogen is an essential macronutrient required for plant growth and productivity. In most plants, inorganic nitrogen (ammonium and or nitrate) is the predominant source of nitrogen present and taken up from the soil. Once taken up by the plant, ammonium and nitrate can be either stored in their ionic form within cellular organelles (i.e. vacuoles) or readily assimilated using enzyme pathways localized across multiple cellular organelles and cell types located across both root and shoot tissues. The ease by which nitrogen is assimilated is dependent on its relative oxidative state. Nitrate is highly oxidised (+5) while ammonium is significantly reduced (-3). Thus plants that utilize nitrate must first reduce it to ammonium through an energy intensive set of enzymatic reactions. Once ammonium is generated plants utilize a common set of GS (glutamine synthetase)/GOGAT (glutamate synthetase) pathways and transamination reactions that converts ammonium into amino acids. Amino acids are then used by plants to produce protein, nucleic acids and various N-containing organic molecules (Taiz and Zeiger, 2002).

2.1.1 Nitrate assimilation

Nitrate assimilation can take place in both shoot and root tissues. Depending on the plant species, the location of nitrate assimilation (root versus shoot) can vary (Heldt, 2005). When plant roots accumulate excessive quantities of nitrate, nitrate

can be temporarily stored in vacuoles or transported into leaves via the xylem (Heldt, 2005). It takes two steps to reduce nitrate into ammonium. In the first step, nitrate is reduced into nitrite by an enzyme called nitrate reductase (NR) located in the cytoplasm. NR has two isoforms, which are NADH isoform in green tissue and NADPH isoform in roots (Oaks, 1994). NR activity requires energy, which is supplied through electron donations from the reduced molecules NADH or NADPH (Taiz and Zeiger, 2002).

Nitrate reductase reaction:

$$NO_3^- + NAD(P)H + H^+ + 2e^- \rightarrow NO_2^- + NAD(P)^+ + H_2O$$

NR is a homodimer, and each monomer comprises three prosthetic groups: 1) flavin adenine dinucleotide (FAD), 2) a heme and 3) a molybdenum cofactor (MoCo) (Masclaux-Daubresse et al., 2010). These three groups comprise the electron transport chain of NR. Firstly, FAD receives two electrons from NAD(P)H, and then the electrons are passed by the heme component onto MoCo, where nitrate binds and is reduced to nitrite (Heldt, 2005). Nitrite then enters the chloroplast (leaves) or plastids (roots), where nitrite reductase (NiR) reduces it further to ammonium. NiR is a single polypeptide, containing two prosthetic electron transfer groups: a 4Fe-4S cluster and a siroheme (Taiz and Zeiger, 2002).

Nitrite Reductase Reaction:

$$NO_2^- + 6Fd_{reduced} + 8H^+ + 6e^- \rightarrow NH_4^+ + 6Fd_{oxidised} + 2H_2O$$

In chloroplasts, the electron donor is reduced ferredoxin (Fd), which is generated from photosynthesis, while in root plastids, the reduced ferredoxin required is first reduced by NADPH generated from the pentose phosphate pathway (Heldt, 2005).

2.1.2 Ammonium assimilation

Ammonium derived from root absorption, nitrate assimilation and or photorespiration, is assimilated in either the cytosol or in the plastids of plant cells. Through the GS/GOGAT pathway, ammonium is converted to glutamine and glutamate (Taiz and Zeiger, 2002; Masclaux-Daubresse et al., 2010). In the first reaction, glutamine synthetase (GS) fixes ammonium to one glutamate molecule, which generates one glutamine molecule. Glutamate synthetase (GOGAT) then converts glutamine with 2-oxoglutarate to two molecules of glutamate.

Glutamate synthetase reaction:

$$\text{Glutamate} + NH_4^+ + \text{ATP} \rightarrow \text{glutamine} + \text{ADP} + P_i$$

$$\text{Glutamine} + \text{2-oxoglutarate} + \text{NADH} + H^+ \rightarrow 2\ \text{glutamate} + NAD^+$$

$$\text{Glutamine} + \text{2-oxoglutarate} + Fd_{reduced} \rightarrow 2\ \text{glutamate} + Fd_{oxidised}$$

In plants, two isoforms of GS exist, the cytosolic glutamine synthetase (GS1) and the plastid localized glutamine synthetase (GS2) (Taiz and Zeiger, 2002). These two isoenzymes perform separate function in plants (Edwards et al., 1990). GS1 is expressed predominantly in roots where it functions in the assimilation of nitrogen taken up from the rhizosphere. (Peterman and Goodman, 1991; Bernard and Habash, 2009). In addition, GS1 is also found expressed in the vascular bundles of roots and shoots, especially during the seed germination and during leaf

senescence (a stage where massive amounts of ammonium is discharged as proteins and nucleic acids break down). GS1 is thus an important enzyme for efficient recycling of ammonium (Lam et al., 1996; Bernard and Habash, 2009). GS2 is predominantly located in chloroplasts of green tissues. However, GS2 has also been identified in root plastids (Lam et al., 1996). GS2 functions in the assimilation of ammonium generated from nitrate reduction and photorespiration (Edwards et al., 1990). The activity of GS2 can be regulated by light as shown in *Pisum sativum* and *Arabidopsis thaliana* leaves (Edwards and Coruzzi, 1989; Peterman and Goodman, 1991).

Similar to GS, plants have two types of glutamate synthetases of which the electron carriers are NAD(P)H (NAD(P)H-GOGAT) or ferredoxin (Fd-GOGAT) (Suzuki and Knaff, 2005). NAD(P)H-GOGAT is expressed primarily in root and vascular bundles, while Fd-GOGAT is mainly present in chloroplasts in leaves (Lam et al., 1996; Taiz and Zeiger, 2002). Since the two enzymes have similar locations with GS1 and GS2 respectively, they are proposed to function co-ordinately with GS1 and GS2 (Lam et al., 1996; Taiz and Zeiger, 2002).

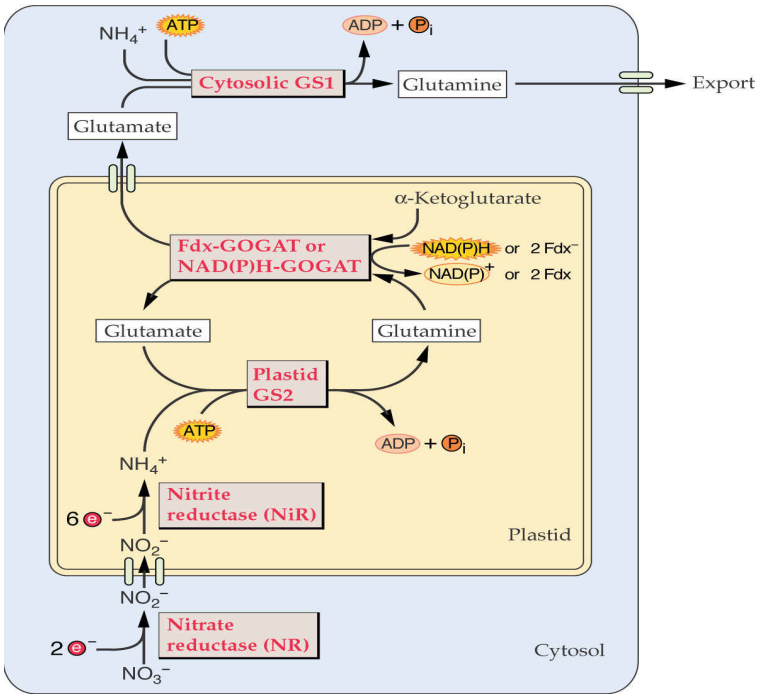

Figure 2.1 GS/GOGAT cycle.

Nitrate absorbed by plants is reduced into ammonium followed by assimilation into amino acids. Ammonium assimilation is mainly the GS/GOGAT pathway, where ammonium is first transformed into glutamine by the enzyme GS, and subsequently glutamine is converted into glutamate by the enzyme GOGAT. Glutamine and glutamate can be the precursors to produce other amino acids. Illustration is from (Hildebrand, 2013).

2.1.3 The role of glutamate dehydrogenase

Previously, glutamate dehydrogenase (GDH, EC 1.4.1.3) was considered as a major contributor to the assimilation of ammonium into amino acids (Miflin and Lea, 1976). However, because of its low activities in chloroplasts and its high K_m for ammonium (Lea and Thurman, 1972), GDH is now not considered as significant as GS in ammonium assimilation (Lea and Miflin, 1974). Nevertheless, GDH still plays an important role in plants where it catalyses a reversible reaction that synthesises

or deaminates glutamate (Taiz and Zeiger, 2002). There are two forms of GDH in plants, which are NADH-dependent form functioning in mitochondria, and NADPH-dependent form found in chloroplast (Lam et al., 1996).

Glutamate dehydrogenase reaction:

2-Oxoglutarate+NH_4^++ NAD(P)H ↔ glutamate+H_2O+$NAD(P)^+$

GDH is important for balancing carbon and nitrogen levels within the cell. GDH can respond to high levels of ammonium to avoid ammonium toxicity. GDH can also deaminate glutamate to produce carbon skeletons that can be used in various carbon-metabolic reactions and the tri-carboxylic acid cycle (Miflin and Habash, 2002).

2.1.4 Transamination reactions transfer nitrogen

The glutamate and glutamine generated from ammonium assimilation can produce other important amino acids such as asparagine and aspartate through transamination reactions. This process requires carbon skeletons (such as sucrose, sugar and alcohols) generated through CO_2 assimilation (Taiz and Zeiger, 2002).

Glutamate and glutamine are important precursors for the synthesis of other amino acids, such as asparagine (Heldt, 2005). Asparagine has a high N:C ratio (2:4), which makes it an important molecule for the storage and transport of nitrogen in both leguminous and non-leguminous plants (Lam et al., 1996; Lea et al., 2007).

Asparagine is generated by the enzyme asparagine synthetase (AS), where an amino group is transferred from glutamine to aspartate to form asparagine (Taiz

and Zeiger, 2002). AS can also utilize ammonium directly as the substrate to generate asparagine, particularly when the concentration of ammonium in the cell is high (Oaks and Ross, 1984; Gaufichon et al., 2010). The expression of AS can be regulated by light and carbohydrate to coordinate the nitrogen and carbon balance of the cell (Lam et al., 1996).

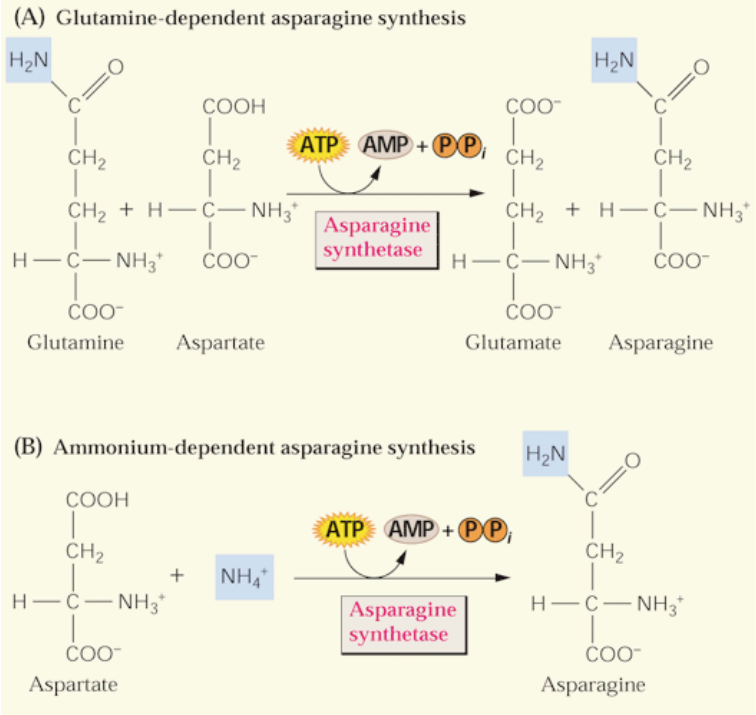

Figure 2.2 The generation of asparagine

Asparagine can be produced either through glutamine or directly through ammonium. Illustration is from (Hildebrand, 2013).

Aspartate can be produced through the reaction between glutamate and oxaloacetate by the enzyme aspartate aminotransferase (Asp-AT) (Taiz and Zeiger, 2002). Aspartate is also an important precursor for other amino acids, such as lysine, isoleucine and threonine (Taiz and Zeiger, 2002).

2.2 Ammonium uptake from soil

2.2.1 Biochemical process

In plants, ammonium transport is mainly facilitated by membrane transporters (Glass et al., 2002; Yuan et al., 2007b). Physiological studies in plant roots have revealed that two kinetically different transport pathways function in ammonium uptake (Fried et al., 1965; Vale et al., 1988; Wang et al., 1993). One is the high affinity transport system (HATS), which operates predominantly at low external ammonium concentrations and exhibits saturation kinetics (Sohlenkamp et al., 2000). The second one is the low affinity transport system (LATS). It works at high external ammonium concentrations (typically > 0.5 mM) and predominantly shows a linear uptake response to external ammonium concentrations (< 20 mM) (Wang et al., 1993; Sohlenkamp et al., 2000; Nacry et al., 2013).

The transport mechanism in plant AMTs is different to those identified in yeast (MEP), bacteria (AmtB) and humans (Rh transporters). Electrophysiology studies showed that in plants, AMTs conduct electrogenic currents and can depolarize membrane potentials while transporting ammonium. Consequently, AMTs are proposed to provide the main route for ammonium transport across plant membranes (Ludewig et al., 2002; Mayer et al., 2006; Wood et al., 2006; Ludewig et al., 2007). The Rh membrane protein is proposed to either conduct NH_4^+/H^+ in an antiport manner or function as a ammonia channel (Ludewig et al., 2007). Prokaryotic AmtB orthologs, recruit ammonium, then deprotonate the ion to ammonia which is transferred as a gas through hydrophobic non-polar pores formed in the centre of each protein subunit (Ludewig et al., 2007).

The HATS pathway and its molecular regulation has been characterized across various plant species, especially in the model plant *Arabidopsis thaliana* (Nacry et al., 2013). In contrast, the genetic identity of the LATS ammonium transport system remains to be identified.

2.2.2 Plant genes involved in ammonium transport

Genes encoding HATS proteins belong to the AMT family which is a part of the large group ammonium transporter family: Ammonium Transporter / Methylammonium Permease / Rhesus (AMT/MEP/Rh) family (Nacry et al., 2013). In Arabidopsis, six genes belong to the AMT family, where *AtAMT1;1 - AtAMT1;5* belong to the AMT1 clade, while the remaining *AtAMT2* is more closely related to the MEP/ AmtB subfamily found in yeast and bacteria (Yuan et al., 2007b; Nacry et al., 2013). Individually AMT1;1 and AMT1;3 are responsible for ~ 30-35% of the net HATS ammonium uptake capacity in nitrogen-deficient roots. Together they contribute additively to approximately 65-70% to ammonium uptake capacity in the roots under nitrogen deficiency (Loqué et al., 2006; Yuan et al., 2007b). AtAMT1;1 and AtAMT1;3 show a very similar affinity for ammonium with K_m values of 50 and 61 µM respectively. This activity suits their enhanced expression in rhizodermal cells and root hairs under nitrogen deficiency where ammonium concentrations in the soil solution are often low in the µM range (Loqué et al., 2006; Yuan et al., 2007b). Studies of *AtAMT1;2* expression in yeast, indicated that AtAMT1;2 exhibited biphasic kinetics for methylammonium uptake at both a high-affinity (K_m of 36 µM) and a low-affinity phase (K_m of 3.0 mM) (Shelden et al., 2001). Subsequently, Yuan compared the contribution of AtAMT1;2 to high affinity and low affinity ammonium transport, which indicated that AtAMT1;2 is primarily a high-affinity

ammonium transporter (Yuan et al., 2007b). However, AtAMT1;2 shows lower substrate affinity (K_m 234 μM) and lower capacity (18-26%) compared with AtAMT1;1 and AtAMT1;3. This activity is consistent with its location in the inner endodermal and cortical cell layers (Yuan et al., 2007b). Thus, AtAMT1;2 is proposed to mediate in the uptake of higher concentrations of ammonium entering the root via the apoplasmic transport pathway (Yuan et al., 2007b). Yuan et al (2007a), found that in an *amt1;1 amt1;2 amt1;3 amt2;1* quadruple mutant in Arabidopsis, high affinity ammonium influx still increases under nitrogen deficiency, which maintained approximately 5-10% of ammonium uptake capacity of wild-type plants. It was suggested that AtAMT1;5 accounted for the remainder of this transport activity (Yuan et al., 2007b). AtAMT1;5 is a high affinity transporter (K_m 4.5 μM), but its transport capacity is low (Yuan et al., 2007b). AtAMT1;5 is expressed in rhizodermal cells and root hairs under nitrogen deficiency (Yuan et al., 2007b). AtAMT1;4 is found as a high affinity plasma membrane transporter (K_m ~17 μM) and is exclusively expressed in pollen in Arabidopsis (Yuan et al., 2009).

AtAMT2 exhibits a high affinity ammonium transport activity where expression is upregulated in roots under nitrogen deficiency (Sohlenkamp et al., 2002). AtAMT2 in yeast shows similar growth complementation at acidic and neutral external pH, which indicates that ammonium is the predominant substrate instead of ammonia (Sohlenkamp et al., 2002; Neuhäuser et al., 2009). However, when *AtAMT2* is expressed in *Xenopus* oocytes, AtAMT2 shows electroneutral transport where no currents are elicited in the presence of either MA or ammonium. This indicates that potentially after recruiting ammonium, AtAMT2 may deprotonate the ion to ammonia, before transfer across the membrane (Neuhäuser et al., 2009). AtAMT2

is found expressed in shoots, roots and photosynthetic tissues (Sohlenkamp et al., 2002; Neuhäuser et al., 2009), and the expression in roots is lower than in shoots (Sohlenkamp et al., 2000). AtAMT2 is expressed in the rhizodermal cells of lateral roots and plasma membrane of the root hairs, which is co-localized with AtAMT1 transporters (Neuhäuser et al., 2009).

Rice, which is commonly grown in flooded paddy fields, will preferentially utilize ammonium as a nitrogen source and is often considered ammonium tolerant (Li et al., 2009). To date, at least 12 AMT genes have been identified in rice plants which are subdivided into five clades from OsAMT1 to OsAMT5 (Li et al., 2009; Bu et al., 2011). The subfamily OsAMT4 and OsAMT5 contain one and two member respectively, whereas the subfamily OsAMT1 to OsAMT3 all contain three members (Li et al., 2009; Bu et al., 2011). Except OsAMT4 and OsAMT5, the other OsAMTs all contain 11 putative transmembrane domains (Sonoda et al., 2003; Bu et al., 2011). *OsAMT1;1* performed constitutive expression in shoots and roots while OsAMT1;2 and OsAMT1;3 are root-specific transporters (Sonoda et al., 2003). OsAMT1;2 is localized in the central cylinder and cell surface of root tips (Sonoda et al., 2003).

Poplar as a perennial woody plant is found to possess an expanded family of 14 AMTs assigned into two subfamilies: AMT1 (six genes) and AMT2 (eight genes) (Couturier et al., 2007). It is proposed that the larger family of AMTs in poplar may be important in the longer time-scale of the plants life relative to annual plant species (Couturier et al., 2007). In tomato, three AMT genes (which are *LeAMT1;1*, *LeAMT1;2* and *LeAMT1;3*) has been identified (Von Wirén et al., 2000). *LeAMT1;1* is preferably expressed in root hairs, while *LeAMT1;3* is mainly present in leaves. *LeAMT1;2* is expressed both in root hairs and leaves (Von Wirén et al., 2000).

Maize roots shows a relative preference of high affinity uptake for ammonium over nitrate when supplied at equimolar concentrations (Gu et al., 2013). In maize, two ammonium transporters, ZmAMT1;1a and ZmAMT1;3 have been characterized (Gu et al., 2013). Both of these were localized on the rhizodermis, and were proposed to be the major high affinity ammonium transport component in maize with K_m values of 48 and 33 μM, respectively (Gu et al., 2013).

2.2.3 Regulation of plant AMTs

The regulatory features of ammonium transporters vary depending on the plant species and the nitrogen status of the plant.

2.2.3.1 AMT response to nitrogen status

Root nitrogen uptake can be regulated in response to either the external nitrogen supply or the nitrogen demand of the whole plant (Nacry et al., 2013). AMTs' expression pattern varies under different nitrogen status. The expression of *AMT* genes varies across plant species and nitrogen status. In hydroponically grown *Arabidopsis* plants, the expression of *AMT1;1* increased 5-fold in roots when plants were transferred from nutrient solution containing 1mM NH_4NO_3 to nitrogen free nutrient solution for 3 days (Gazzarrini et al., 1999), This nitrogen-deficiency induced gene expression pattern is also observed in Arabidopsis shoots, when Arabidopsis T-DNA insertion line *atamt1;1-1* was transformed and overexpressed with *AtAMT1;1* and starved for nitrogen for 3d (Yuan et al., 2007a). When tobacco plants were introduced with *AtAMT1;1* gene driven by cauliflower mosaic virus 35s promoter, *AtAMT1;1* expression was also increased in both shoots and roots when starved for N for 3d, while the increased expression in roots declined when

resupplied with nitrogen (Yuan et al., 2007a). Conversely in maize, AMT genes showed substrate-inducible expression. When maize seedlings were transferred from nutrient solution containing 2 mM NH_4NO_3 to nutrient solution free of nitrogen for 24, 48, 72 and 96h, the transcription of *ZmAMT1;1a* and *ZmAMT1;3* decreased about half during the nitrogen starvation period. However, when the nitrogen starved maize roots resupplied with ammonium, the expression of *ZmAMT1;1a* and *ZmAMT1;3* in maize roots increased 2 to 3-fold within 24h (Gu et al., 2013). In hydroponically grown tomato roots, *LeAMT1;1* expression was strongly induced after two days of nitrogen starvation and declined by resupply of ammonium. Conversely, *LeAMT1;2* expression was only slightly increased after nitrogen starvation, but the transcription was significantly increased by the resupply of ammonium in roots (Von Wirén et al., 2000). In rice, *OsAMT1;2* expression also increased with a re-supply of ammonium, while the expression of *OsAMT1;3* was induced under nitrogen deficiency (Sonoda et al., 2003).

2.2.3.2 Diurnal regulation of *AMT* genes

The expression of *AMT* genes shows diurnal regulation. In *Arabidopsis* roots, the expression of *AtAMT1;3* was regulated by light where its expression peaked at the end of light period (Gazzarrini et al., 1999). As carbohydrates are at a high level at the end of light period and required for ammonium assimilation, it has been suggested that AtAMT1;3 may play an important role in carbon and nitrogen metabolism in plants (Gazzarrini et al., 1999). In tomato leaves, the expression of *LeAMT1;3* peaked in the dark while the expression of *LeAMT1;2* performed highest expression after onset of the light period and then decreased to its lowest level before the end of light period (Von Wirén et al., 2000).

2.2.3.3 Posttranslational regulation of AMT activity

The transcriptional regulation of AMT expression is also complemented by posttranslational modifications that directly influence AMT activity. Plant AMTs form trimers within the membrane, where each subunit forms a hydrophobic pore capable of transporting ammonium (Lanquar and Frommer, 2010). Interactions between subunits will ultimately regulate the transport activity of the AMT trimer (Graff et al., 2011), thus providing a form of allosteric regulation occurring directly within the membrane (Nacry et al., 2013). In many AMT orthologs, the cytosolic C-terminus of AMTs are highly conserved. Phosphorylation of the conserved Threonine-460 located within this region has recently been proposed to be an important regulatory mechanism that influences AMT activity (Lanquar and Frommer, 2010). When phosphorylated, subunit conformation changes, rendering AMTs inactive. Disruptions in the cytosolic C-terminus can also inactive neighbouring subunits and lead to a loss of transport activity (Loque et al., 2007; Neuhäuser et al., 2007). In *Arabidopsis*, the cytosolic carboxy terminus of ammonium transporters can act as an allosteric regulator (Loque et al., 2007).

2.3 Ammonium once inside the plant

2.3.1 Ammonium transport between root and shoot in plants

Once mineral nutrients are absorbed by roots they need to be transported to the shoots to support growth. The xylem is the principle way to transport nutrients to the shoots (Jeschke and Hartung, 2000). However, whether ammonium is transported from roots to shoots, through the xylem, remains unclear. Since ammonium at high concentrations is toxic to plants, it is generally suggested that

ammonium absorbed from the soil is first assimilated in roots, rather than transported to the shoots to be assimilated (Peuke et al., 1994). Ammonium observed in plant tissues is mainly generated by nitrogen metabolism such as protein breakdown and photorespiration (Schjoerring et al., 2002). However, significant amounts of nitrate is taken up by roots and transported to the shoots where it is assimilated (Engels and Marschner, 1993; Peuke et al., 1994). Studies of xylem sap composition have often shown that nitrate and reduced nitrogen (mainly glutamine) are major components of the sap transported to the shoot (Engels and Marschner, 1993; Peuke et al., 1994; Kronzucker et al., 1998). However, when xylem sap is analysed amino acids amines and ammonium is often detected, suggesting root to shoot ammonium transport may occur across some plant species (Husted et al., 2000; Schjoerring et al., 2002). When identified, the concentration of ammonium in xylem sap will increase as the external ammonium concentrations increases; ammonium in the sap has been estimated at ~11% v/v of the translocated N in the xylem sap (Schjoerring et al., 2002).

The cycling of nitrogen between root and shoot is an important mechanism to regulate nitrogen nutrition of plants. However, the ammonium transporters responsible for this process, especially the low affinity ammonium transporters still remain to be identified.

2.3.2 Ammonium generation inside plants

2.3.2.1 Nitrogen remobilization

The process of tissue nitrogen remobilization is an ongoing activity across a plant canopy to ensure that nitrogen released during tissue senescence is conserved and

reallocated. Tissue (leaves, stems) senescence involves the degradation of organic molecules, such as protein, nucleic acids and lipids into amino acids, peptides and inorganic ammonium (Liu et al., 2008). Chloroplasts which account for 70% of the nitrogen in a leaf, is a major source for available nitrogen for remobilization (Liu et al., 2008; Bieker and Zentgraf, 2013).

Remobilized nitrogen is an important nutrient source for plants across both vegetative and reproductive growth periods. Before anthesis, nitrogen remobilization supports the growing meristematic regions of the plant including leaves and reproductive organs. When plants began begin to flower and set fruit, remobilized nitrogen from senescing tissues increases and becomes a significant component of the final accumulated nitrogen in the reproductive tissues (Bieker and Zentgraf, 2013). In cereals, remobilization of shoot nitrogen is particularly relevant, especially during the important grain filling stages.

As plant tissues senesce, protein and nucleic acids are degraded into amino acids, amides and ammonium. Ammonium is generally re-assimilated during this process through enhanced GS1 activity in senescing tissues where it is converted back into amino acids and transported through the phloem to seeds (Gregersen et al., 2008). Glutamine derived from this process is the primary component of the transported nitrogen in the phloem (Liu et al., 2008). GDH is also proposed to play important roles in nitrogen remobilization (Miflin and Habash, 2002) where its activity is found induced in older leaves (Masclaux et al., 2000).

Improving the efficiency of nitrogen remobilization is proposed to be an important way to improve grain yield and to enhance nitrogen fertilizer utilization (Gregersen

et al., 2008; Liu et al., 2008; Masclaux‐Daubresse et al., 2008; Bieker and Zentgraf, 2013). Ammonium is an important by-product produced during leaf senescence. The role of ammonium transporters in the re-capture of this remobilized ammonium is therefore important in plant nitrogen metabolism and nitrogen remobilization efficiency.

2.3.2.2 Ammonium and the synthesis of lignin

In addition to photorespiration, the biosynthesis of lignin is thought to be a significant source of ammonium generation in plant cells, especially in trees which require lignin to form wood (Cantón et al., 2005). The first step of lignin biosynthesis is the deamination of phenylalanine to yield cinnamate, which is catalyzed by phenylalanine ammonia-lyase (PAL) (Whetten and Sederoff, 1995). The amino group cleaved from this reaction is released as ammonia (Whetten and Sederoff, 1995). The ammonia generated is proposed to enter in the cytosolic GS/GOGAT pathway located in vascular bundles (Suárez et al., 2002). Efficient re-capture of this ammonia is important to conserve plant nitrogen reserves.

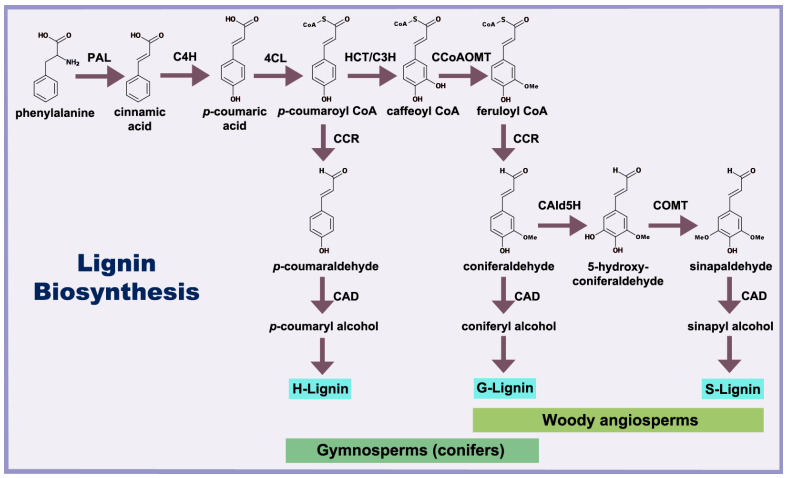

Figure 2.3 The lignin biosynthesis pathway

In the first step of lignin biosynthesis, ammonia is released during the formation of phenylalanine to cinnamic acid. Illustration is from (Diouf, 2004).

2.3.2.3 Photorespiration

Photorespiration takes place simultaneously with photosynthesis in all oxygen (O_2)-producing photosynthetic organisms, especially when light is intense and external O_2 is elevated (Bauwe et al., 2010). Since photorespiration diminishes about 25% of CO_2 fixation in C3 plants, it was previously viewed as a wasteful process (Rachmilevitch et al., 2004). However, as photorespiration can act as an energy sink promoting the flow of electrons along the photosynthetic electron chain, photorespiration can prevent photoinhibition with high light and drought stress (Wingler et al., 2000; Rachmilevitch et al., 2004). In addition, photorespiration can also generate amino acids such as glycine, serine, which can be used for other metabolic pathways (Wingler et al., 2000). A by-product of photorespiration is the generation of ammonia from the decarboxylation of glycine to serine in the mitochondria. In C3 plants, the amount of ammonia released during photorespiration has been calculated to be at least 10-fold that produced from primary nitrate assimilation (Lam et al., 1996).

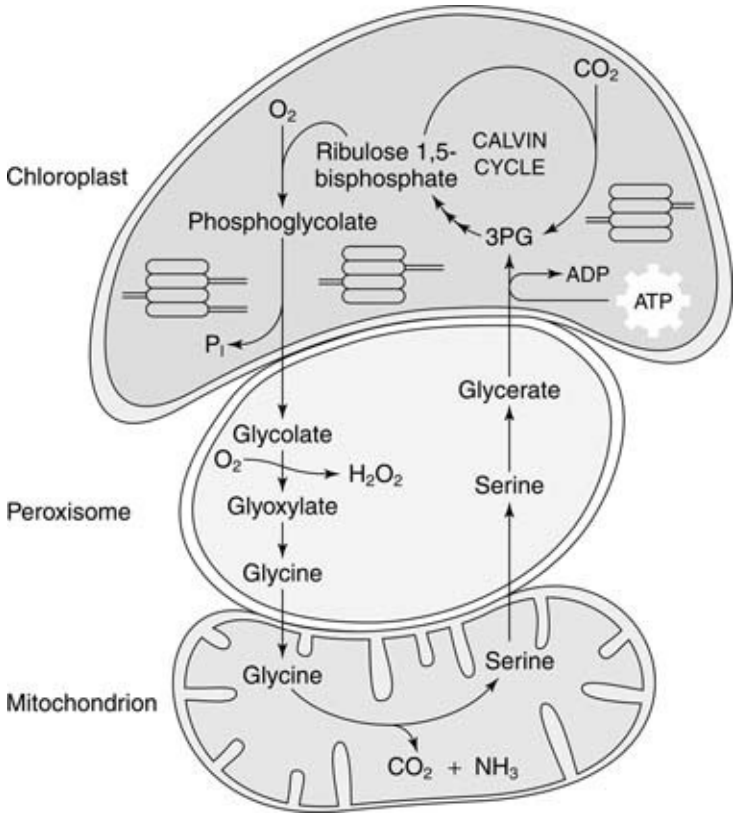

Figure 2.4 Photorespiration pathway.

Photorespiration involves a series of reactions in chloroplasts, peroxisomes and mitochondria. 2-phosphoglycolate produced in chloroplast enters into peroxisomes where it is transformed into glycine, which enters the mitochondria where two molecules of glycine react to produce one molecule of serine and one molecule of CO_2 and NH_3. Illustration is retrieved from (https://www.emedicalprep.com/study-material/biology/plant-physiology/photosynthesis-in-higher-plants/).

The whole process of photorespiration involves three organelles, which include chloroplasts, peroxisomes and mitochondria. The first step of photorespiration takes place in the chloroplast, where instead of photosynthetic CO_2 fixation by Rubisco, O_2 is fixed onto ribulose bis phosphate (RuBP). This process produces 3-phosphoglycerate (PGA) and 2-phosphoglycolate (2PG, or PG). PGA is the normal product of carboxylation, and can re-enter the Calvin cycle. Phosphoglycolate,

however, is toxic, and is converted into glycolate in the peroxisome, and finally through transamination, turns into glycine. Glycine then enters into mitochondrion where two molecules of glycine react and generate one molecule of serine as well as one molecule of CO_2 and NH_3.

Reaction: 2 GLYCINE + H_2O → SERINE + CO_2 + NH_3 + $2H^-$ + $2e^-$

Ammonium released from photorespiration must be reassimilated quickly to avoid ammonium toxicity. The ammonium is reassimilated in the chloroplast by GS2 (Oliveira et al., 2002).

2.4 AMF

2.4.1 Identification of the AMF1 class of ammonium transporters

Although high affinity ammonium transporters have been studied across various plant species, genetic information on the low-affinity ammonium transporter is lacking. GmSAT1 is a basic helix-loop-helix transcription factor found located on the symbiosome membrane of soybean nodules (Kaiser et al., 1998). It has recently also been shown to be localized across other membranes within the infected cell (Chiasson et al., 2014). It was previously characterized as a putative transport protein (Kaiser et al., 1998), however Marini et al (2000) (Marini et al., 2000) found that GmSAT1 was involved indirectly in ammonium transport. Recent work has shown that GmSAT1 is a membrane localized DNA-binding bHLH transcription factor, and it was renamed as GmbHLHm1. When GmbHLHm1 is expressed in yeast, the expression of a yeast gene (ScAMF1) is significantly unregulated (approximately 50-fold) through direct binding of the TF to the

promoter of ScAMF1 (Chiasson et al., 2014). ScAMF1 is an uncharacterized membrane transport protein located on the plasma membrane, and it is a member of the major facilitator superfamily (MFS) with 14 predicted transmembrane spanning domains. When independently expressed in yeast, ScAMF1 transports ammonium into the cell (Chiasson et al., 2014).

2.4.2 AMF activity

ScAMF1 orthologs have been found in many plants including maize, soybean and *Arabidopsis* and *Medicago*. In most situations sequence identity is ~45% between yeast and plant orthologs; although the identities amongst the plant orthologs are ~70-80% (Chiasson et al., 2014). Interestingly, in dicotyledenous plants both bHLHm1 and AMF1 genes share a conserved location at the chromosomal level. Through electrophysiological studies in *Xenopus* oocytes, ScAMF1 and a soybean homolog, GmAMF3, have been found to conduct low-affinity ammonium transport (Chiasson et al., 2014). Using a fusion of *GmAMF3* promoter with GUS, GmAMF3 has been found expressed in soybean root vascular bundles and in the nodule parenchyma cell layer. Using a YFP::GmAMF3 construct, transient expression in onion cells, show that GmAMF3 is localized to the plasma membrane.

In maize, two candidates of AMF have been identified, *AMF1;1* and *AMF1;2*, however, their activities remain to be characterized.

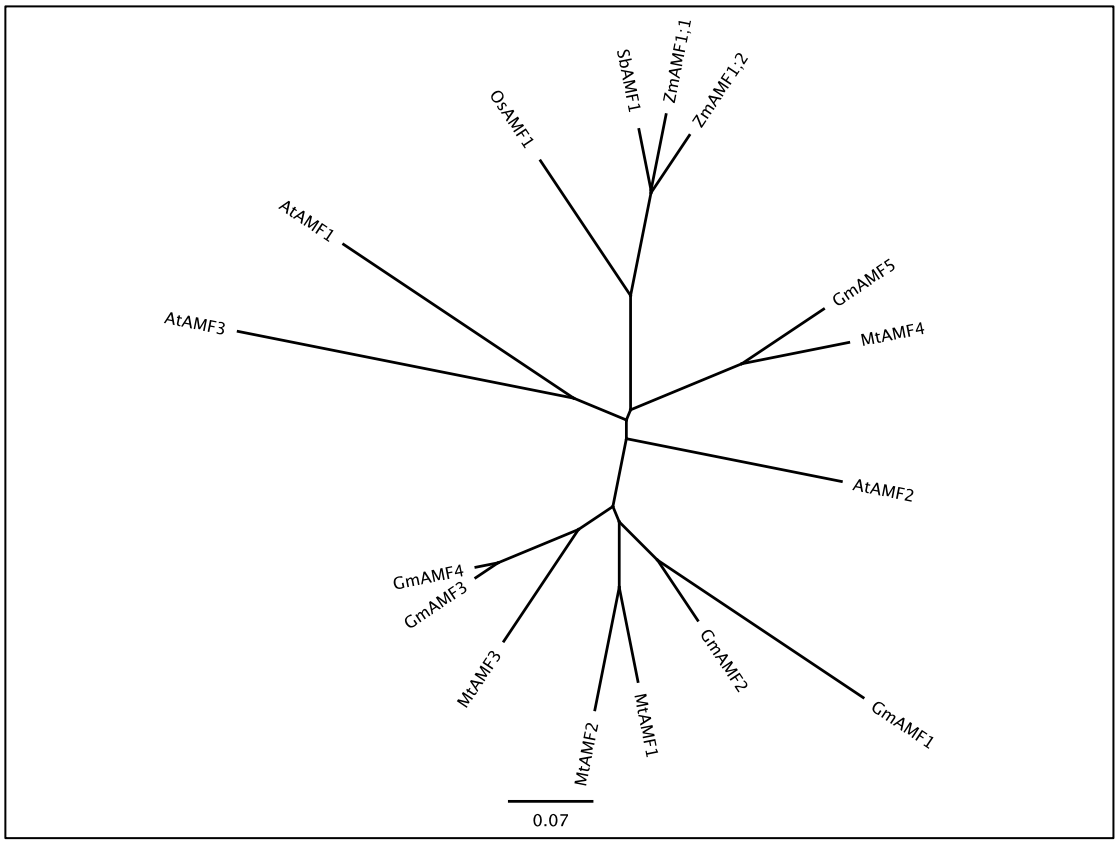

Figure 2.5 Phylogenetic tree of *Arabidopsis*, maize, soybean, *Medicago*, rice and sorghum AMFs.

The phylogenetic tree was built up with Geneious 6.0.6 software based on neighboring-joining method with Jukes-Cantor genetic distance model. The scale represents the number of amino acid substitutions per unite. The phylogenetic tree contains ZmAMF1;1 (grmzm2g062024), ZmAMF1;2 (grmzm2g164743), OsAMF1 (LOC_Os04g44430), SbAMF1 (Sb06g023125.1), AtAMF1 (At2g22730), AtAMF2 (At5g64500), AtAMF3 (At5g65687), GmAMF1(Glyma15g06660), GmAMF2 (Glyma13g32670), GmAMF3 (Glyma08g06880), GmAMF4 (Glyma09g30370), GmAMF5 (Glyma09g33680), MtAMF1 (Medtr2g010370.1), MtAMF2 (Medtr2g010350.1), MtAMF3 (Medtr4g092770.1), MtAMF4(Medtr5g030580.1).

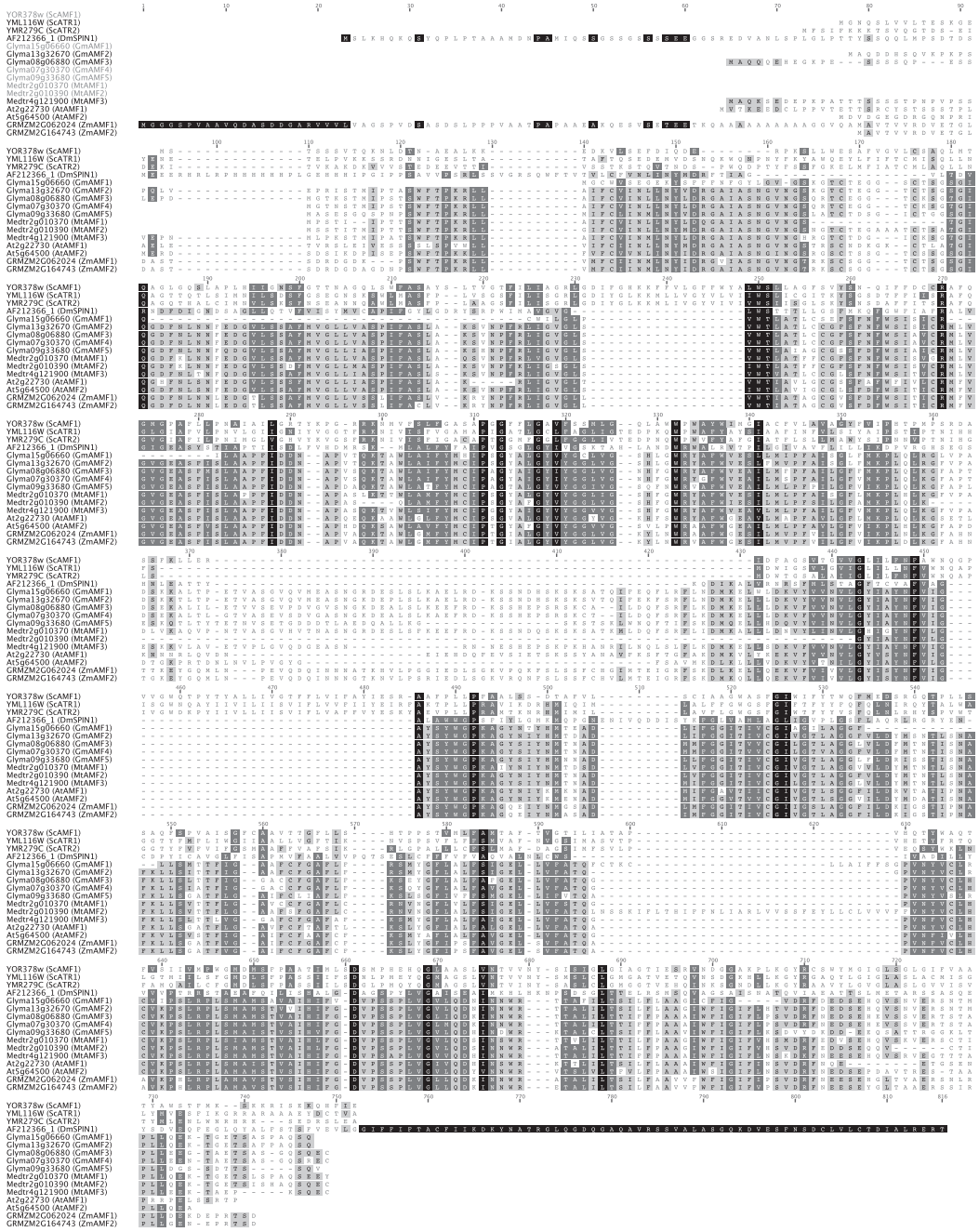

Figure 2.6 Amino acid alignment of predicted plant proteins of AMF1 family and close orthologs. Illustration is from (Chiasson et al., 2014).

The alignment contains *Saccharomyces cerevisiae* (YOR378w, YML116W, YMR279C), *Drosophila melanogaster* (AF212366_1), *Glycine max* (Glyma15g06660, Glyma13g32670, Glyma08g06880, Glyma07g30370, Glyma09g33680), *Medicago truncatula* (Medtr2g010370, Medtr2g010390, Medtr4g121900), *Arabidopsis thaliana* (At2g22730, At5g64500) and *Zea mays* (GRZM2G062024, GRZM2G164743). Related sequences were identified using BLAST. Sequence alignment was generated by Geneious Pro v 5.6.5.

2.5 Conclusion

Nitrogen has an important role in plant growth and development. Ammonium is a major inorganic form of nitrogen utilized by plants. Its transport across different organelles and tissues in plants involves two systems, a high affinity and low affinity pathway. Up to now, transporters responsible for the high affinity transport pathway have been studied in various kinds of plants. This examination has included their transport properties, location, expression and regulation. However, the information about low affinity ammonium transporters in plants including maize is lacking. The identification of the AMF1 class of proteins offers an exciting opportunity to further understand the pathways which may be responsible for low-affinity ammonium transport in plants.

This study aims to understand the functional activity of two AMF1 candidate genes (*ZmAMF1;1* an *ZmAMF1;2*) in maize, which includes the role of AMF1 proteins to plant nitrogen transport and metabolism, their role as low-affinity ammonium transporters and their ability to influence maize growth and development. It is intended this research will lead to strategies that improve nitrogen use efficiency and agricultural plant production.

Chapter 3 Development of TUSC lines

3.1 Introduction

3.1.1 *Mu* transposon - a class of highly active transposons in Maize

Transposon insertional mutagenesis has been a useful way to study gene function in maize which has several well-characterized transposon mutated populations. Transposons in maize, commonly known as the Ac (activator) / Ds (dissociation) system, were first identified by Barbara McClintock (McClintock, 1950). McClintock found that chromosomal Ds element insertions created mutational events, which can affect the expression of neighboring genes or give rise to a loss of a genes activity or physical presence in the genome. Ds elements move or 'jump' across the chromosome when in the presence of a nearby activator Ac element (McClintock, 1950). Ac is an autonomous transposon able to self-mobilize across the chromosome. This activation and insertion was confirmed in a study where a Ds element was found inserted into the coloured aleurone allele *C* which is dominant to the colourless aleurone *c* of chromosome 9 in maize. The colourless phenotype indicated the function of the *C* allele was disrupted. The same experiment also showed the activity of *C* could be restored when Dc was transposed from the *C* locus in the presence of an Ac activation element (McClintock, 1950). Both Ds and Ac have 11 bp terminal inverted repeats, and the insertion of Ds or Ac will generate 8 bp target site duplications (Du et al., 2011).

In 1978, Roberson (1978) discovered a new class of highly active transposon mutators (*Mu*), which displayed a 30-fold increase in the mutation frequency than that of the natural spontaneous mutation rate in maize. Since then, the *Mu* transposon has been a useful resource for both forward and reverse genetics studies in maize to activate or silence genes.

3.1.2 Characteristics of *Mu* transposon

The *Mu* transposon consists of two types of transposons, those which are either autonomous or those considered non-autonomous. Autonomous transposons are known as *MuDR* and can independently transpose within the genome. Non-autonomous transposons such as *Mu1*, *Mu2*, *Mu3*, *Mu4*, *Mu5*, *Mu6/Mu7* and *Mu8* (Robertson, 1978) requires the presence of *MuDR* for their transposition (Robertson, 1978). The majority of *Mu* transposons contain ~220 bp of conserved terminal inverted repeats (TIR) separated by nonconserved internal sequences (Bennetzen and Springer, 1994; Bennetzen, 1996; Dietrich et al., 2002; Tan et al., 2011).

Mu transposons are often found at high copy number in the genomes of active *Mu* transposon lines. The high copy number can result in a mutation rate of $\sim 10^{-4}$ mutations per locus per individual line (Lisch, 2002). Characterized *Mu* transposon loci, have revealed a preference for insertion into predicted gene sequences across the maize genome (Talbert et al., 1989; Lisch, 2002). This has allowed for the design of PCR primers that can conveniently identify the *Mu* transposon TIRs for PCR genotyping and the identification of the flanking gene sequences. Moreover, the use of the *Mu* transposon system in maize is supported by its relative ease to

outcross to remove non-specific insertions in the genome through traditional backcrossing programs. Consequently, several maize transposon panels (TUSC, Rescue *Mu* and Uniform *Mu*) have been developed for the identification of gene specific maize mutations (McCarty and Meeley, 2009).

3.1.3 Trait Utility System for Corn (TUSC)

Trait Utility System for Corn (TUSC) is a *Mu*-based reverse-genetic resource. It has a population of 41,472 mutagenized maize lines (McCarty and Meeley, 2009). The TUSC population was initially constructed by crossing *Mu*-active maize lines with a number of adapted and diverse maize inbreds. The TUSC resource has two sub-populations which are PV03 and BT94 (McCarty and Meeley, 2009). PV03 was constructed by crossing 350 inbreds with 65 different *Mu* lines. Approximately 6% of the background of this population is from maize line B73. (McCarty and Meeley, 2009). BT94 has less background complexity, and was built up by a single hybrid crossing with smaller set of *Mu* lines (McCarty and Meeley, 2009). With the development of the TUSC population, mutant populations are available for both forward and reverse genetic analysis. For example, Leonard *et al.* (2014) utilized TUSC lines to help confirm the genetic loci responsible for the *tassel-less 1* (*tls1*) inflorescence mutant. Map-based cloning identified that a deletion of *ZmNIP3;1* was a likely contributor to the *tls1* phenotype. Two TUSC mutants displaying a *tls1* phenotype were shown to carry *Mu* insertions in *ZmNIP3;1* (Leonard et al., 2014). Slewinski et al. (2009) utilized a *sut1* mutant isolated from the TUSC resource to demonstrate that *SUT1* functions in phloem loading in maize leaves. Gallavotti et al. (2004) utilized TUSC lines to study the function of *barren stalk1* in the architecture of maize.

In this chapter, I have utilized a collection of TUSC lines which carry putative insertions of the *Mu* transposon within *ZmAMF1;1* and *ZmAMF1;2*. These mutants were used to characterize the functional role of *AMF1* genes in maize. This chapter describes the process by which multiple lines were imported and screened for the *Mu* insertion at either loci and the subsequent steps used to backcross both *Mu* lines to the dwarf maize line, GASPE Flint (Garnett et al., 2013) and the common maize inbred B73.

3.2 Materials and methods

3.2.1 Mutant stocks and plant growth conditions

Seven independent *Mu* transposon mutants for *ZmAMF1;1* and 10 independent mutants for *ZmAMF1;2* were isolated and imported from the transposon resource, Trait Utility System for Corn (TUSC, Dr. Bob Meeley, DuPont Pioneer, Johnson Iowa, US). Multiple seeds per line were planted and selected for *Mu* insertions. As the seeds were imported, the first selection occurred within quarantine containment at the University of Adelaide Plant Research Centre. The glasshouse had day and night temperatures set at 28°C and 25°C respectively and supplemental lighting by 1000 watt metal halide lamps provided from 5:00 am to 9:00 am and 5:00 pm to 9:00 pm. Lights in the growth chamber were turned on from 7:00 am to 9:00 pm, and the light intensity was maintained at 400 μmol m^{-2} s^{-1} at canopy level. The temperature of the chamber was 28°C in the day and 25°C at night. The humidity in the chamber was 80% in the day and 50% at night. Before planting, seeds were surface sterilized by submerging in 70% (v/v) ethanol for 1 min followed by soaking into 0.5% (v/v) sodium hypochlorite for 20 min. Seeds were then washed

5 times in reverse osmosis (RO) water. To help seeds germinate after surface sterilization, seeds were soaked into RO water with aeration using an air stone and pump for 4 h. Osmocote Premium Potting Mix (Scotts) which contains a 4-month slow release fertilizer was used as a potting mix. B73 and TUSC lines were planted in 290 mm square × 300 mm deep pots, and GASPE was planted in 183 mm square × 240 mm deep pots. All plants were watered daily or as necessary to retain sufficient moisture in the pots. When seedlings were at the 3-leaf stage, Aquasol Soluble Fertilizer (total nitrogen 23% (w/w), total phosphorus 3.95%, total potassium 14%) was used to apply to both the potting mix and surface of the plants. When reproductive organs emerged Aquasol fertilizers were applied again. As plants developed, tissue samples were collected for genotype analysis. At the end of the growth cycle, cobs were allowed to dry on the plant and then harvested.

3.2.2 TUSC lines crossing

3.2.2.1 TUSC lines backcrossing

Backcrossing was conducted by collecting pollen from either B73 or GASPE to apply on the silks of each TUSC line. As TUSC lines predominantly come from different backgrounds, the silking time was found to vary from 2 -3 months after planting. To overcome the differences in TUSC silking times, the first backcross with B73 required B73 plants to be planted 4 weeks before each TUSC planting, and then was planted twice a week for 3 weeks after the planting of the TUSC lines. As GASPE has a short life cycle, which is about 60 days, the first planting of GASPE occurred 3 weeks after the initial TUSC planting, which then continued 3 times per week until 8 weeks after the TUSC lines were planted. To avoid pollen

contamination, Tassels of TUSC lines were removed before they started to produce pollen, and cobs were covered with bags when the silks emerged. Pollination was carried out between 10:00 and 11:00 am in the morning. When the silks began to shrink, pollination was considered complete. When pollination finished, watering continued until plants began to senesce. Thereafter, plants were ultimately left to dry until leaves and stalks were fully senesced and seeds felt hard for harvesting.

In the second backcross, B73 plantings started 4 weeks before the backcrossed TUSC lines were planted and then twice a week until 3 weeks after TUSC lines planting. GASPE pollen donors were planted at the same time of backcrossed TUSC lines continuing for another 8 weeks after the initial TUSC line planting. Pollination was carried as described in first backcrossing. In the third backcross, the backcrossed TUSC lines showed more similar flowering and silking times to the B73 and GASPE line. For the third GASPE backcross, GASPE seeds were planted 1 week earlier than the backcrossed TUSC lines, continuing every second day for 4 weeks after TUSC lines planting. In the B73 backcrosses, B73 was planted 2 weeks earlier than TUSC lines, and the planting continued with one pot every second day until 3 weeks after TUSC lines planting.

3.2.2.2 TUSC lines self-crossing

Self-crossing involved collection of individual plant pollen which was then applied to its silks as they emerged. The TUSC line tassels were covered with bags before they produced pollen. When silks emerged, the cobs of TUSC lines were also covered with paper bags. Pollen was collected by tapping anthers to disperse pollen into the bags. The homozygous mutants had poor tassel development and

pollen shedding, which delayed the process to collect enough seeds to conduct experiments.

3.2.3 DNA extraction and *Mu* transposon genotyping

After each backcrossing, DNA was isolated from multiple seedlings of TUSC lines (on average 15 seedlings were tested. Seedling DNA was purified (see below) and tested by PCR for the presence of the *Mu* insertion. Heterozygotes, containing the *Mu* insertion were allowed to grow to be backcrossed or selfed. After three backcross events, positive *Mu* genotypes were selfed and then the subsequent seed genotyped (20 seeds) to identify homozygous events.

DNA extraction was done using a modified extraction method of Edwards (1991). Fresh leaf tissue was collected in a 1.5 ml microfuge tubes, and Extraction buffer (200 mM Tris-HCl pH 7.5, 250 mM NaCl, 25 mM EDTA, 0.5% SDS) added and ground for 2 min at 1500 x rpm in a Genogrinder (SPEX® SamplePrep). The mixture was centrifuged at 13,000 x *g*, 4°C for 15 min and the supernatant transferred to a new microfuge tube. The supernatant was then mixed with equal volume of 100% isopropanol and incubated for 15 min at room temperature. The mixture was then centrifuged at 13,000 x *g*, 4°C for 15 min to pellet insoluble DNA. The DNA pellet was washed by 75% (v/v) ethanol and dried in a 37°C oven. Once dry, the pellet was resuspended in 50 µl of sterile milli- Q water.

To identify the location of the *Mu* insertion, a universal PCR primer, 9242 was used. 9242 has been previously designed against the conserved TIRs of the *Mu* transposon (Chuck et al., 1998). 9242 is located 71 bp into the TIR, and possess a

region of high sequence identity. The 9242 primer can allow amplification from both the left and right TIRs of the *Mu* transposon (McCarty and Meeley, 2009). For *ZmAMF1;1* TUSC lines, the gene specific primer 157308 and 157309 were designed against upstream and downstream regions of *Mu* insertion respectively (Bob Meeley, DuPont Pioneer). With the PCR, the PCR primers 157308 and 9242 or 9242 and 157309, enable the identification of the *Mu* insertion and its 5' and 3' flanking regions. To identify homozygous *Mu* insertion lines, the upstream and downstream PCR primers *ZmAMF1;1 F-g* and *ZmAMF1;1 R-g* were designed (Figure 3.3B).

PCR primers, 157313 and 157316 were designed for *ZmAMF1;2*. Each was designed to be upstream and downstream of the *Mu* insertion (Bob Meeley, DuPont Pioneer). PCR primer combinations of 157313 and 9242 or 9242 and 157316 allowed for the amplification of the flanking regions of the *Mu* insertion. Homozygous *Mu* lines were identified by PCR using 157313 and 157316 (Figure 3.3C). For all PCR genotyping experiments, the PCR was carried with an initial denature of 95°C for 3min, followed by 35 cycles of 95°C for 15s, 60°C for 15s and 72°C for 1 min. At the end of the 35 cycles a final extension occurred at 72°C for 5 min.

3.2.4 *Mu* insertion location analysis

PCR products were purified using the ISOLATE II PCR and Gel Kit (Bioline) and then cloned into the pGEM T-EASY vector (Promega) following the manufacturer instructions. All cloned constructs were transformed into XL I-BLUE *Escherichia coli* competent cells. Plasmid extraction for sequence analysis was completed using the ISOLATE II Plasmid Mini Kit (Bioline) according to the manufacturer's

instructions. All constructs were first verified by restriction enzyme digestion and then sent for sequencing by genotyping primers mentioned in 3.2.3 (AGRF, Sydney). *Mu* insertion location was analyzed by alignment against *ZmAMF1;1* and *ZmAMF1;2* predicted gene sequence from Phytozome by Geneious 6.0.6, and partial sequence from sequencing results of the *Mu* transposon was aligned using BLAST (NCBI) to identify the category of *Mu* transposon.

3.2.5 RT-PCR

3.2.5.1 Plant growth

TUSC seeds for ADL112, 114, 119 and the wild-type GASPE were surface sterilized with 70% (v/v) ethanol for 1 min, then submerged in 0.5% (v/v) sodium hypochlorite (Chem-supply) for 20 min. Seeds were rinsed with reverse osmosis water 5 times, and then soaked in reverse osmosis water with aeration for 4 h. Seeds were placed into prewashed vermiculite to germinate in a temperature-controlled growth chamber for 4 days. Germinated seedlings (~1 cm tall shoots) were transferred to a recirculating hydroponics system. The hydroponics system consisted of two 70 L black plastic tanks, one tank to support the plants and receive nutrient solution and the second placed below to store nutrient solution that drained from the top tank. Each seedling was placed on a mesh collar inside a 30 mm wide pvc tube that rests inside a larger pvc pipe to keep the plants elevated and the roots separated inside the tank. Seedlings were provided nutrient solution via a submerged pump in the bottom tank which filled the top tank in 10 minutes. After 5 minutes, the tank pump was turned off and the solution eluted back to the bottom tank. The pump was set to turn off and on every 15 minutes which

provided continuous aeration for the submerged root system. Plants were grown with two nitrogen levels: 0.5 and 5 mM NH_4NO_3, supplemented with basal nutrients, including $MgSO_4 \cdot 7H_2O$ 0.5 mM, KH_2PO_4 0.5 mM, H_3BO_3 25 µM, $MnSO_4 \cdot H_2O$ 2 µM, $ZnSO_4 \cdot 7H_2O$ 2 µM, $CuSO_4 \cdot 5H_2O$ 0.5 µM, $Na_2MoO_4 \cdot 2H_2O$ 0.5 µM, KCl 1.05 mM, Fe-EDTA 0.1 mM, Fe-EDDHA 0.1 mM, K_2SO_4 1.25 mM, $CaCl_2 \cdot 2H_2O$ 0.25 mM, $CaSO_4 \cdot 2H_2O$ 1.75 mM (pH 6.5). Nutrient solutions were changed weekly.

3.2.5.2 RNA extraction and RT-PCR

Plants were harvested on the 15th day after the radical emerged from the seeds for ADL 112 and 119, and 15th and 26th day for ADL 114, under both 0.5 and 5 mM NH_4NO_3 growth condition. RNA was extracted from roots of ADL 112, 114 and 119 plants. Each TUSC line mutant had a GASPE control grown at the sample time to collect RNA samples. Plant total RNA was extracted by Spectrum™ Plant Total RNA Kit (Sigma). 100 mg ground root tissue was used for RNA extraction following the manufacturer's instructions. RNA integrity was checked on a 1% w/v agarose 1X TAE gel. Primers (EF1A F1 and EF1A R1) were designed against the maize elongation factor gene *ZmElF1* (GRMZM2G154218) across an intron span to test for potential genomic DNA contamination in all cDNA samples. Prior to the RT step, potential genomic DNA contamination was removed by DNase I treatment with the RNase Free DNase I kit following the manufacturer's instructions (New England Biolabs).

For ADL 112 and 114, primers 157308, 157309 and the universal *Mu* primer 9242 were used to characterize the *Mu* insertion in TUSC line transcripts. Primers located in the 3' CDS (*ZmAMF1;1 qPCR F1*, *R1*) were also used to check for transcript expression.

For ADL 119, primer *ZmAMF1;2 F3*, *R3* and 9242 were used to check for the presence of the transposon. Primers located in the 3' CDS (*ZmAMF1;2 qPCR F1*, *R1*) were also designed to check cDNA abundance.

The PCR program for cDNA amplification was as follows: 1) initial denature of 95°C for 1min, 2) followed by 35 cycles of 95°C for 15s, anneal at (60°C for 157308, 9242 and 157308, 157309; 58 °C for 9242 and *ZmAMF1;2 R3*, *ZmAMF1;1 qPCR F1* and *R1*, *ZmAMF1;2 qPCR F1* and *R1*; 55 °C for *ZmAMF1;2 F3* and *R3*) for 15s and an extension at 72°C for 30s. At the end of the 35 cycles a final extension occurred at 72°C for 5 min. PCR products were validated (size) on 1% (w/v) 1 X TAE agarose (Bioline) gel.

3.2.6 TUSC lines phenotype comparison with GASPE

Seeds surface sterilization method of ADL 112, 114, 119, double mutant and GASPE was described as 3.2.1. Seeds were germinated in potting mix (Grange Garden Health, nitrogen ~ 200 mg/L, phosphorous ~ 8-40 mg/L, potassium ~ 50 mg/L) in 290 mm square × 300 mm deep pots in a growth chamber. Plants were grown in temperature-controlled growth chamber, and growth environment in the growth chamber was same as described in 3.2.1. Plants randomly placed in the growth chamber and were watered daily or more according to the demand of plants. The phenotype capture was conducted before the reproductive stage (on the 22nd day after planting). Plant height, leaf number and stem thickness were captured. Plant height was determined by measuring from the surface of the potting mix to the top most extended leaf. Stem thickness was measured between the 1st and 2nd leaf. Leaf numbers were counted of leaf at least 70 to 80% extended.

3.3 Results

3.3.1 Importation and release of TUSC lines from quarantine

Seven independent TUSC lines for *ZmAMF1;1* and 10 independent TUSC lines for *ZmAMF1;2* were imported from Dr. Bob Meeley, DuPont Pioneer (Johnson Iowa, US) in Dec 2013. All TUSC lines were given importation names, which will be used in this chapter (Table 3.1). Prior to their arrival in Australia, each line was PCR genotyped for the location of the *Mu* transposon (Bob Meeley, personal communications). In the *ZmAMF1;1* TUSC lines, *Mu* transposons were predicted to be in the 5' UTR of two lines while the other five lines were predicted to possess a *Mu* insertion in exon1 (Table 3.1). In the ten lines for *ZmAMF1;2*, six had a predicted *Mu* transposon insertion in the promoter region, while the remaining four lines had a *Mu* transposon in the first exon (Table 3.1)

TUSC lines were grown in a glasshouse under quarantine (QC2 containment) at the Waite Campus of the University of Adelaide. At flowering, both silks and tassels were bagged and then selfed using the collected pollen. Pollination occurred between 10:00 am to 11:00 am. In total, six *Mu* lines of *ZmAMF1;1* (ADL 110 to 115) and nine *Mu* lines of *ZmAMF1;2* (ADL 117 to 124, and 126) were selfed and harvested seed successfully released from quarantine. The cob shapes of the TUSC lines varied significantly from each other (Figure 3.1, 3.2).

PCR on isolated genomic DNA was used to genotype each TUSC line before and after self-crossing during the initial quarantine entry period. The universal primer 9242, previously designed to bind 71bp into the conserved TIRs of the *Mu* transposon (Figure 3.3A), was used to assist amplifying both the 5' and 3' ends of

the *Mu* terminal repeat regions (Chuck et al., 1998). For *ZmAMF1;1* TUSC lines, *Mu* insertions were identified by PCR with primer combinations of 9242 with 157308 (-392 bp) or 157309 (+304 bp) (Figure 3.3B). The homozygous *ZmAMF1;1* TUSC lines were identified by PCR with the *ZmAMF1;1 F-g* (-484 bp) and *ZmAMF1;1 R-g* (+487 bp) primers (Figure 3.3B). Similarly, *Mu* insertions in *ZmAMF1;2* TUSC lines were identified by PCR using the 9242 primer with 157313 (-689 bp) or 157316 (+147 bp), while the homozygous lines were identified using PCR primers 157313 (-689 bp) and 157316 (+147 bp) (Figure 3.3C). Using these primer sets, ADL 112 and 114 were genotyped as homozygous *ZmAMF1;1 Mu* events (Figure 3.4). For *ZmAMF1;2*, ADL 119, 121 and 123 were identified as homozygous lines for the *Mu* transposon (Figure 3.5). Although the insert transposon is relatively small (~1.4 kb) it was not possible to amplify across the insertion site when testing for homozygous lines. Attempts were made with long-read PCR where extended extension times were used but no product was amplified. It is possible that multiple transposons may be present at the identified insertion sites.

3.3.2 TUSC backcrossing with GASPE and the selection of homozygous lines

To eliminate the genetic background complexity of the TUSC parental lines, a backcrossing program was initiated with the maize inbred B73 and the dwarf maize GASPE. TUSC lines were finished three times of backcrossing with GASPE and B73. Unfortunately, facility access and timing limited the self-crossing only to the GASPE crossed TUSC lines. With each successive backcross, the phenology of the lines (time to tassel, set cob and the production of silks) increasingly resembled that of the GASPE parents (Figure 3.6). Wildtype GASPE produced tassels, cobs and silks around 23, 25 and 33 days after planting, respectively. Initially, ADL 112

developed tassels, cobs and silks 56, 68, 73 days after planting, respectively. At the conclusion of three backcrosses to GASPE, ADL 112 tassel and cobs developed around 40 days after planting while the silks occurred approximately 45 days after planting. With ADL 114, tassel, cob and silks developed at 93, 93 and 103 days, respectively, and after three backcrosses to GASPE, the tassels, cobs and silks developed around 34, 34 and 41 days, respectively. In ADL 119, the tassel, cob and silks initially developed at 54, 56 and 65 days after planting but after three backcrosses to GASPE they were around 43, 39 and 45 days, respectively. Apart from key changes in the reproductive developmental stages of the plants, the TUSC cob phenotypes became less abnormal and varied to that similar to the GASPE parents (Figure 3.7).

Upon completion of the three successions of backcrosses to GASPE, the TUSC lines were self-pollinated to select for homozygous TUSC *Mu* lines. PCR genotyping identified that ADL 112, 114 and 119 were all homozygous for the *Mu* insertion (Figures 3.8-3.10).

3.3.3 TUSC *Mu* insertion sequence mapping and verification

To confirm the location of the TUSC *Mu* insertion, PCR genotyping of ADL 112, 114 and 119 was completed. DNA fragments amplified using PRC primers described in 3.2.3 were cloned individually, sequenced and aligned against genomic sequence of *ZmAMF1;1* and *ZmAMF1;2* (Phytozome). ADL 112 amplified a 506bp PCR product with primer 157308 and 9242 and a 377bp product with primer 9242 and 157309. ADL 112 was found to have a *Mu* inserted in the first exon (Figure 3.11) which resulted in a 10 bp duplication of the targeted gene sequence. In ADL 114, a 421bp

PCR product was amplified by primer 157308 and 9242, while 478bp product with primer 9242 and 157309. ADL 114 was found to have *Mu* insertion in 5'UTR (Figure 3.12), resulting in a 10 bp duplication in the gene sequence. ADL 119 had a 371bp PCR product with primer 157313 and 9242, and 470 bp product with primer 9242 and 157316. In ADL 119, the *Mu* was identified in 5'UTR (Figure 3.13), but instead of an insertion, the *Mu* also resulted in a 8 bp deletion at the insertion site. When compare the sequence of the ADL 119 PCR product to the genomic sequence of *ZmAMF1;2* annotated in the Phytozome database, a 177 bp section was missing in the upstream region of the insertion site. Partial sequence analysis of the *Mu* transposon using BLAST (NCBI), confirmed the 1.4 kb *Mu1* transposon had inserted into 112, 114 and 119 (Lillis and Freeling, 1986).

3.3.4 RT-PCR on TUSC line cDNA

To determine the impact of transposon insertion on gene expression, reverse transcription PCR (RT-PCR) was completed on ADL 112, 114, 119 and GASPE cDNA samples. With primers 157308 and 9242, transcript that included a component of the transposon was identified in ADL 112 and 114. Using primers 157308 and 157309 which flank the transposon, no product was amplified in either ADL 112 or 114 but was present in the GASPE control. Using PCR primers that targeted the 3'-end of the transcript, a PCR product was identified for ADL 112, 114 and GASPE (Figure 3.14). These results indicated that the transposon insertion disrupted the 5'-end of the transcript, while full-length transcript could be generated and then amplified from the 3'-end in ADL 112 and 114. At this stage it is uncertain whether the TUSC mutation disrupts potential splicing in ADL 112 and 114 resulting in a defective but transcribed transcript.

Similarly in ADL119, the primer 9242 with *ZmAMF1;2 R3* amplified a cDNA product, while primers *ZmAMF1;2 F3* and *R3* did not amplify a product but could in the GASPE control (Figure 3.15). Consequently, the transposon is still present in ADL 119 transcript, and the impact on protein level needs to be further elaborated.

3.3.5 TUSC line growth relative to GASPE

To understand the impact that a loss of ZmAMF1;1 and/or ZmAMF1;2 has on plant growth, plants were grown under controlled conditions and growth phenotypes characterized. Plant height, leaf number and stem thickness were compared between ADL 112, ADL 114, ADL 119, the double mutant (ADL 112 × ADL 119) and GASPE up to the onset of the reproductive stage. ZmAMF1;1 mutants (ADL 112 and ADL 114) produced more leaves than GASPE. ADL 114 was taller and had thicker stems than GASPE. In contrast, the ZmAMF1;2 mutant (ADL 119) showed no significant difference in plant growth compared to GASPE (Table 3.2). Nevertheless, when there was a loss of both *AMF* genes in maize, plants grew better than GASPE, with greater plant height, stem thickness and leaf numbers than the GASPE control (Table 3.2).

Table 3.1 TUSC (Trait Utility System for Corn) lines imported for *ZmAMF1;1* and *ZmAMF1;2*.

Insertion sites were based on the start of the gene coding region (+1). ADL= Adelaide importation number.

Gene	Public code	Importation name	Predicted insertion site
ZmAMF1;1	BT94 9 F-11	ADL110	+12, exon1
	BT94 90 E-08	ADL111	+202, exon1
	PV03 102 A-06	ADL112	+52, exon1
	PV03 20 F-06	ADL113	+52, exon1
	PV03 51 B-04	ADL114	-38, 5'UTR
	PV03 56 H-05	ADL115	-38, 5'UTR
	PV03 79 D-05	ADL116	+2, exon1
ZmAMF1;2	PV03 103 A-05	ADL117	-360, promoter
	PV03 103 F-03	ADL118	+15, exon1
	PV03 55 C-09	ADL119	-410, promoter
	PV03 56 G-03	ADL120	+18, exon1
	PV03 71 C-03	ADL121	+68, exon1
	PV03 71 E-07	ADL122	+68, exon1
	PV03 78 F-04	ADL123	-360, promoter
	PV03 80 C-11	ADL124	-385, promoter
	PV03 97 D-01	ADL125	-385, promoter
	PV03 97 F-05	ADL126	-385, promoter

Figure 3.1 Cob phenotypes of *ZmAMF1;1 Mu* TUSC lines

ZmAMF1;1 TUCS lines were grown in a temperature-controlled quarantine containment glasshouse at the Waite Campus of the University of Adelaide. Panels A (ADL110), B (ADL111), C (ADL112), D (ADL113), E (ADL114) and F (ADL115) represent variability in cob development at harvest across the independent TUSC lines.

Figure 3.2 Cob phenotypes of *ZmAMF1;2 Mu* TUSC lines

ZmAMF1;2 TUCS lines were grown in a temperature-controlled quarantine containment glasshouse at the Waite Campus of the University of Adelaide. Panels A (ADL117), B (ADL118), C (ADL119), D (ADL120), E (ADL121), F (ADL122), G (ADL123), H (ADL124), I (ADL124) and J (ADL126) represent variability in cob development at harvest across the independent TUSC lines.

A


9242
9242
TIR
Mu
TIR
~220bp
~1.4kb
~220bp

B

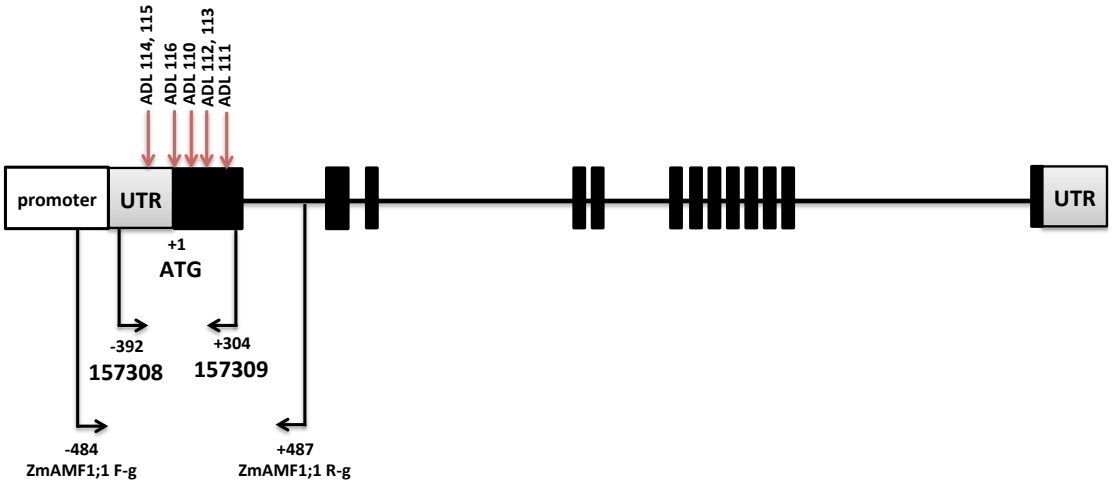
ADL 114, 115
ADL 116
ADL 110
ADL 112, 113
ADL 111
promoter
UTR
UTR
+1
ATG
-392
157308
+304
157309
-484
ZmAMF1;1 F-g
+487
ZmAMF1;1 R-g

C

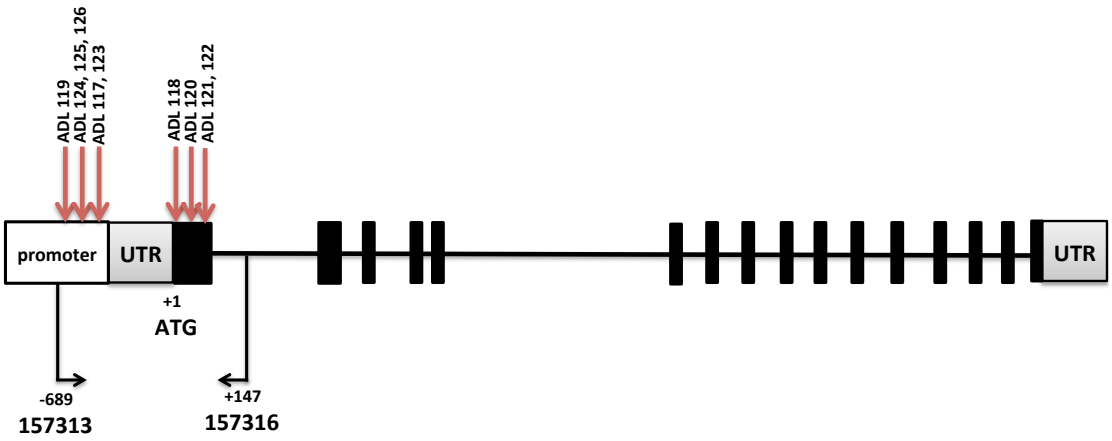
ADL 119
ADL 124, 125, 126
ADL 117, 123
ADL 118
ADL 120
ADL 121, 122
promoter
UTR
UTR
+1
ATG
-689
157313
+147
157316

Figure 3.3 PCR primer locations for transposon genotyping

(A) The universal PCR primer 9242 is designed to bind 71bp into both TIRs of the *Mu* element. (B) Primers (*ZmAMF1;1 F-g*, 157308, 157309, *ZmAMF1;1 R-g*) designed for *ZmAMF1;1* TUSC line genotyping. (C) Primers (157313 and 157316) designed for *ZmAMF1;2* TUSC line genotyping. Exons are shown as black boxes, and introns are shown as black lines. UTRs are shown in grey boxes. Promoter is shown as an empty box. Primer binding locations are shown using black arrows, and the predicted *Mu* insertions are shown using red arrows.

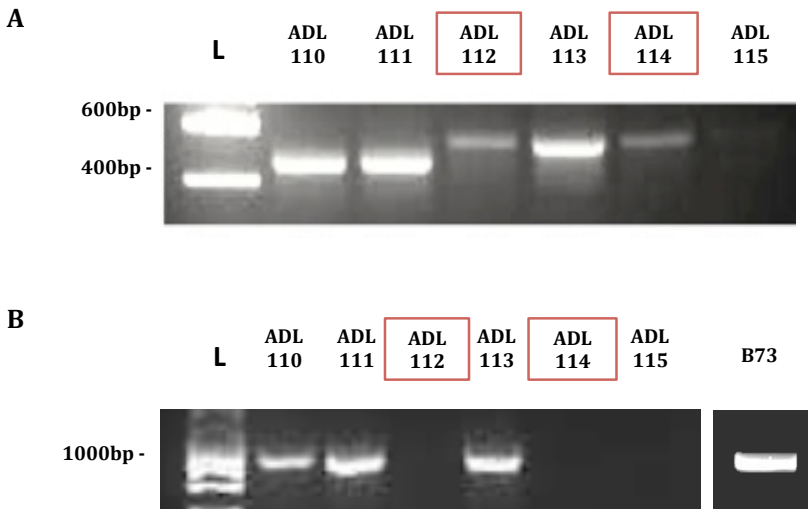

Figure 3.4 PCR genotyping result of *ZmAMF1;1* TUSC lines.

(A) *Mu* insertions were identified in ADL 110, 111, 112, 113, 114 and 115 with the gene specific primer 157308, and the universal *Mu* primer 9242. (B) Selection of homozygous *Mu* TUSC lines determined using the primer combination of *ZmAMF1;1 F-g* and *ZmAMF1;1R-g*. A separate experiment was conducted using B73 DNA as a positive control. No PCR products were identified in ADL 112 or ADL 114 with primer *ZmAMF1;1 F-g* and *ZmAMF1;1R-g*, the remaining lines were assumed to be heterozygous for the *Mu* transposon after the initial selfing. L = Ladder (Hyper Ladder I, Bioline).

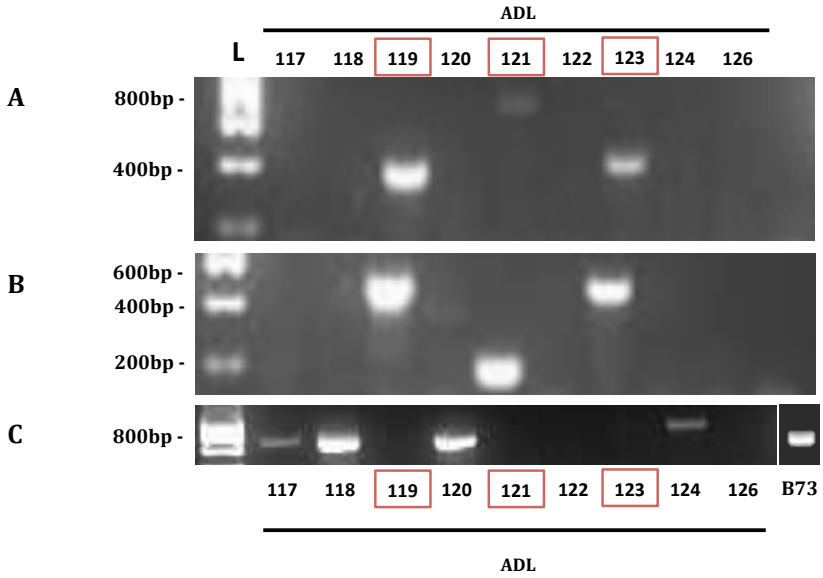

Figure 3.5 PCR genotyping result of *ZmAMF1;2* TUSC lines

(A, B) *Mu* insertions were identified in ADL 119, 121 and 123 with either the gene specific primers 157313 (A), 157316 (B) partnered with the universal *Mu* primer 9242. (C) Selection of homozygous *Mu* TUSC lines determined using the primer combination of 157316 and 157313. A separate experiment was conducted using B73 genomic DNA as a positive control for the expected 800bp product. No PCR products (putative homozygous lines) were identified in ADL 119, ADL 121 and ADL 123 with primer 157313 and 157316. L = Ladder (Hyper Ladder I, Bioline).

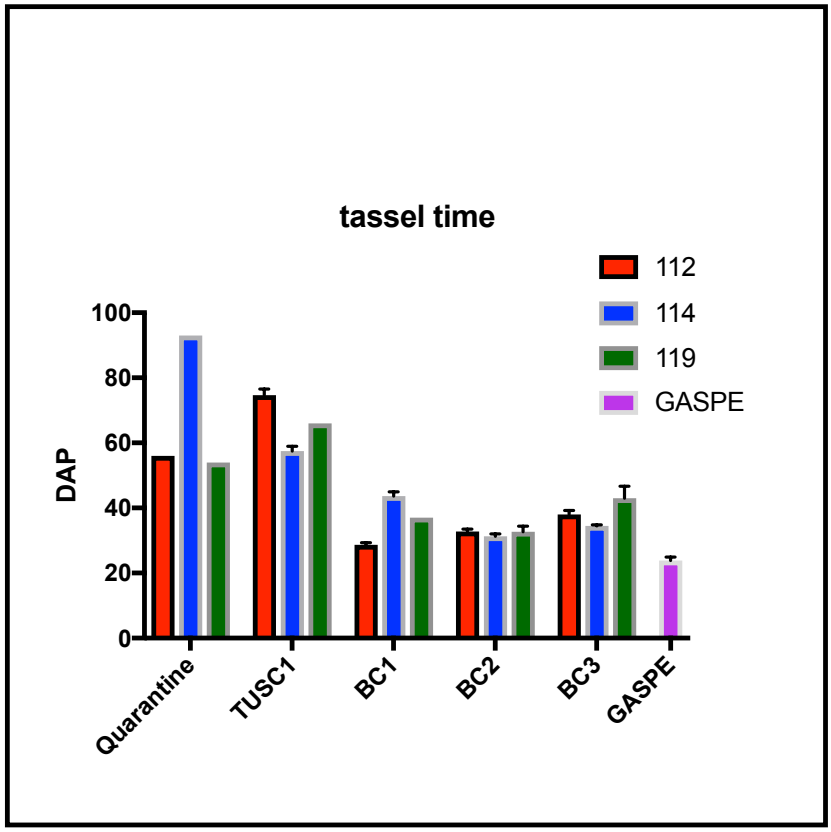
tassel time
112
114
119
GASPE
DAP
100
80
60
40
20
0
Quarantine
TUSC1
BC1
BC2
BC3
GASPE

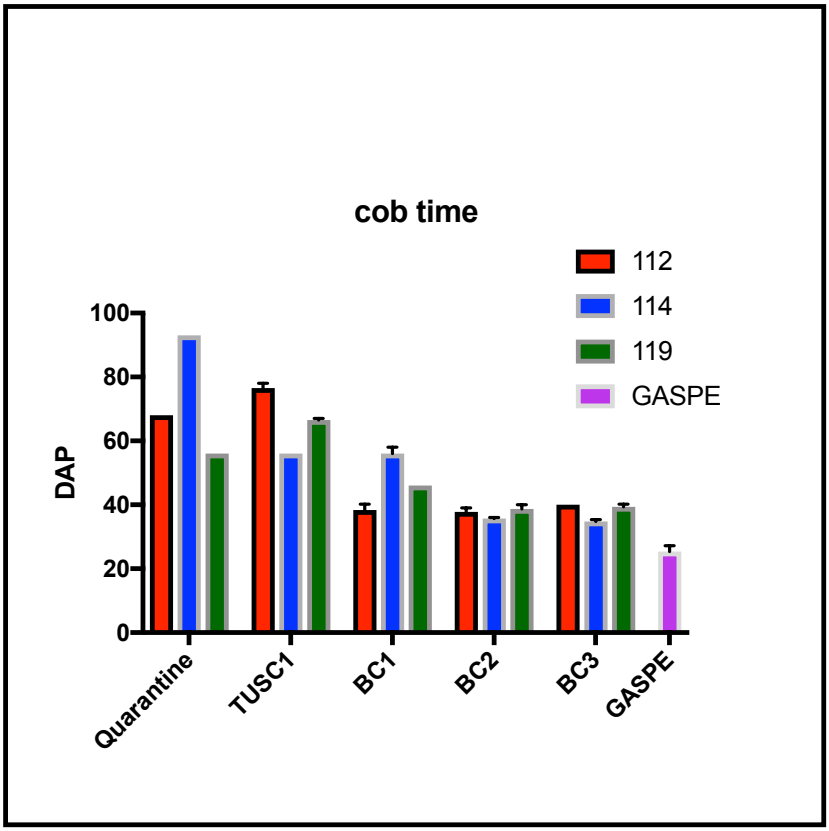
cob time
112
114
119
GASPE
DAP
100
80
60
40
20
0
Quarantine
TUSC1
BC1
BC2
BC3
GASPE

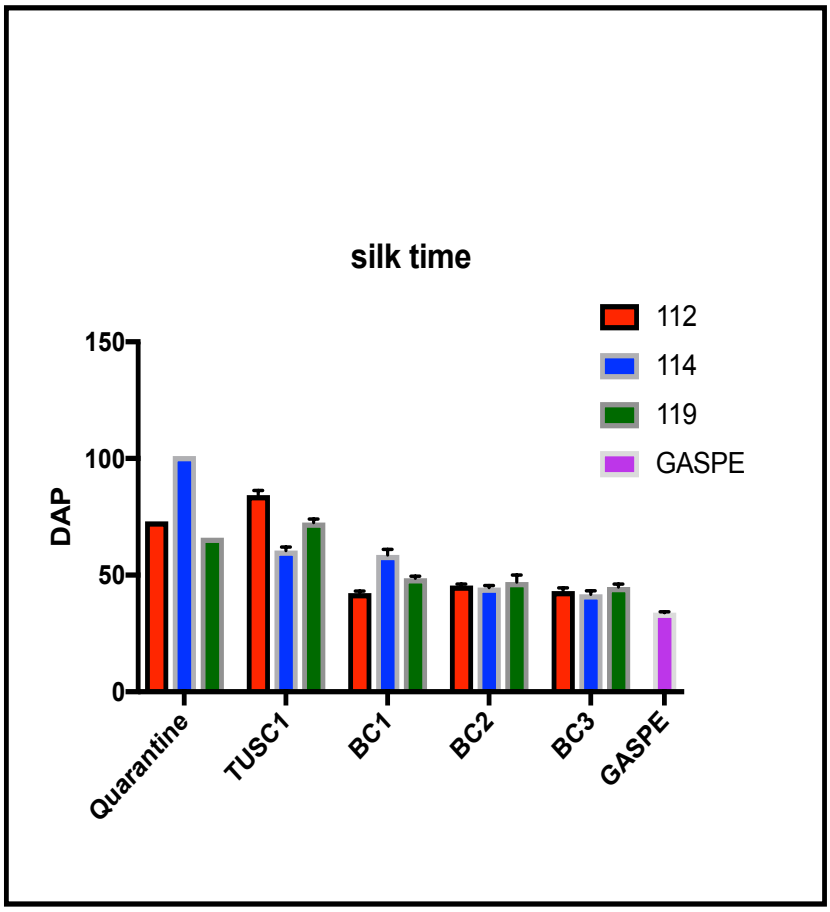

Figure 3.6 Visual changes in TUSC line plant phenology with repetitive backcrossing to GASPE.

Observed time periods from planting to develop tassels, cobs and silks of parental and TUSC backcrossing events. Quarantine = Original TUSC self-crossing in quarantine glasshouse. TUSC1 = after self-crossing in quarantine, BC1 = first backcross with GASPE, BC2 = second backcross with GASPE, BC3 = third backcross with GASPE, GASPE = Wild-type GASPE growth. DAP= day after planting. Values= mean ± SEM (n=1 to 11 plants).

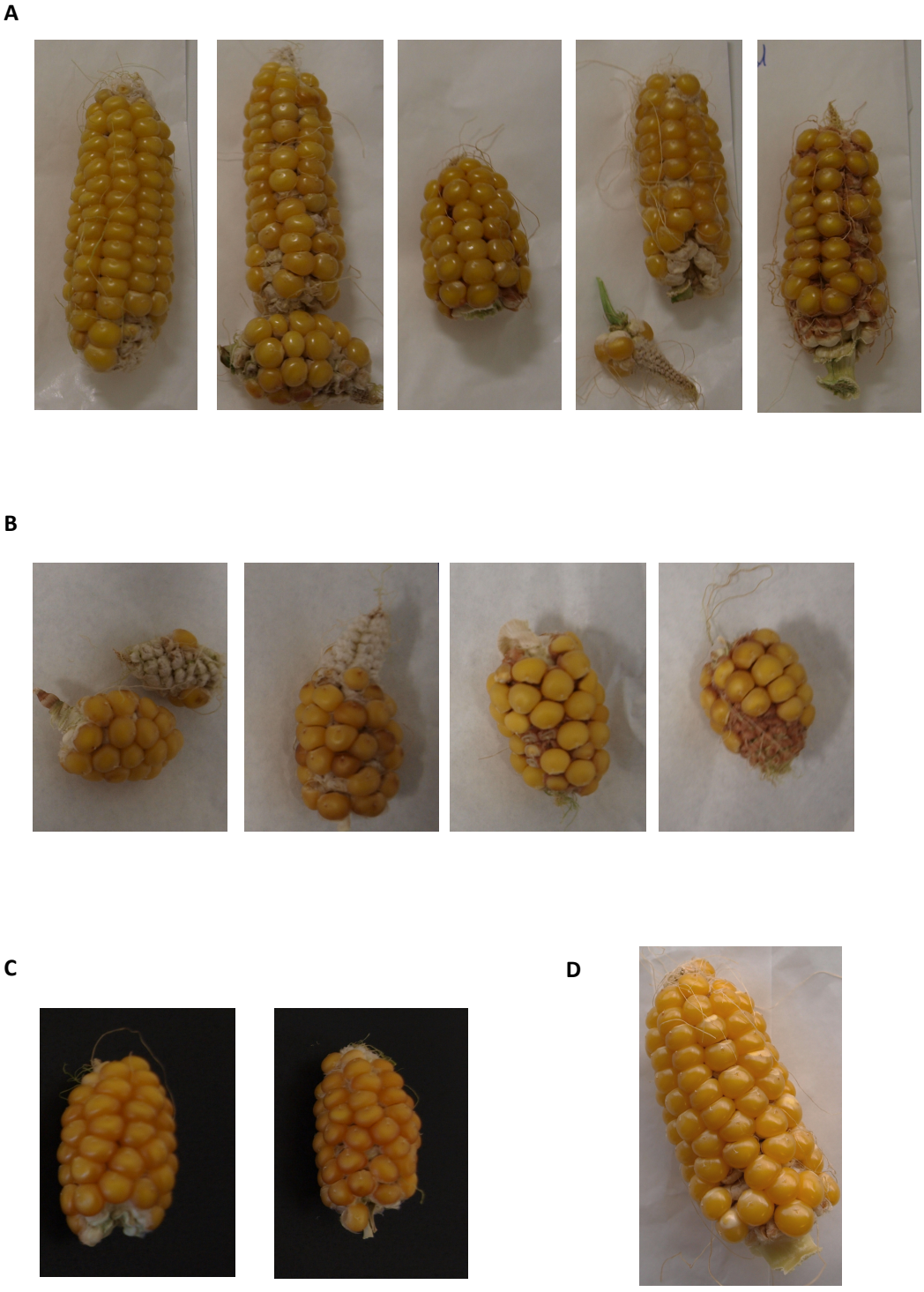

Figure 3.7 TUSC lines cob phenotypes after three times backcrossing with GASPE and first time of self-crossing

A) TUSC ADL 112 BC3SC1 cob phenotype; B) TUSC ADL 114 BC3SC1 cob phenotype; C) TUSC ADL 119 BC3SC1 cob phenotype; D) GASPE cob phenotype.

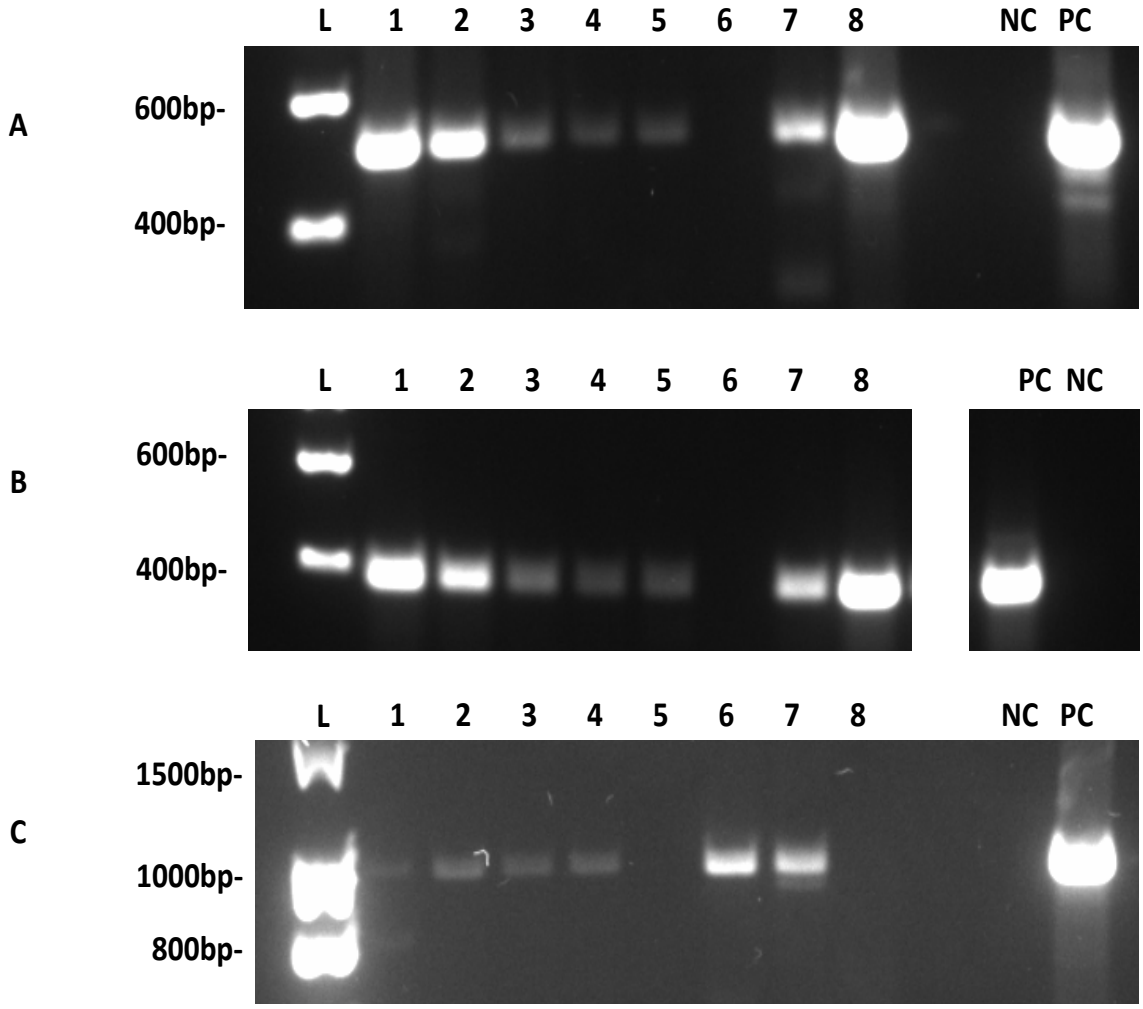

Figure 3.8 Genotypic characterization of BC3SC1 ADL 112 seed and *Mu* localization within the genome.

A, B) PCR amplification of the flanking regions in TUSC ADL 112 DNA using PCR primers 157308 or 157309 with the universal *Mu* primer 9242. PCR products amplified from 7 of 8 plants got same size band with positive control. C) Amplification of genomic DNA using primers *ZmAMF1;1 F-g* and *ZmAMF1;1 R-g.* No DNA band (putative homozygous lines) were identified in samples 5 and 8. Lanes in A-C are: L = Ladder (Hyper Ladder I, Bioline); 1-8 = independent BC3SC1 seedlings, PC = Positive control from DNA purified from the original TUSC line ADL 112 (quarantine imported material); NC= Negative water control.

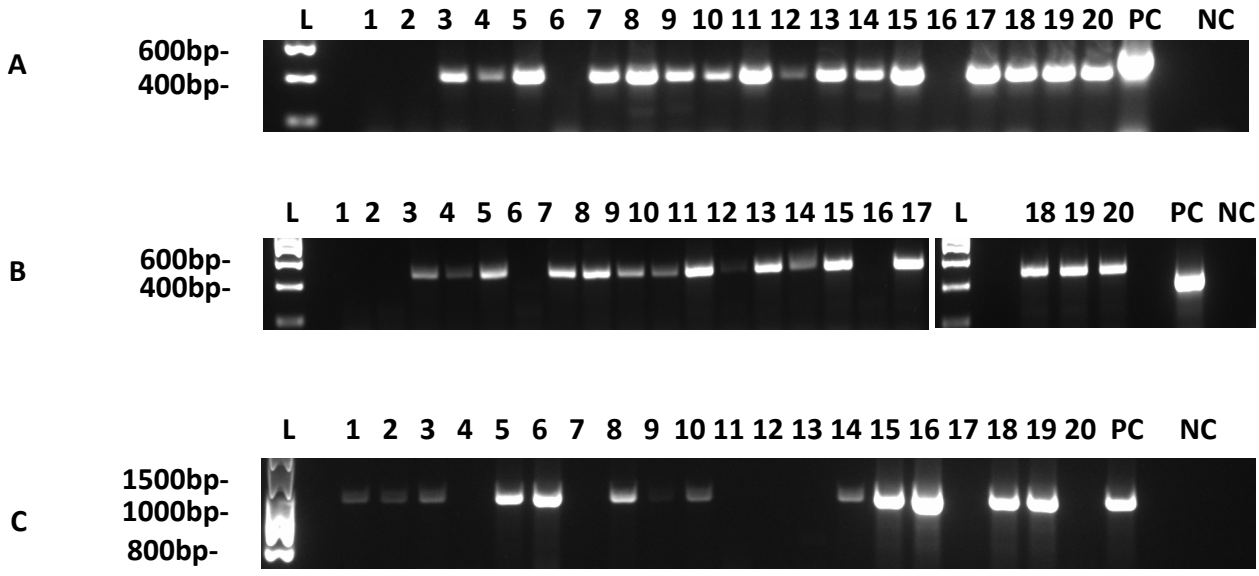

Figure 3.9 Genotypic characterization of BC3SC1 ADL 114 seed and *Mu* localization within the genome.

A, B) PCR amplification of the flanking regions in TUSC ADL 114 DNA using PCR primers 157308 or 157309 with the universal *Mu* primer 9242. Expected 400 to 600bp PCR products were amplified from 16 of 20 plants. C) Amplification of genomic DNA using primers *ZmAMF1;1F-g* and *ZmAMF1;1 R-g*. No DNA band (putative homozygous lines) were identified in samples 4, 7, 9, 11-13, 17 and 20. Lanes in A-C are: L = Ladder (Hyper Ladder I, Bioline); 1-20 = independent BC3SC1 seedlings; PC = Positive control from DNA purified from the original TUSC line ADL 112 (quarantine imported material); NC= negative water control.

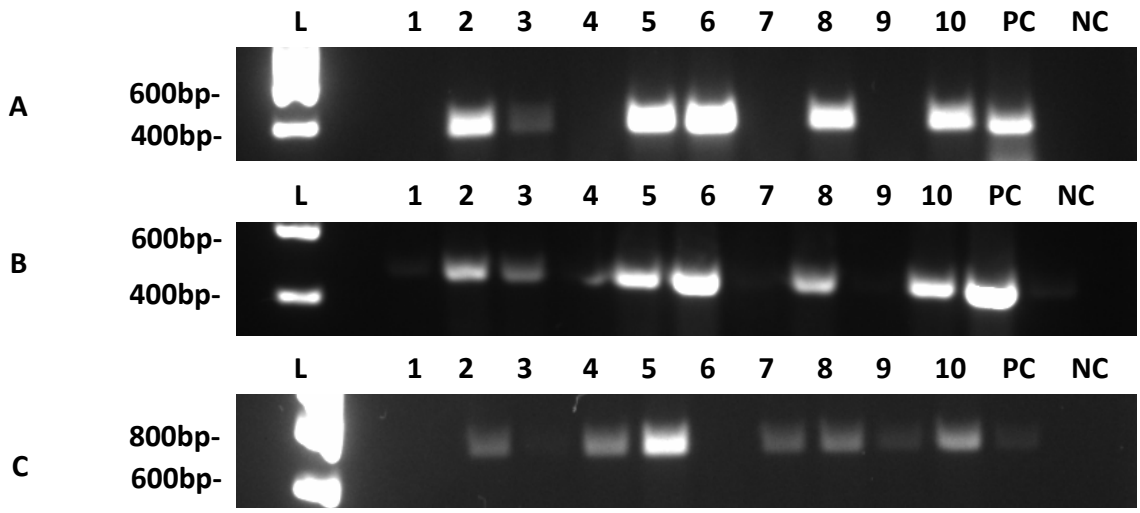

Figure 3.10 Genotypic characterization of BC3SC1 ADL 119 seed and *Mu* localization within the genome.

A, B) PCR amplification of the flanking regions in TUSC ADL 119 DNA using PCR primers 157313 or 157316 with the universal *Mu* primer 9242. PCR products amplified from 6 of 10 plants got same size band with positive control. C) Amplification of genomic DNA using primers 157313 and 157316. No DNA band (putative homozygous lines) were identified in samples 3 and 6. Lanes in A-C are: L = Ladder (Hyper Ladder I, Bioline); 1-10 = independent BC3SC1 seedlings; PC = Positive control from DNA purified from the original TUSC line ADL 119 (quarantine imported material); NC= negative water control.

A

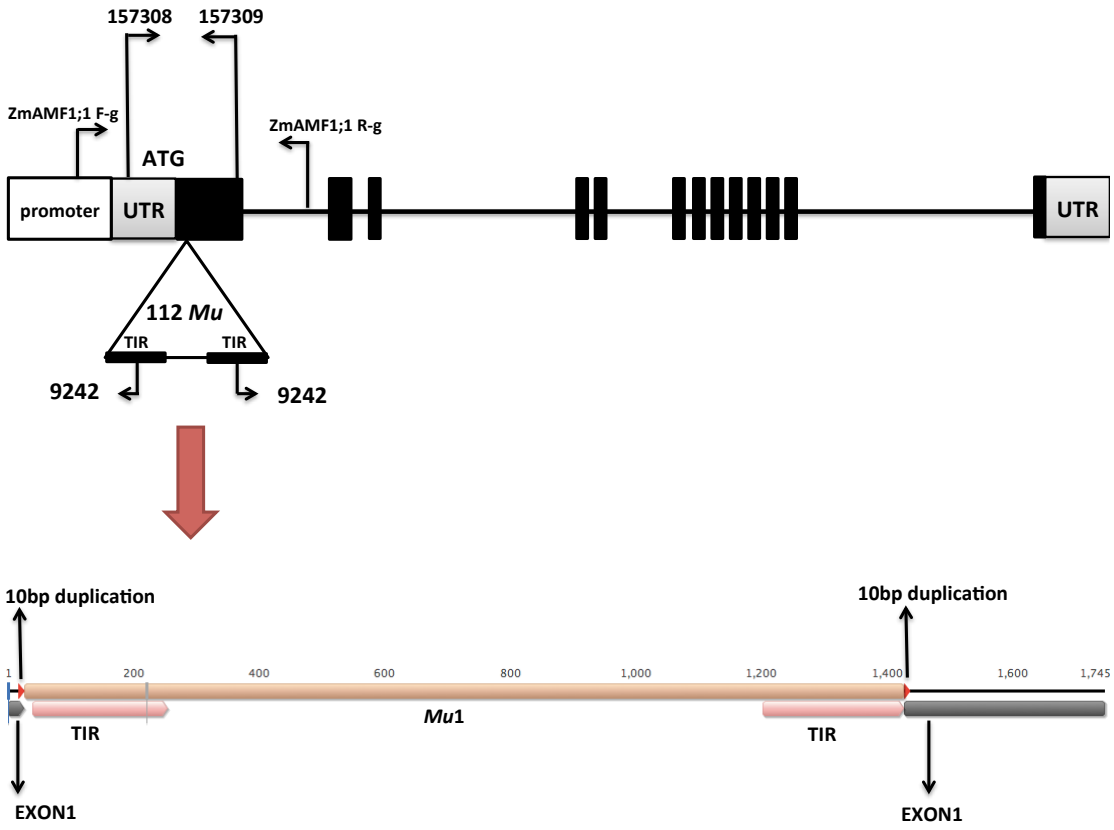

B

'5CTGTCTCCCTCGTTGCAATCACCACGCCGCCGGAGTCCGGAGGGCAGCGTGCGAACTGCGAAACCGAACTC
GGGGAGAGGAAGGAATCTCCTACCAGCCGGCAGCCAACACCCAGCATTCGTGCTCCCGTAGCCTTCGTCGTC
CCCAGCCCCACGGCCGCTGCGTCGCCTTCCCCTCTCGGTCGAAACCACAACGGTCTCTTCCGGCATAACAAT
ATGCACCGAATATTCAGCTCATCCGCTCTCCTATAAAAACGAAGCGCAAATCCAAAAAAAAAAACCCGCCCG
CACGACGCATTGTCCGTTCCGTTTGGACCCATGATATATCTCGCTGGGATCTTGACCGTGCGCGAGACGAAT
CTCCTCGTGCGGTAACCGATACCCCCCAAGTCAAAAATCAGCCCATAAAATTTTTATGGGCGGAGGATCAC
CCGTCGCCGCGAGATAATTGCTATTATGGACGAAGAGGGAAGGGGATTCGACGAAATAGAGGCGATGGCG
TTGGCTT……*Mu*1……..AGAGAAGCCAACGCCAACGCCTCTATTTCGTCGAATCCCCTTCCCTCTTCG
TCCATAATGGCAATTATCT**CCGTCGCCGC**AGTTCAGGACGCGAGCGACGACGGCGCCAGGGTCGTGGTGCT
AGTCGCGGGTTCTCCCGTCGATTCCGCCTCCGATTCCCTCCCTCCTCCCGTTGCGGCGACTCCTGCTCCTGCG
GCGGAGGCCAAGCAGGAGTCGGTGTCGGAGACGGAGGAAACTAAGCAGGCGGCGGCGGCAGCAGCAGCAGC
GGCAGGAGGTGTGCAGGCCATGGCGGTCACCGTAGTGCGGGACGTCGAGACGGGCCTGGACGCGAGCACCA
GCGACCGGGACGGTGACAAGCCTTCCTGGTTCACACCTAA-3'

Figure 3.11 Transposon insertion map of ADL 112 line (A) and detailed sequence analysis (B). *ZmAMF1;1* Gene sequence is shown in black letters, and primer 157308 and 157309 sequence are in red. *Mu* sequence is highlighted in yellow, and 10bp duplication caused by *Mu* insertion is shown in blue letters.

PCR products of ADL 112 event by different primers sets (A) were cloned into pGEM T-EASY vector and transformed into XLI-BLUE competent cell. Plasmids were extracted and verified by restriction digestion. After verification with sequencing, alignment of PCR product from genotyping and *ZmAMF1;1* gene sequence was carried with Geneious 6.0.6 software. Exons are shown as black boxes, and introns are shown as black lines. UTRs are shown in grey boxes. Promoter is shown as an empty box. Primer binding locations are shown using black arrows. *Mu* insertion in ADL 112 event was found in exon1 and caused 10bp duplication (blue letters). Partial sequence from *Mu* transposon was used to BLAST (NCBI) and found the transposon inserted in ADL 112 line is *Mu*1 transposon.

A

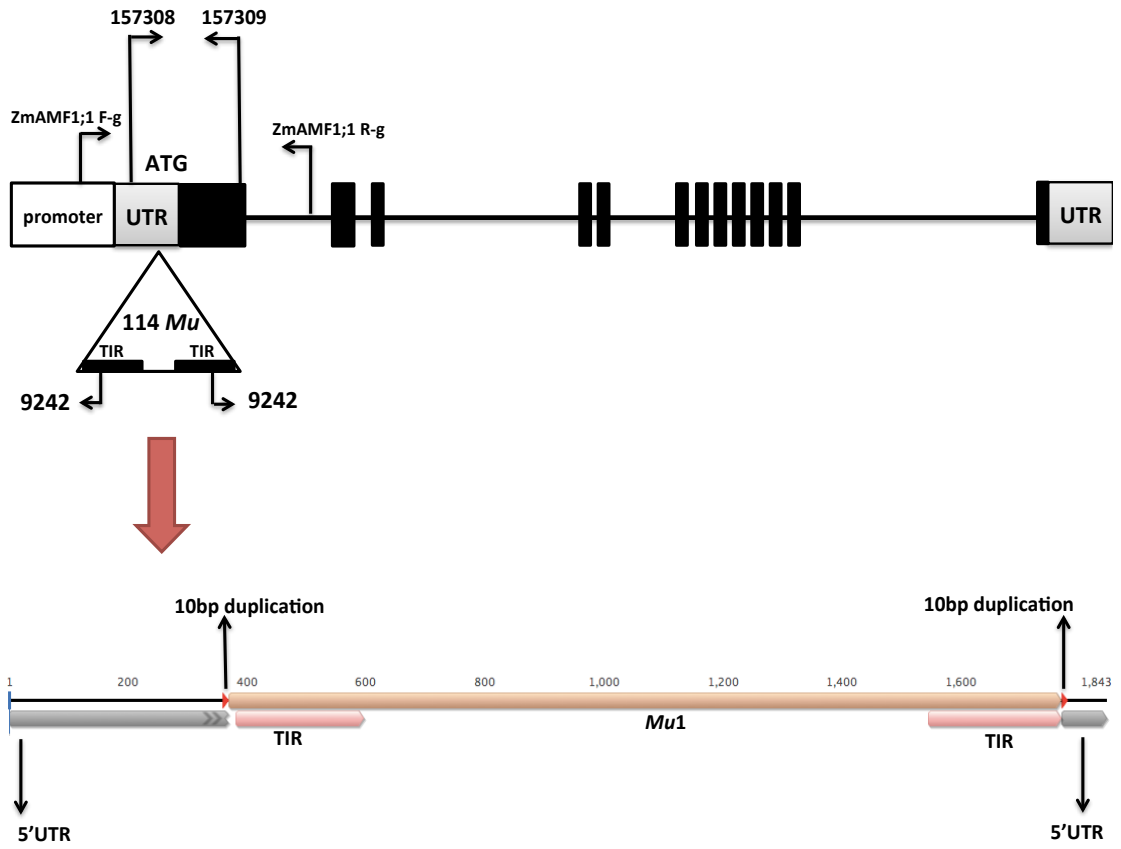

B

'5CTGTCTCCCTCGTTGCAATCACCACGCCGCCGGAGTCCGGAGGGCAGCGTGCGAACTGCGAAACCG
AACTCGGGGAGAGGAAGGAATCTCCTACCAGCCGGCAGCCAACACCCAGCATTCGTGCTCCCGTAGC
CTTCGTCGTCCCCAGCCCCACGGCCGCTGCGTCGCCTTCCCCTCTCGGTCGAAACCACAACGGCCTCTT
CCGGCATAACAATATGCACCGAATATTCAGCTCATCCGCTCTCCTATAAAAACGAAGCGCAAATCCA
AAAAAAAAAAACCCCGCCCGCACGACGCATTGTCCGTTCCGTTTGGACCCATGATATATCTCGCTGG
GATCTTGACCGTGCGAGATAATTGCCATTATAGACGAAGAGCGGAAGGGATTCGACGAAATAGAGG
CGATGGCGTTGGCTTCTCT……*Mu*1……AGAGAAGCCAACGCCAACGCCTCT
ATTTCGTCGAATCCCTTCCGCTCTTCGTCTATAATGGCAATTATCTCTGACCGTGCGCGAGACGAAT
CTCCTCGTGCGGTAACCGATACCCCCCAAGTCAAAAATCAGCCCATAAAATTTTTATGGGCGGAGGA
TCACCCGTCGCCGCAGTTCAGGACGCGAGCGACGACGGCGCCAGGGTCGTGGTGCTAGTCGCGGGTTC
TCCCGTCGATTCCGCCTCCGATTCCCTCCCTCCTCCCGTTGCGGCGACTCCTGCTCCTGCGGCGGAGGC
CAAGCAGGAGTCGGTGTCGGAGACGGAGGAAACTAAGCAGGCGGCGGCGGCGGCGGCAGCACCAGCA
ACAGCGGCAGGAGGTGTGCAGGCCATGGCGGTCACCGTAGTGCGGGACGTCGAGACGGGCCTGGACG
CGAGCACCAGCGACCGGGACGGTGACAAGCCTTCCTGGTTCACACCTAA3'

Figure 3.12 Transposon insertion map of ADL 114 line (A) and detailed sequence analysis (B). *ZmAMF1;1* Gene sequence is shown in black letters, and primer 157308 and 157309 are in red. *Mu* sequence is highlighted in yellow, and 10bp duplication caused by *Mu* insertion is shown in blue letters.

PCR products of ADL 114 event by different primer sets (A) were cloned into pGEM T-EASY vector and transformed into XLI-BLUE competent cell. Plasmids were extracted and verified by restriction digestion. After verification with sequencing, alignment of PCR product from genotyping and *ZmAMF1;1* gene sequence was carried with Geneious 6.0.6 software. Exons are shown as black boxes, and introns are shown as black lines. UTRs are shown in grey boxes. Promoter is shown as an empty box. Primer binding locations are shown using black arrows. *Mu* insertion in ADL 114 event was found in 5'UTR and caused 10bp duplication (blue letters). Partial sequence from *Mu* transposon was used to BLAST (NCBI) and found the transposon inserted in ADL 114 line is *Mu*1 transposon.

A

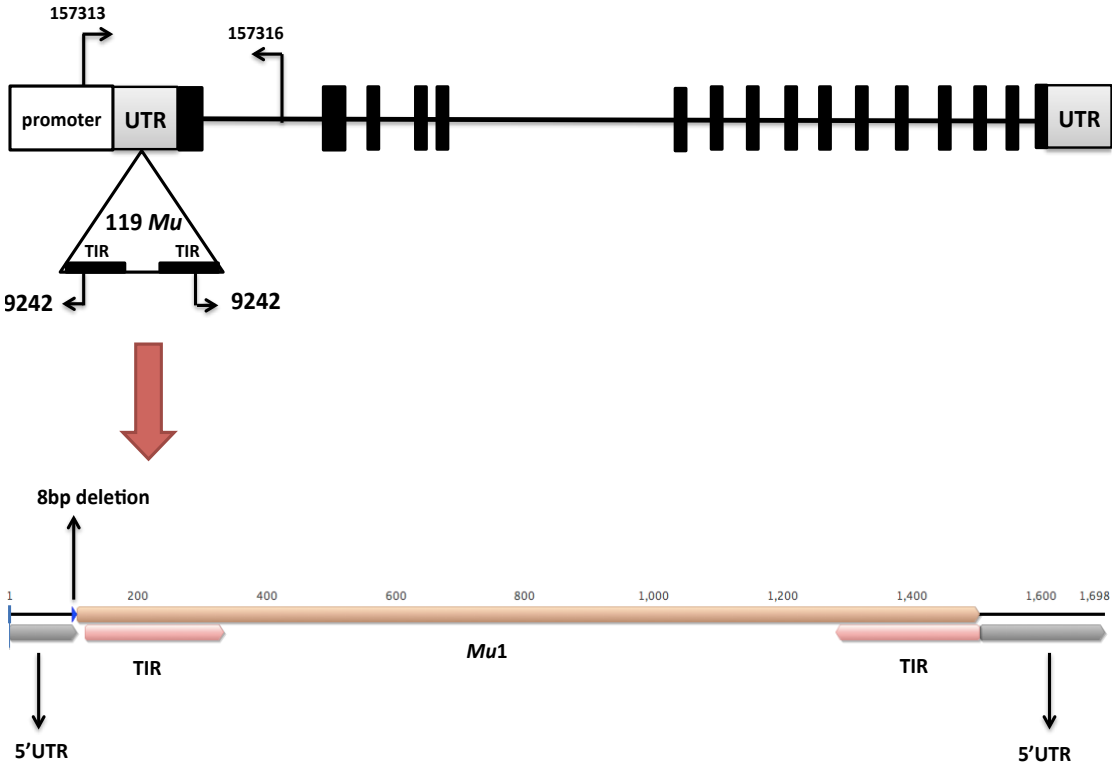

B

'5GCCGTGGCCTTCTCATTCCGTTCAAAACCACAGCACACTAGCTTTAATCCGCATGACTTATATTAATT
CTACAGTATCTTGTCTTTATATATTTCAGCTACAACAGTATTTTATCTTTATAAATTGCAGCTACAGT
CTAACAGCTGGCTTTGACCTTAATTAGAAGGTAACAGCCCGGAAGCAAACAAAAGATAACCCGCCCGC
GCACGCATTACCCATTCCGTTTGGACCCATGAGATTTTTCGCTGGGATGACCGTGCACGAGACGAATCC
CGTTCGGTAACCGATACCCCAAGTCAAGGCGGATCATAGATAATTGCCATTATGGACGAAGAGGGAAG
GGGATTCGACGAAATAGAGGCGTTGGCGTTGGCTCTCT……*Mu*1……AGAGAAGCCAACGCCAT
CGCCTCCATTTCGTCGAATCCGCTTCTCTCTTCGTCCATAATGGCAATTATCTCCAAGTCAAGGCGGAT
CACCCGTCCCGTCAGTCCGTCACCGCAGTCCAGGAAGCGAGCGACGACGACGCCAGGGTCGGTGCTAGT
TGCGGGGTCCCGGTCCGTCGAGTCCGCCTCCGGTTCTCCCCCTCCTCCCGTTGCGGCGACTCCGGCGGCG
GAGACAGAGGAGCCTAAGCAGGAGGAGGAGGAGGAGGCGGCGGCAGCAGCAGCAGGTGTGCA
GGCCATGGCTGTCACGGTAGTGCGGGACGTCGAGACGGGCCTGGACGCGAGCACCAGCGACCGGGACGG
TGACGCCGGGGACAACCCTTCCTGGTTCACACCTAAGAGGTAACCCAACCCATAGCAGAGCTCGATTGA
GTACCATCGCCCTAGACTCGGCTGTGGTAGGCTTGATCT3'

Figure 3.13 Transposon insertion map of ADL 119 line (A) and detailed sequence analysis (B). *ZmAMF1;2* Gene sequence is shown in black letters, and primer 157313 and 157316 are in red. *Mu* sequence is highlighted in yellow, and *Mu* insertion caused 8bp deletion (CGGATCAT) is shown in green letters.

PCR products of ADL 119 event were cloned into pGEM T-EASY vector and transformed into XLI-BLUE competent cell. Plasmids were extracted and verified by restriction digestion. After verification with sequencing, alignment of PCR product from genotyping and *ZmAMF1;2* gene sequence was carried with Geneious 6.0.6 software. Exons are shown as black boxes, and introns are shown as black lines. UTRs are shown in grey boxes. Promoter is shown as an empty box. Primer binding locations are shown using black arrows. The *Mu* insertion in ADL 119 event was found in the 5'UTR resulting in a 8bp deletion (CGGATCAT) at the insertion site. 177 bp fragment was also found missing in the upstream region of the insertion site relative to the predicted *ZmAMF1;2* genomic sequence (Phytozome). Partial sequence from *Mu* transposon was used to BLAST (NCBI) and found the transposon inserted in ADL 119 line is *Mu*1 transposon.

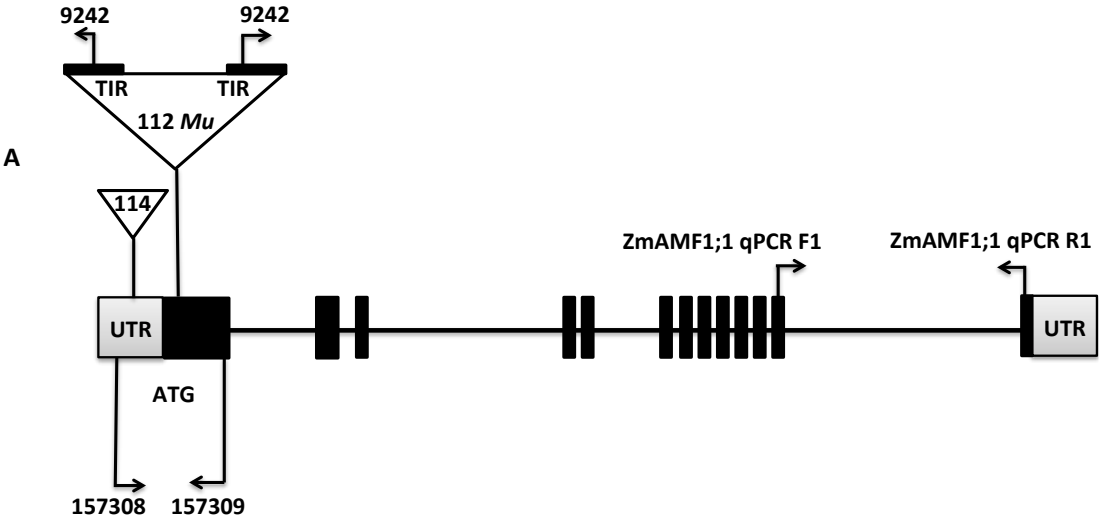
A
9242
9242
TIR
TIR
112 Mu
114
ZmAMF1;1 qPCR F1
ZmAMF1;1 qPCR R1
UTR
UTR
ATG
157308
157309

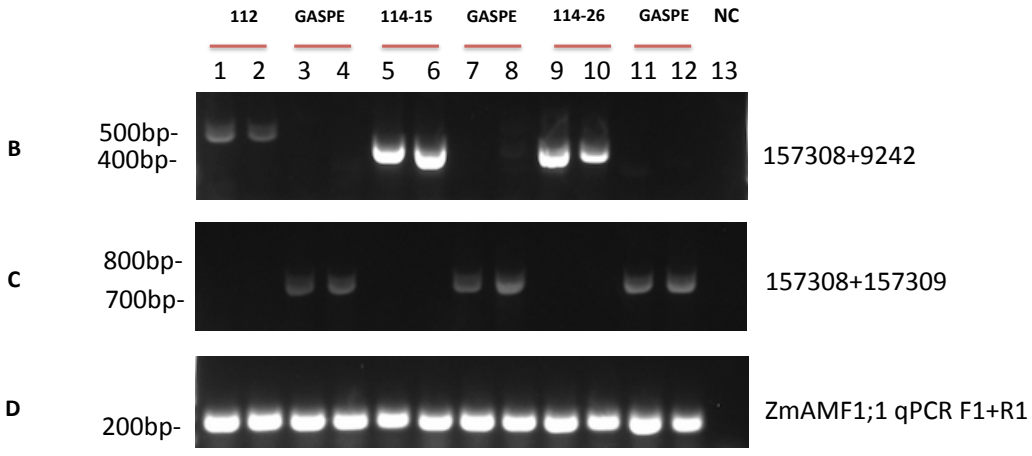
112
GASPE
114-15
GASPE
114-26
GASPE
NC
1 2 3 4 5 6 7 8 9 10 11 12 13
B
500bp-
400bp-
157308+9242
C
800bp-
700bp-
157308+157309
D
200bp-
ZmAMF1;1 qPCR F1+R1

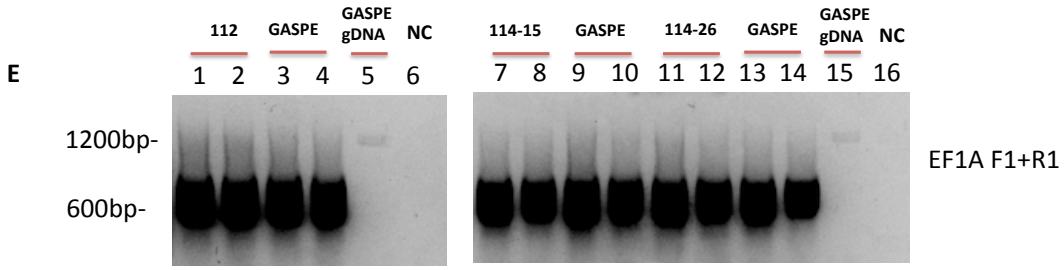
E
112
GASPE
GASPE gDNA
NC
114-15
GASPE
114-26
GASPE
GASPE gDNA
NC
1 2 3 4 5 6 7 8 9 10 11 12 13 14 15 16
1200bp-
600bp-
EF1A F1+R1

Figure 3.14 RT-PCR on ADL 112, ADL 114 and GASPE cDNA

Primers used in RT-PCR were shown in (A), 9242 is a universal *Mu* primer, Exons are shown as black boxes, and introns are shown as black lines. UTRs are shown in grey boxes. Primer binding locations are shown using black arrows. RT-PCR was carried with primer 157308, 9242 (B); 157308, 157309 (C); ZmAMF1;1 qPCR F1, R1 (D). 1,2- ADL 112 cDNA; 3,4 – GASPE control for ADL 112; 5,6- ADL 114 (15 days old plants) cDNA; 7,8- GASPE control for ADL 114 (15 days); 9,10- ADL 114(26 days old plants) cDNA; 11, 12- GASPE control for ADL 114 (26 days); 13- Negative water control. Genomic DNA contamination was checked with primer EF1A F1 and EF1A R1 (E): 1 to 2- ADL 112 cDNA; 3 to 4- GASPE control for ADL 112; 5- GASPE genomic DNA; 6- Negative water control; 7 to 8- ADL 114 (15 days) cDNA; 9 to 10- GASPE control for ADL 114 (15 days); 11 to 12- ADL 114 (26 days) cDNA; 13 to 14- GASPE control for ADL 114 (26 days); 15- GASPE genomic DNA; 16-Negative water control.

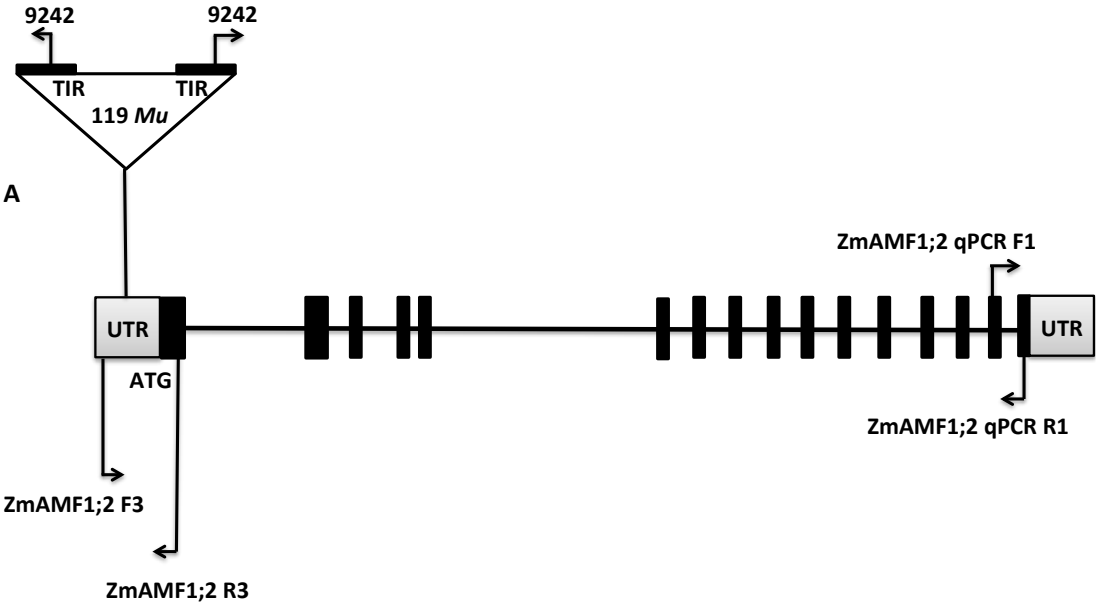
9242
9242
TIR
TIR
119 Mu
A
ZmAMF1;2 qPCR F1
UTR
UTR
ATG
ZmAMF1;2 qPCR R1
ZmAMF1;2 F3
ZmAMF1;2 R3

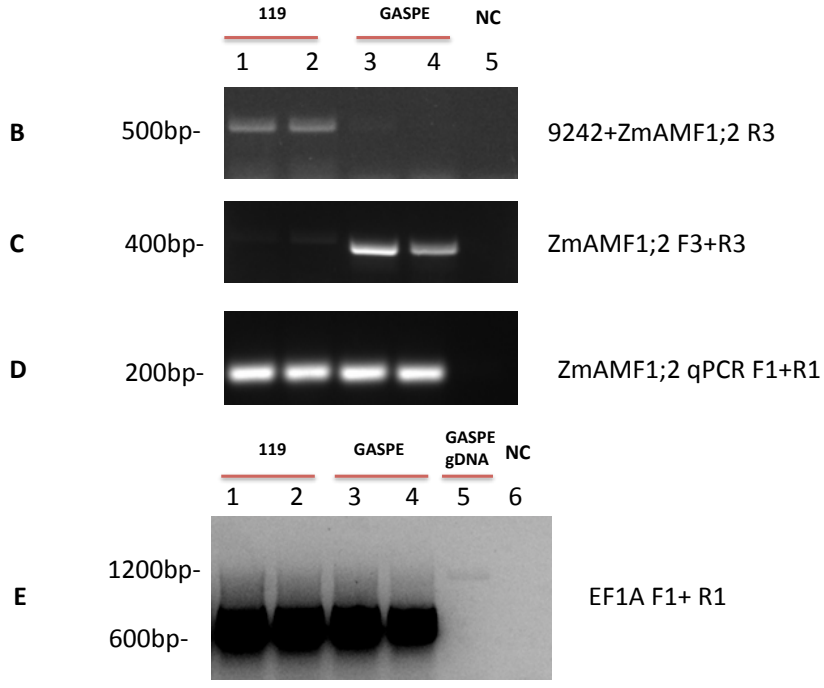
119
GASPE
NC
1 2 3 4 5
B
500bp-
9242+ZmAMF1;2 R3
C
400bp-
ZmAMF1;2 F3+R3
D
200bp-
ZmAMF1;2 qPCR F1+R1
119
GASPE
GASPE gDNA
NC
1 2 3 4 5 6
E
1200bp-
600bp-
EF1A F1+ R1

Figure 3.15 RT-PCR on ADL 119 and GASPE cDNA

Primers used in RT-PCR were shown in (A), 9242 is a universal *Mu* primer, Exons are shown as black boxes, and introns are shown as black lines. UTRs are shown in grey boxes. Primer binding locations are shown using black arrows. RT-PCR was carried with primer 9242, ZmAMF1;2 R3 (B); ZmAMF1;2 F3, R3 (C); ZmAMF1;2 qPCR F1, R1 (D). 1,2- ADL 119 cDNA; 3,4 – GASPE control; 5- Negative water control. Genomic DNA contamination was checked with primer EF1A F1 and EF1A R1 (E): 1,2- ADL 119 cDNA; 3,4 – GASPE control; 5-GASPE genomic DNA; 6-Negative water control.

Table 3.2 Phenotypic comparison between TUSC line mutant and GASPE before reproductive stage

Line	Plant Height (cm)	Leaf Number	Stem Thickness (cm)
ADL 112	32.4 ±2.56	6.9 ± 0.26**	3.3 ± 0.32
ADL 114	39.0 ±0.85**	6.9 ± 0.22***	3.4 ± 0.20*
ADL 119	33.9 ±2.00	6.0 ± 0.25	2.8 ± 0.19
Double mutant	41.1±2.41*	7.0 ± 0.29**	3.8 ± 0.33*
GASPE	33.4 ±1.57	5.7 ± 0.16	2.9 ± 0.12

Plant height, leaf number and stem thickness of TUSC lines and GASPE control were measured on the 22nd day after planting. Values= mean ± SEM (n= 7 to 14). Significant differences between TUSC lines and GASPE control were represented by star (unpaired t test with Welch's correction, $P< 0.05$).

3.4 Discussion

TUSC has been a useful resource for maize forward and reverse genetic studies. In the current study, we imported multiple TUSC lines potentially carrying *Mu* insertions within or near the *ZmAMF1;1* and *ZmAMF1;2* locus for functional studies of these two genes. The lines were developed through genotypic selection and through a backcrossing program (3 crosses) with the dwarf maize inbred, GASPE to eliminate potential background mutations and normalize the genetic background of the variable parents the TUSC populations represent. Through self-crossing, backcrossed homozygous TUSC lines were selected and the *Mu* insertion located through PCR analysis, cDNA cloning and sequencing. From the initial ADL 110 to ADL 115 lines for *ZmAMF1;1* and ADL 117 to ADL 126 lines for *ZmAMF1;2*, and ADL 112, 114 and 119 were selected as lines which retained the *Mu* insertion and after backcrossing resulted in a homozygous insertion of the *Mu* element.

Characterized *Mu* transposons have traditionally been located within gene sequences (McCarty and Meeley, 2009) potentially with a preference in the 5'UTR region (Dietrich et al., 2002). In this study, we also found that the *Mu* insertion in 114 and 119 was in the 5'UTR of *ZmAMF1;1* and *ZmAMF1;2* respectively. *Mu* insertions have been reported to introduce a 9 bp target site duplication change to the genome (Dietrich et al., 2002; Tan et al., 2011), but in this study we found it induced a 10 bp duplication event (ALD112 and 114) or a 8 bp deletion (ADL119) in the insertion site. The population of parental TUSC lines represents a mixed population of lines (41,472 mutagenized maize lines) and *Mu* transposons (McCarty and Meeley, 2009). Sequence analysis of cloned cDNA of flanking and internal *Mu* PCR products of the *Mu* transposon TIRs has been completed and the

sequence suggested the *Mu* transposon for each identified line was that of the 1.4 kb *Mu1* element (Lillis and Freeling, 1986). Unfortunately, the ability to amplify and sequence the entire *Mu* transposon in each line proved difficult, where only flanking regions of the transposon could be sequenced. Reasons for this are unclear but may relate to the actual physical insertion of the *Mu* element and possible transpositions and or deletions of the element with *Mu* insertion. RT-PCR results also indicated that the *Mu* insertion in ADL 112, 114, and 119 is also present in the transcripts but insertion may disrupt 5' sequence stability but not sequence at the 3'-end of the transcribed cDNA. This may indicate the impact of transposon insertion is more on translational level. Whether the transcripts are still translated, or the translated protein is still functional needs to be further studied.

ScAMF1 and GmAMF3 have been reported to conduct low affinity ammonium transport (Chiasson et al., 2014). It is unknown if other AMF1 orthologs including ZmAMF1;1 and ZmAMF1;2 behave in a similar manner to the previously two characterized low affinity ammonium transporters. It is interesting that loss of both *AMF1* genes in maize improved vegetative growth, a phenotype that requires further study across the reproductive growth phase. The development of backcrossed homozygous AMF1 TUSC lines will allow for the *in planta* reverse-genetic characterization of ZmAMF1;1 and ZmAMF1;2 activities in maize. Important questions that need to be addressed include their role in N transport into and within the plant, the functional properties of both proteins and their genetic regulation across developmental time lines.

Chapter 4 Characterization of ZmAMF1;1 and ZmAMF1;2 in a yeast expression system

4.1 Introduction

ScAMF1 and GmAMF3 have been previously identified to be involved in low affinity ammonium transport (Chiasson et al., 2014). However, whether ZmAMF1;1 and ZmAMF1;2 also have the ability to transport ammonium or other substrates are unclear. Sequence BLAST searches of these two transporters identify similarity to predicted boron and carbohydrate transporters, most of which have not been shown biochemically. In this chapter, the function of ZmAMF1;1 and ZmAMF1;2 were studied using different yeast mutant strains to test for possible transport activities.

4.1.1 A novel class of low affinity ammonium transport family -AMF1

4.1.1.1 GmbHLHm1 is a membrane bound transcription factor

GmbHLHm1 (formerly named GmSAT1) has been previously characterized as a peribacteriod membrane located ammonium channel (Kaiser et al., 1998). It was identified by its ability to rescue the growth of an ammonium transport deficient yeast strain 26972c and its ability to facilitate methylammonium uptake into yeast cells (Kaiser et al., 1998). Subsequently, it was later found that GmbHLHm1 failed

to complement the growth of a different ammonium deficient strain, 31019b (*mep1*Δ *mep2*Δ *mep3*Δ) when grown on medium containing low concentrations of ammonium (Marini et al., 2000). This suggested that GmbHLHm1 restored ammonium uptake in 26972c possibly in an indirect manner. Since these initial studies, the functional properties of the yeast mutants used to characterize GmbHLHm1 and other AMT1-like transport proteins have been described in detail. In the ethyl methane sulphonate (EMS) derived yeast mutant strain 26972c, the *mep2-2* allele is completely deleted and *mep1-1* has a single point mutant which results in the substitution of glycine 413 residue to aspartate 413 in cytoplasmic C-terminus (Marini et al., 1997; Marini et al., 2000). The mutation of mep1 trans-inhibits MEP3 at a post-translational level, however the overexpression of *MEP3* can compensate this inhibition (Marini et al., 2000). The indirect complementation of GmbHLHm1 in 26972c may be due to that GmbHLHm1 increased the expression level of MEP3 to overcome the trans-inhibition of mep1 mutation (Marini et al., 2000).

Subsequently, GmbHLHm1 has been identified as a membrane-localized transcription factor possessing a basic helix-loop-helix (bHLH) motif (Kaiser et al., 1998; Chiasson et al., 2014) which belongs to the superfamily of plant bHLH transcriptional factors (Heim et al., 2003; Chiasson et al., 2014). The bHLH motif can recognize the palindromic CANNTG "E-box" elements in the promoters of most bHLH transcriptional factors regulated genes (Chiasson et al., 2014). The mechanism of GmbHLHm1 activity has been suggested to first involve an unknown proteolytic event in the upstream of its C terminal tail and together with a modification of its N terminus, assists in the delivery of GmbHLHm1 into nucleus to

regulate gene transcription (Chiasson et al., 2014). GmbHLHm1 orthologs have been found in both monocot and dicot plant species including soybean, *Arabidopsis*, *Medicago*, maize and rice (Chiasson et al., 2014).

4.1.1.2 GmbHLHm1 identified a novel class of low affinity ammonium transporter family – AMF1

The expression of *MEP3* has been examined in the yeast 26972c strain transformed with pYES3-GmbHLHm1. It was found that the expression of *MEP3* was upregulated ~2-fold compared to cells transformed with empty pYES3 vector (Chiasson et al., 2014). However, when physically deleted in 26972c (*mep3Δ*), the transformation of GmbHLHm1 was still able to increase MA uptake. Using microarray analysis, a second gene (*YOR378w*) was found to be up-regulated ~56.5 fold (p= $8.6E^{-14}$) in 26972c cells transformed with GmbHLHm1 (Mazurkiewicz, 2013; Chiasson et al., 2014). *YOR378w* was subsequently named *ScAMF1* (*Saccharomyces cerevisiae Ammonium Facilitator 1*). ScAMF1 was able to transport methylammonium (MA) at sufficient levels which were toxic to both yeast strains, 26972c and 31019b. When ScAMF1 was deleted from 26972c, GmbHLHm1-dependent MA toxicity was eliminated (Mazurkiewicz, 2013; Chiasson et al., 2014). When fused with GFP, ScAMF1 was found located on the plasma membrane (Mazurkiewicz, 2013; Chiasson et al., 2014). However, ScAMF1 failed to rescue 26972c growth on 1 mM NH_4^+, and in *Xenopus laevis* oocytes ScAMF1 conducted a concentration-dependent [^{14}C] MA uptake, which suggested ScAMF1 is a low affinity ammonium transporter (Mazurkiewicz, 2013; Chiasson et al., 2014). The orthologs of ScAMF1 have been found in various plant species, including soybean, *Medicago*, *Arabidopsis*, and maize (Chiasson et al., 2014). In soybean, GmAMF3 was

found to conduct low affinity MA uptake in both yeast and *X. laevis* oocytes (Chiasson et al., 2014). In maize, two paralogs *ZmAMF1;1* (GRMZM2G062024) and *ZmAMF1;2* (GRMZM2G164743) have been identified by sequence analysis, but the function of these two genes remain to be discovered.

4.1.3 ScATR1, the paralog of ScAMF1, is required for boron resistance in yeast

ScATR1 shares 38.7% identity with ScAMF1, and has been found to be involved in boron resistance in yeast (Kaya et al., 2009). The overexpression of ScATR1 can increase boron tolerance in the wild type yeast strain BY4741 by lowering the boron concentration inside the cell by 25%. In contrast, the deletion of *ScATR1* (*atr1*Δ) results in the hyper accumulation of boron in cells (Kaya et al., 2009). However, when overexpressed, *ScATR1* reduces the intracellular boron level by 47% in the *art1*Δ mutant (Kaya et al., 2009). The boron resistance of ScAMF1 was also examined in these studies. When the wildtype *ScAMF1* was deleted (*yor378w*Δ), there was no change to boron tolerance, which suggested ScAMF1 was not involved in boron transport (Kaya et al., 2009). Overexpression of *ScAMF1* by the constitutive GAPDH promoter also resulted in no significant changes to boron sensitivity (Bozdag et al., 2011). The expression response of *ScAMF1* to boron stress was also tested, but there was no significant change in gene expression (Bozdag et al., 2011). It would appear, ScAMF1 is not a functioning boron efflux pump. However, whether ZmAMF1;1 and ZmAMF1;2 are involved in boron resistance is unclear and should be investigated.

4.1.4 SUSY7, a sucrose uptake deficient strain, is used to test the ability of ZmAMF1;1 and ZmAMF1;2 to transport sucrose

ZmAMF1;1 and ZmAMF1;2 are classified as members of the major facilitator superfamily, and both of them have been predicted as sugar transporters based on sequence comparisons. To rule out whether they are involved in sugar transport, the yeast strain SUSY7 which is deficient in sucrose uptake was used in this study. To utilize sucrose, wildtype yeast utilize extracellular invertase activity to hydrolyse sucrose into hexose, and subsequently uptake hexose through a hexose transport system (Riesmeier et al., 1992). The yeast mutant strain SUSY7, lacks the extracellular invertase, which results in its deficiency to utilize sucrose (Riesmeier et al., 1992; Deol et al., 2013). The SUSY7 yeast strain has been used widely in sucrose studies to clone sucrose transport proteins. For example, in wheat, TaSUT2 was found to rescue SUSY7/ura3 yeast strain growth when grown on medium with sucrose as sole carbon source, and was identified as a sucrose transporter in wheat (Deol et al., 2013). Expression of *AtSUT4* allowed yeast SUSY7 to grow on the medium with sucrose as the only carbon source. When exposed to ^{14}C-sucrose, AtSUT4 showed liner low affinity uptake of the isotope, which indicated AtSUT4 as a low affinity sucrose transporter (Weise et al., 2000).

4.1.5 Potassium transport in yeast- the genetic basis to test the ability of ZmAMF1;1 and ZmAMF1;2 to transport potassium

In yeast, there are two primary transport systems for K^+ uptake, a high affinity transport system and low affinity one (Rodríguez-Navarro and Ramos, 1984). In medium free of NH_4^+ and Na^+, the K^+ transport activities in yeast display a high-affinity system with a K_m of 24 μM while a low-affinity system operated with a

estimated K_m of 2 mM (Rodríguez-Navarro and Ramos, 1984). Subsequently, TRK1 a plasma membrane located protein, was found to be required for high affinity potassium uptake. Loss of TRK1 in yeast cells limits the uptake of K^+ when extracellular K^+ is less than 1 mM (Gaber et al., 1988). Later, by mutagenizing the *trk1*Δ mutant with EMS and screening mutants that required higher potassium concentrations to grow, a mutant defective in low affinity potassium uptake was isolated(Ko et al., 1990). The identified gene, *TRK2* encoded a low affinity potassium transporter (Ko et al., 1990). TRK2 shares 55% identity with TRK1 (Ko and Gaber, 1991). The *trk1*Δ *trk2*Δ double mutant is hypersensitive to low external pH, and this sensitivity can be suppressed by high concentrations of potassium (100 mM) on a complete yeast nutrient media (Ko et al., 1990). However when the *trk1*Δ *trk2*Δ yeast cells are transformed with *TRK1*, cells grow on medium with only 0.2 mM K^+, and the hypersensitivity to low pH is eliminated (Ko et al., 1990; Ko and Gaber, 1991). Yeast cells were able to accumulate potassium in *trk1*Δ *trk2*Δ yeast strain when external potassium increased to 15 mM, which revealed the existence of additional potassium transport systems (Bihler et al., 2002). The remaining potassium transporter(s) are hypersensitive to external pH, and cannot transport potassium efficiently when pH is below 4, which suggested the remaining transporter(s) are functioned differently to TRK1 and TRK2 (Ko and Gaber, 1991). Subsequently, the remaining potassium transport systems in *trk1*Δ *trk2*Δ yeast cells are identified as the non-selective cation channel NSC1 (Bihler et al., 2002). NSC1 can be blocked by elevating external Ca^{2+}, at low extracellular pH, and with the addition of hygromycin B and TEA^+ (Bihler et al., 2002). It has also been shown that NH_4^+ can substitute K^+ transport by NSC1 (Bihler et al., 2002). Proteins that are responsible for potassium efflux have been identified in yeast. TOK1 is an

outwardly rectifying potassium channel, opening when the membrane potential is above the K^+ equilibrium potential (Ketchum et al., 1995). NhaI has been found to be both a Na^+/H^+ and K^+/H^+ antiporter, and involved in both Na^+ and K^+ efflux, and *ENA* genes which encode a Na-ATPases for Na^+ efflux have also been found to participate in K^+ efflux in yeast (BaAueIos et al., 1998; Bañuelos and Rodríguez-Navarro, 1998).

In this chapter, the ability of ZmAMF1;1 and ZmAMF1;2 to transport potassium was studied using the potassium uptake deficient strain CY162 (MATα *ura3-52 trklΔ his3Δ200 his4-15 trk2Δl*::pCK64).

4.2 Materials and Methods

4.2.1 Maize growth and cDNA library synthesis

B73 was cultivated in 10 cm pots placed in a drip tray system in glasshouse with nutrient solution containing NH_4NO_3 2.5 mM, $MgSO_4 \bullet 7H_2O$ 0.5 mM, KH_2PO_4 0.5 mM, H_3BO_3 25 μM, $MnSO_4 \bullet H_2O$ 2 μM, $ZnSO_4 \bullet 7H_2O$ 2 μM, $CuSO_4 \bullet 5H_2O$ 0.5 μM, $Na_2MoO_4 \bullet 2H_2O$ 0.5 μM, KCl 1.05 mM, Fe-EDTA 0.1 mM, Fe-EDDHA 0.1 mM, K_2SO_4 1.25 mM, $CaCl_2 \bullet 2H_2O$ 0.25 mM, $CaSO_4 \bullet 2H_2O$ 1.75 mM (pH 5.5). The nutrient solution in the hydroponic system was refreshed weekly. After 4 weeks of growth, shoots and roots were separately harvested and frozen in liquid nitrogen and stored at -80°C before being ground into powder with a frozen mortar and pestle. Total RNA was extracted from both root and shoot frozen ground samples with Trizol (Invitrogen) and cDNA was synthesized by 1 μg RNA with SuperScript™ III Reverse Transcriptase (Invitrogen), according to the manufacturer's instructions.

Primers (EF1A F1 and EF1A R1) were designed on maize elongation factor gene *ZmElF1* (GRMZM2G154218) across its intron to check genomic DNA contamination in all cDNA samples. Genomic DNA contamination was removed by DNase I (RNase free) kit from New England Biolabs.

4.2.2 Amplification of *ZmAMF1;1* and *ZmAMF1;2* CDS

The *ZmAMF1;1* and *ZmAMF1;2* CDS were cloned from a 4-week-old B73 shoot cDNA library. Primers were designed based on the *ZmAMF1;1* and *ZmAMF1;2* predicted gene sequence in Phytozome. The CDS for both genes were amplified with primers *ZmAMF1;1 F2/R2* (forward and reverse) and *ZmAMF1;2 F2/R2* (forward and reverse) designed against their 5'-UTR and 3'-UTR regions. Both genes were amplified using Phusion High-Fidelity DNA Polymerase (Thermo Scientific). The PCR protocol involved an initial denaturation at 98°C for 30S, followed by 35 cycles of 98°C for 10 s, 61°C for 30s, 72°C for 1min, before a final extension of 72°C for 10 min.

4.2.3 Gateway cloning

Both AMF PCR products were readied for Gateway© cloning by the addition of a 3'-adenine overhang with the addition of *Taq* polymerase (New England Biolabs) and incubated at 72°C for 20min. Both PCR products were then cloned into the *pCR8/GW/TOPO* entry vector using a pCR™8/GW/TOPO®TA Cloning® Kit (Invitrogen) and following the manufacturer's instructions. The recombinant plasmid was transformed into One Shot® Chemically Competent *E. coli* cells (Invitrogen) by heat shock and selected on a solid 0.5 x salt LB medium (1.0% (w/v)

Tryptone, 0.5% (w/v) Yeast Extract, 0.5% NaCl and 2% agar) containing 100 μg·ml^{-1} spectinomycin. Transformed cells were selected by incubating for 2-4 days at 28°C. Several promising colonies were selected, cultured in new liquid media (half salt LB) prepared with 100 μg·ml^{-1} spectinomycin. Once grown, plasmid DNA was extracted with an EZ-10 Spin Column Plasmid DNA Miniprep Kit (Bio Basic) following the manufacturers instructions. Each cloned cDNA was confirmed by restriction enzyme digestion and sequencing by the AGRF (Waite campus, The University of Adelaide).

ZmAMF1;1 and *ZmAMF1;2* were then subcloned into *pYES3-DEST* vector with Gateway® LR Clonase™ II Enzyme Mix (Invitrogen) following the manufacturers instructions. *pYES3-ZmAMF1;1* and *pYES3-ZmAMF1;2* were then transformed into One Shot® Chemically Competent *E. coli* cells (Invitrogen) by heat shock, and then selected on half salt LB medium mixed with 100 μg·ml^{-1} carbenicillin. Plasmid DNA was isolated using a EZ-10 Spin Column Plasmid DNA miniprep kit (Bio Basic) and insertion of genes were verified by restriction digestion and sequencing.

4.2.4 Cloning of *ZmAMF1;1* , *ZmAMF1;2* and *ScAMF1* CDS into PDR196 vector

Primers *ZmAMF1;1 restriction F* and *ZmAMF1;1 restriction R*, and *ZmAMF1;2 restriction F* and *ZmAMF1;2 restriction R* were designed to amplify the *ZmAMF1;1* and *ZmAMF1;2* CDS with flanking *Spe*I and *Xho*I restriction sites. Primer *ScAMF1 Res-F* and *Res-R* were designed to clone the *ScAMF1* CDS with flanking restriction sites *Pst*I and *Xho*I. Plasmids of *ZmAMF1;1* and *ZmAMF1;2* in *pCR8/GW/TOPO* were used to amplify *ZmAMF1;1* and *ZmAMF1;2* CDS, while plasmid of *ScAMF1* in *pYES3* (Mazurkiewicz, 2013) was used to clone the *ScAMF1* CDS. All amplifications were

conducted using Phusion High-Fidelity DNA Polymerase (Thermo Scientific) to ensure high-fidelity and minimal amplification errors. The PCR programmes were as follows: Initial denaturation 98°C for 30S, followed by 35 cycles of denaturation at 98°C for 10S, anneal at 65°C for *ZmAMF1;1*, 61°C for *ZmAMF1;2* and 55°C for *ScAMF1* for 30S, extension at 72°C for 2min, and then followed by a final extension of 72°C for 5min. PCR products of *ZmAMF1;1* and *ZmAMF1;2* and the empty *PRD196* vector were digested with *Spe*I and *Xho*I. AMF cDNAs after digestion were purified from a 1% (w/v) agarose gel with ISOLATE II PCR and Gel Kit (Bioline). Similarly, the PCR product of *ScAMF1* and the empty *PRD196* vector were digested with *Pst*I and *Xho*I. Digested PCR products were gel purified and then ligated with digested *PDR196* using T4-ligase (New England, Biolabs) and then transformed into XLI-BLUE chemically competent *E. coli* cells. Colonies were selected on solid 0.5 X salt LB medium containing 100 $\mu g \cdot ml^{-1}$ ampicillin and incubated for 2-4 days at 28°C. Selected colonies were inoculated into fresh 0.5 X salt LB medium with 100$\mu g \cdot ml^{-1}$ ampicillin. Containing plasmids were isolated with ISOLATE II Plasmid Mini Kit (Bioline) according to manufacturer's instructions. Isolated plasmids were verified by restriction digestion and by sequencing.

4.2.5 Yeast Transformation

The *S. cerevisiae* strains 26972c (MAT**a***::ura3 mep1-1*, *mep2Δ*, *mep3*), SUSY7/ura3 and CY162 (MATα *ura3-52 trklΔ his3Δ200 his4-15 trk2Δl*::pCK64) were used for functional study of *ZmAMF1;1* and *ZmAMF1;2*. Yeast transformation used a modified Lithium Acetate (LiAc) transformation method described by Gietz *et al.* (2007). In brief, a fresh colony of yeast was selected from plates and inoculated into 20 ml of YPD medium (1% (w/v) Bacto yeast extract, 2% (w/v) Bacto peptone,

and 2% (w/v) D-glucose). For experiments involving the CY162 yeast strain, 100 mM KCl was added to the YPD medium. Yeast cells were aerobically grown in a sterile 100 ml glass conical flask at 28°C at 200 rpm. An overnight culture was diluted with 2X YPD or YPD with 100 mM KCl to an OD_{600nm} of 0.1 to 0.2 before and then grown to mid-log grow phase (OD_{600nm} of 0.6 to 0.8). The culture was transferred to 50ml sterile falcon tubes and spin at 4000 rpm for 2 min. Cell pellets were washed twice with 40 ml sterile Milli-Q water, and then resuspended in 1ml sterile Milli-Q water and transferred to a 1.5ml sterile Eppendorf tube. The cells were then washed twice in 750 µL of LiAc washing solution (10 mM Tris-HCl + 1 mM EDTA + 0.1 M LiAc, pH 7.5) followed by a suspension in 300 µL of LiAc washing solution. Fifty µL of the cell suspension was transferred to a new tube and mixed of 300µL PEG/LiAc transformation solution (50% (w/v) PEG 4000, 10 mM Tris-HCl + 1 mM EDTA + 0.1 M LiAc, pH 7.5), 5 µL of boiled salmon sperm DNA (Sigma) and approximately 300 ng of plasmid DNA. The mixture was briefly vortexed, then incubated at 28°C with 200 rpm shaking for 30min before incubating in a 42°C water bath for 40 min. Cells were washed twice with 500 µL sterile Milli-Q water, and then resuspended in 500 µL selection medium. For 26972c, the selection medium was 0.17% (w/v) YNB (Nitrogen Base Without Amino Acids and Ammonium Sulphate, Sigma) supplemented with 0.1% (w/v) L-proline and 2% (w/v) glucose. For SUSY7, the selection medium was 0.17% (w/v) YNB supplemented with 5 g/L ammonium sulphate, 20 mg/L tryptophan and 2% glucose. For CY162, the selection medium was 0.17% (w/v) YNB supplemented with 5 g/L ammonium sulphate, 10 mg/L histidine, 20 mg/L methionine, 20 mg/L tryptophan, 100 mM KCl and 2% (w/v) glucose. The cell suspension was then spread on the solid selection medium which is medium described above

supplemented with 2% (w/v) agar. Yeast colonies appeared on the plates after 3-4 days incubation at 28°C and colonies were re-streaked to a new solid selective medium plate to confirm the transformation.

4.2.6 Methylammonium transport test in 26972c or 26972c:Δ*amf1*

Yeast strain 26972c or 26972c:Δ*amf1* generated by Mazurkiewicz (2013) were transformed with plasmid *pYES3-DEST*, *pYES3-GmbHLHm1*, *pYES3-ScAMF1*, *pYES3-ZmAMF1;1* or *pYES3-ZmAMF1;2* and inoculated individually into 20 ml of 0.17% YNB supplemented with 0.1% L-proline and 2% glucose prepared in a sterile 100 ml conical flask and grown overnight at 28°C with agitation at 200 rpm to an OD_{600nm} of 1.5 to 2. The culture was pelleted by centrifugation (4000 rpm for 2 min), washed twice and resuspended with 0.17% YNB. All yeast cultures were resuspended with 0.17% YNB to a uniform OD_{600nm} of 0.1. For spot plate analysis, 10-fold dilution series were prepared and spotted out using 5 µL aliquots on the selective medium. The complementation screens for potential ammonium transport were carried out on 0.17% YNB supplemented with 0.1% L-proline and 0.1 M methylamine hydrochloride (MA) or with 0.15 M MA using 2% glucose or 1.5% galactose and 0.5% raffinose as carbon sources, respectively. The medium was buffered with 50 mM MES/Tris to a pH 4.5 and 6.1. All the plates were incubated at 28°C for 5 d.

4.2.7 Boric acid transport test in 26972c

Yeast strain 26972c transformed with plasmid *pYES3-DEST*, *pYES3-ScAMF1*, *pYES3-ZmAMF1;1* or *pYES3-ZmAMF1;2* were inoculated into 20 ml of 0.17% YNB supplemented with 0.1% L-proline and 2% glucose individually in a sterile 100 ml

glass conical flask and grown at 28°C overnight with shaking (200 rpm). The spot plate experiment was carried as described in 4.2.6. The complementation experiments were screened on 0.17% YNB supplemented with 0.1% L-proline under 0, 50, 75 and 100 mM boric acid with 2% glucose or 1.5% galactose + 0.5% raffinose as carbon sources, respectively. The plates were incubated at 28°C for 5 d.

4.2.8 Sucrose transport test in SUSY7 yeast strain

SUSY7 transformed with empty *PDR196* vector, *PDR196-ZmAMF1;2* and *PDR196-ZmAMF1;2* were inoculated in 20ml of 0.17% (w/v) YNB supplemented with 5 g/L ammonium sulphate, 20 mg/L tryptophan and 2% glucose in a sterile 100 ml glass conical flask and grown overnight at 28°C with shaking (200 rpm). The spot plate experiment was carried as described in 4.2.6. The yeast complementation study of SUSY7 was performed on medium 0.17% (w/v) YNB with 5 g/L ammonium sulphate and 20 mg/L tryptophan and supplemented with 2% glucose or 2% sucrose as carbon source. The plates were incubated at 28°C for 5 d.

4.2.9 Functional analysis of ZmAMF1;1 and ZmAMF1;2 in yeast strain CY162

CY162 transformed with *PDR196*, *PDR196-ScAMF1*, *PDR196-ZmAMF1;1* and *PDR196-ZmAMF1;2* were individually inoculated into 20 ml of medium 0.17% (w/v) YNB supplemented with 5 g/L ammonium sulphate, 1.92 g/L SD-uracil (Yeast Synthetic Drop-out Medium without uracil, Sigma), 2% glucose and 100 mM KCl in a sterile 100 ml flask and incubated with shaking of 200 rpm at 28°C overnight. The spot plate experiments were carried as described in 4.2.6. Yeast complementation 0.17% (w/v) YNB with 5 g/L ammonium sulphate, 1.92 g/L SD-uracil and 2% glucose supplemented with 0 mM or 100 mM added KCl. Plates were incubated at

28°C for 8 d. Phenotypic analysis was also tested on identical medium where ammonium was replaced with either: 1) 10 mg/L histidine + 20mg/L methionine + 20 mg/L tryptophan, 2) 0.1% L-proline or 3) 0.1% L-asparagine. Plates were incubated at 28°C for 5-9 d.

To understand the relationship between the concentration of ammonium, pH and the level of K plates were prepared with 0.17% (w/v) YNB with 1.92 g/L SD-uracil and 2% glucose, supplemented with either 0.5, 1.5 or 5 mM ammonium sulphate with pH 4.5 or 6.1. Plates were incubated at 28°C for 4 d.

Methylammonium toxicity tests were also performed. CY162 transformed with empty *PDR196*, *PDR196-ScAMF1*, *PDR196-ZmAMF1* and *PDR196-ZmAMF2* were inoculated into 20ml of medium 0.17% (w/v) YNB with 5g/L ammonium sulphate, 1.92g/L SD-uracil, 2% glucose and 100mM KCl in a sterile 100ml flask respectively and incubated with shaking of 200 rpm at 28°C overnight. The spot plate experiments were carried out as described in 4.2.6. The spot plates were examined on medium containing 0.17% (w/v) YNB without ammonium sulphate and amino acids, with 1.92 g/L SD-uracil, 0.1% proline and 2% glucose supplemented with 0 or 0.1M MA under 0 mM, 10 mM or 100 mM KCl. The medium was buffered with MES/Tris to reach pH 6.1. The plates were incubated at 28°C for 5 days.

4.3 Results

4.3.1 ZmAMF1;1 and ZmAMF1;2 functional analysis in yeast strain 26972c and 26972c:Δ*amf1*

ScAMF1 has previously been characterized as a putative low affinity ammonium transporter (Chiasson et al., 2014). To test whether the two maize orthologs of ScAMF1 behave the same, *ZmAMF1;1* and *ZmAMF1;2* were cloned into the yeast/*E.coli* shuttle vector *pYES3* which contains a *GAL1* promoter to induce gene expression in the presence of galactose. *pYES3-ZmAMF1;1* and *pYES3-ZmAMF1;2* were transformed into yeast strain 26972c and the 26972c:Δ*amf1* knockout. In each test, the overexpression of *ZmAMF1;1* and *ZmAMF1;2* did not induce an enhanced sensitivity to MA as observed in the control strains expressing *GmbHLHm1* and *ScAMF1*. The loss of background ScAMF1 activity (26972c Δ*amf1*) had no effect on MA sensitivity for ZmAMF1;1 and ZmAMF1;2 (Figure 4.1 and 4.2). With increased pH, both ZmAMF1;1 and ZmAMF1;2 started to show sensitivity to MA, but the phenotype was similar to the empty vector control. Both GmbHLH1 and ScAMF1 showed much more toxicity at elevated pH (Figure 4.1).

4.3.2 Boron test in yeast 26972c

ScATR1 was previously characterized as a boron exporter in yeast (Kaya et al., 2009). Sequence analysis had identified that ScAMF1 was one of ScATR1's closest protein paralogs, however when tested for enhancing boron tolerance, ScAMF1 failed (Bozdag et al., 2011). To help understand the functional properties of ZmAMF1;1 and ZmAMF1;2, a similar test for boron tolerance was conducted. In the presence of increasing boron (0, 50, 75 and 100 mM boric acid) neither ZmAMF1;1

and ZmAMF1;2 improved tolerance to boron, all yeast failed to grow with media supplemented with boric acid (Figure 4.3).

4.3.3 Test of sucrose transport activity by ZmAMF1;1 and ZmAMF1;2 in the external invertase yeast mutant SUSY7

To utilize sucrose, wildtype yeast require extracellular invertase activity to hydrolyse sucrose into hexose, where hexose is subsequently transported into the cell through existing hexose transport pathways (Riesmeier et al., 1992). The yeast mutant strain SUSY7, lacks extracellular invertase, which results in deficiency to utilize sucrose in the growth media (Riesmeier et al., 1992; Deol et al., 2013). Both ZmAMF1;1 and ZmAMF1;2 have been aligned based on sequence comparisons to putative carbohydrate transporters in animal systems. To understand whether ZmAMF1;1 or ZmAMF1;2 function as a sugar transport protein, their activity was examined on the medium containing 0.17% (w/v) YNB supplemented with 5 g/L ammonium sulphate and 20 mg/L tryptophan, and 2% glucose or 2% sucrose as a carbon source. Both ZmAMF1;1 and ZmAMF1;2 failed to rescue the growth when the medium contained 2% sucrose as a carbon source, while SUSY7 transformed with ZmAMF1;1 and ZmAMF1;2 grew well in media supplied with 2% glucose (Figure 4.4).

4.3.4 Characterization of ZmAMF1;1 and ZmAMF1;2 activity in the CY162 yeast strain

We found that expression of both *ZmAMF1;1* and *ZmAMF1;2* in the double potassium transport mutant CY162 (MATα *ura3-52 trklΔ his3Δ200 his4-15 trk2Δl*::pCK64), rescued growth of CY162 in the presence of 5 g/L $(NH_4)_2SO_4$ (37.8

mM) with no additional potassium added to the medium. In contrast, the empty vector *PDR196* and *ScAMF1* (cloned into *PDR196*) both failed to grow. When the strains were plated on similar media containing an additional 100 mM KCl, all yeast transformations grew (Figure 4.5). To test if the growth defect in the control and ScAMF1 was due to the presence of high concentrations of ammonium, we replaced the $(NH_4)_2SO_4$, leaving residual amino acids (20 mg/L histidine +10 mg/L methionine + 20 mg/L tryptophan) in the medium. All strains grew regardless if extra potassium was supplied or not in the YNB medium (Figure 4.5). Different ammonium concentrations (0.5 to 5 mM $(NH_4)_2SO_4$) at either pH 4.5 or 6.1 were also tested. At 0.5 to 1.5 mM $(NH_4)_2SO_4$, yeast transformed with the empty vector *PDR196*, *PDR96-ZmAMF1;1* or *ZmAMF1;2* were all able to grow when there was no extra added potassium in the medium. However, when the $(NH_4)_2SO_4$ increased to 5 mM (pH 4.5) the yeast again became sensitive (Figure 4.7). The growth characterization was also examined with proline and asparagine as a nitrogen source, both alternative nitrogen sources rescued cell growth of all transformed strains at low potassium level (~7.3 mM) (Figure4.6).

Interestingly, when 0.1 mM MA was added to the medium (in a low potassium medium), CY162 transformed with ZmAMF1;1 and ZmAMF1;2 were more susceptible to MA compared to the empty vector and the ScAMF1 transformed control. However, when the potassium concentration was increased, the toxicity was eliminated.

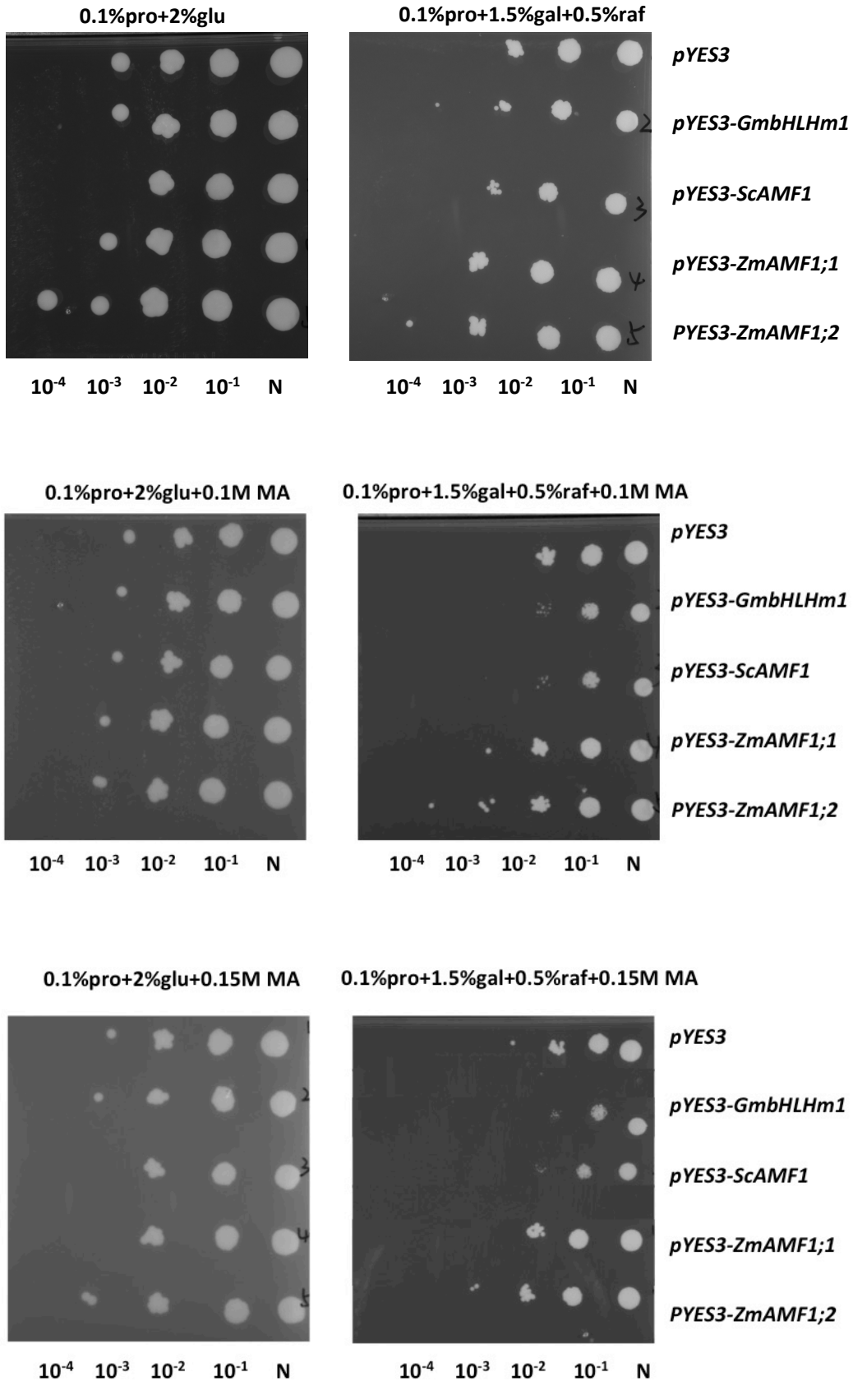
0.1%pro+2%glu
0.1%pro+1.5%gal+0.5%raf
pYES3
pYES3-GmbHLHm1
pYES3-ScAMF1
pYES3-ZmAMF1;1
PYES3-ZmAMF1;2
10-4 10-3 10-2 10-1 N
0.1%pro+2%glu+0.1M MA
0.1%pro+1.5%gal+0.5%raf+0.1M MA
0.1%pro+2%glu+0.15M MA
0.1%pro+1.5%gal+0.5%raf+0.15M MA
pH 4.5

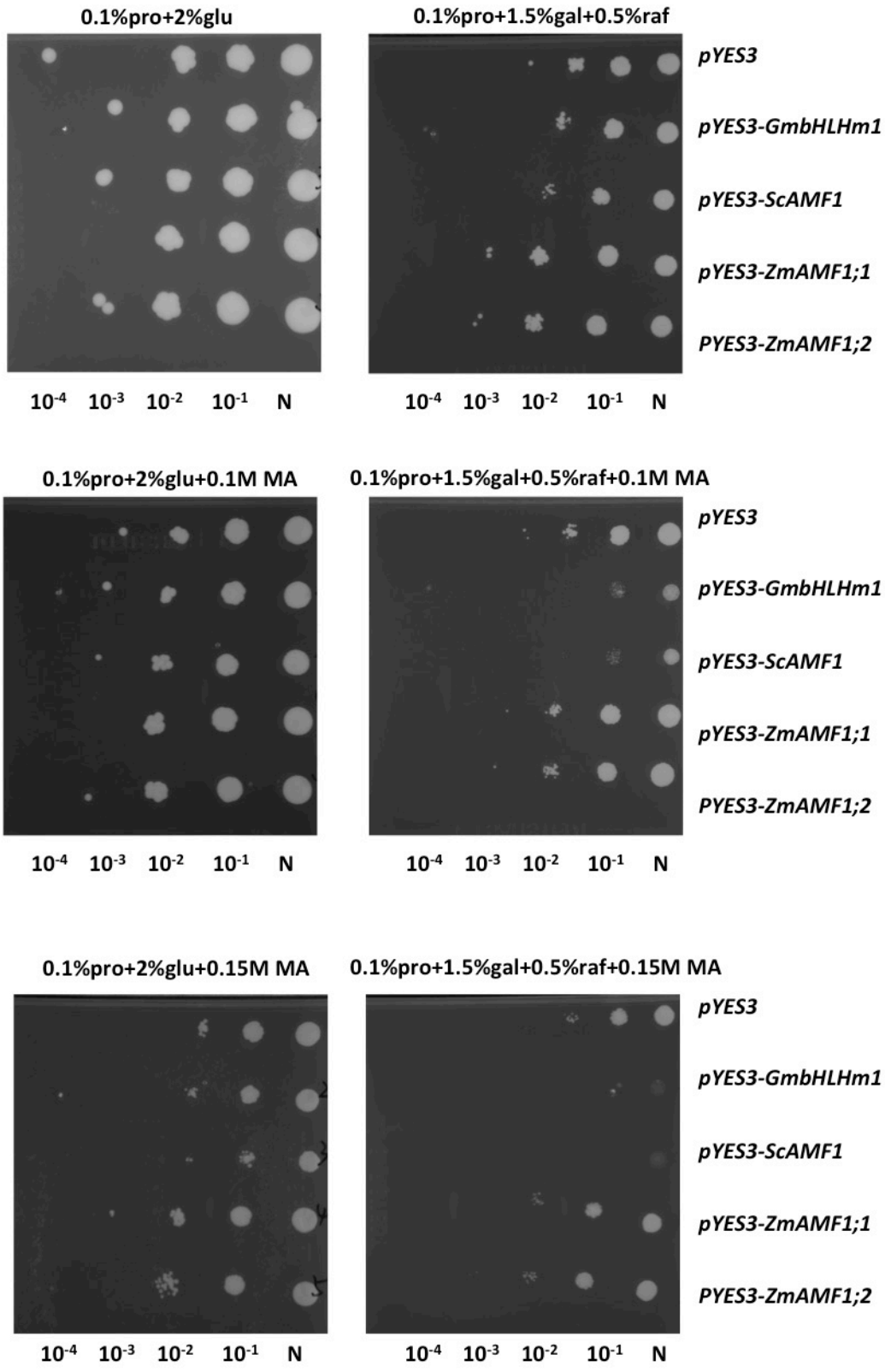
0.1%pro+2%glu
0.1%pro+1.5%gal+0.5%raf
pYES3
pYES3-GmbHLHm1
pYES3-ScAMF1
pYES3-ZmAMF1;1
PYES3-ZmAMF1;2
10-4 10-3 10-2 10-1 N
0.1%pro+2%glu+0.1M MA
0.1%pro+1.5%gal+0.5%raf+0.1M MA
0.1%pro+2%glu+0.15M MA
0.1%pro+1.5%gal+0.5%raf+0.15M MA
pH 6.1

Figure 4.1 Functional analysis of ZmAMF1;1 and ZmAMF1;2 in 26972c

Yeast strain 26972c transformed with *pYES3-DEST*, *pYES3-GmbHLHm1*, *pYES3-ScAMF1*, *pYES3-ZmAMF1;1* or *pYES3-ZmAMF1;2*. All cells were diluted to a uniform OD_{600nm} of 0.1 and then diluted further using a 10-fold dilution series before spotting 5 µL aliquots onto solid media plates containing 0.17% YNB supplemented with 0.1% L-proline (pro), 0.1 M Methylammonium (MA) or 0.15 M MA with 2% glucose (glu) or 1.5% galactose (gal) plus 0.5% raffinose (raf) as a carbon source, respectively. The medium was buffered with 50 mM MES/Tris to a pH of 4.5 and 6.1. All the plates were incubated at 28°C for 5 d.

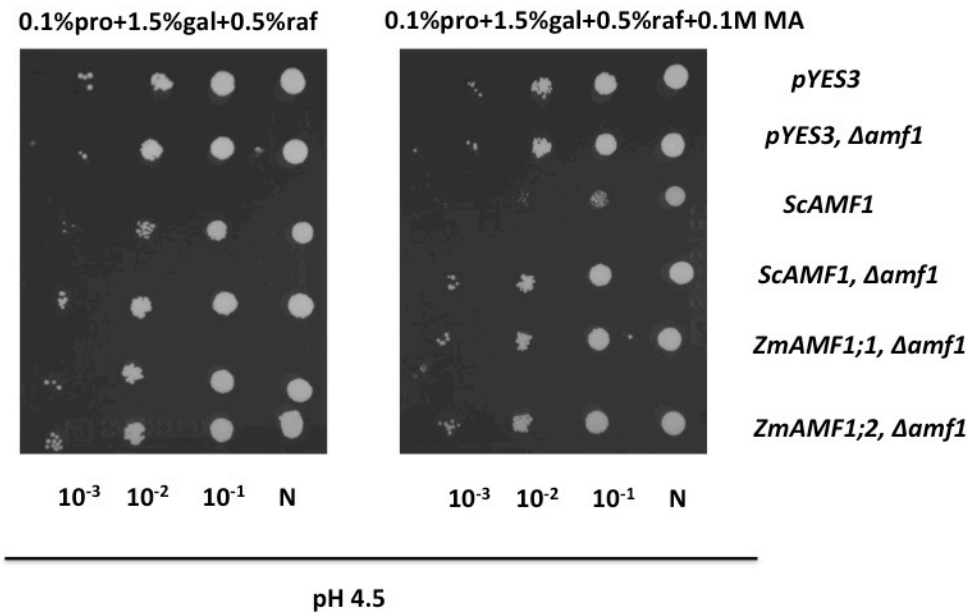
0.1%pro+1.5%gal+0.5%raf
0.1%pro+1.5%gal+0.5%raf+0.1M MA
pYES3
pYES3, Δamf1
ScAMF1
ScAMF1, Δamf1
ZmAMF1;1, Δamf1
ZmAMF1;2, Δamf1
10-3 10-2 10-1 N
10-3 10-2 10-1 N
pH 4.5

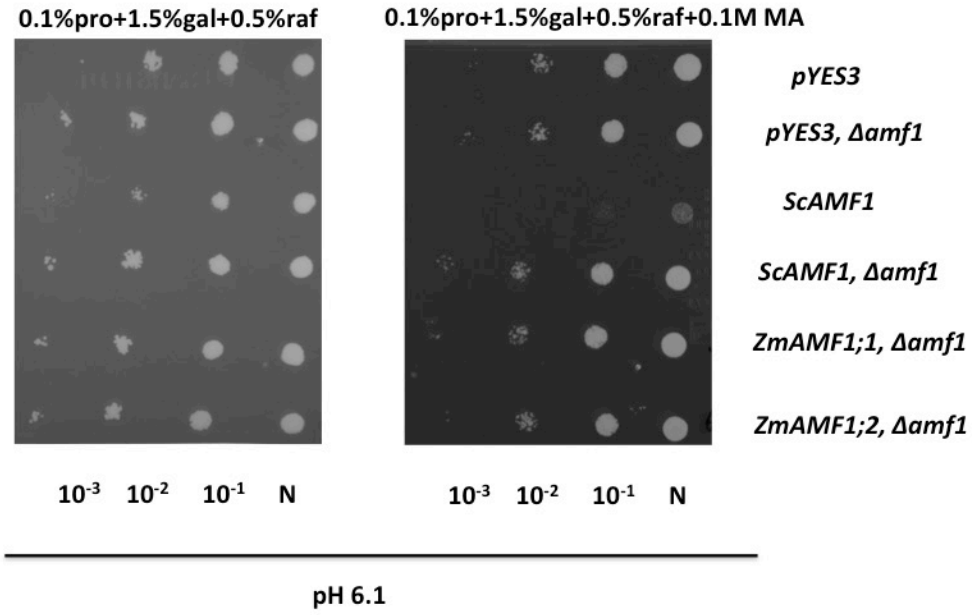
0.1%pro+1.5%gal+0.5%raf
0.1%pro+1.5%gal+0.5%raf+0.1M MA
pYES3
pYES3, Δamf1
ScAMF1
ScAMF1, Δamf1
ZmAMF1;1, Δamf1
ZmAMF1;2, Δamf1
10-3 10-2 10-1 N
10-3 10-2 10-1 N
pH 6.1

Figure 4.2 Functional analysis of ZmAMF1;1 and ZmAMF1;2 in 26972c:*Δamf1*

Yeast strain 26972c or 26972c:*Δamf1* transformed with *pYES3-DEST*, *pYES3-ScAMF1*, *pYES3-ZmAMF1;1* or *pYES3-ZmAMF1;2*. All cells were diluted to a uniform OD_{600nm} of 0.1 and then diluted further using a 10-fold dilution series before spotting 5 μL aliquots onto solid media plates containing 0.17% YNB supplemented with 0.1% L-proline (pro), 0.1 M MA with 2% glucose (glu) or 1.5% galactose (gal) plus 0.5% raffinose (raf) as a carbon source, respectively. The medium was buffered with 50 mM MES/Tris to a pH of 4.5 and 6.1. All the plates were incubated at 28°C for 5d.

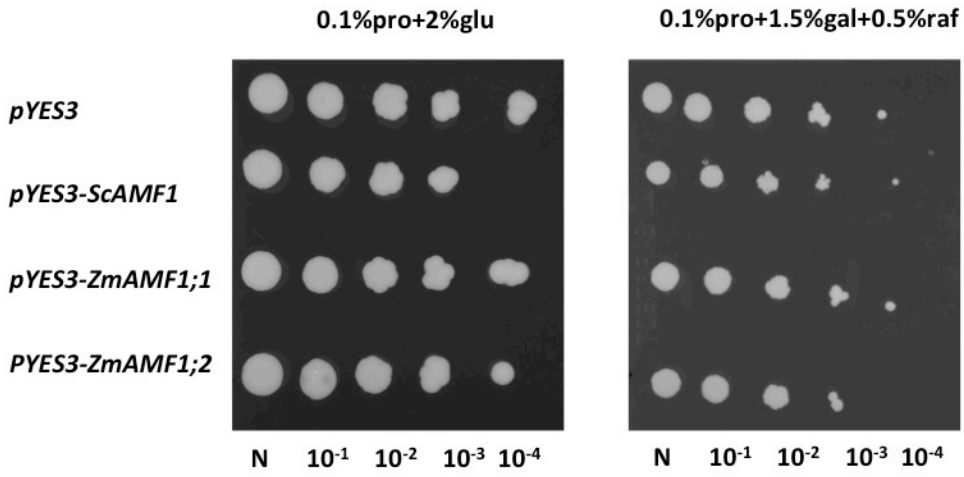
0.1%pro+2%glu
0.1%pro+1.5%gal+0.5%raf
pYES3
pYES3-ScAMF1
pYES3-ZmAMF1;1
PYES3-ZmAMF1;2
N 10-1 10-2 10-3 10-4
N 10-1 10-2 10-3 10-4

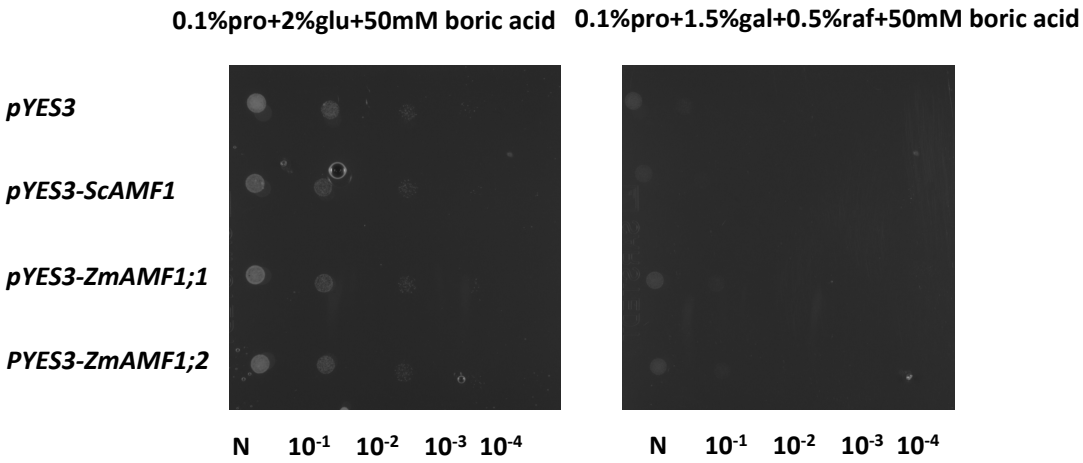
0.1%pro+2%glu+50mM boric acid
0.1%pro+1.5%gal+0.5%raf+50mM boric acid
pYES3
pYES3-ScAMF1
pYES3-ZmAMF1;1
PYES3-ZmAMF1;2
N 10-1 10-2 10-3 10-4
N 10-1 10-2 10-3 10-4

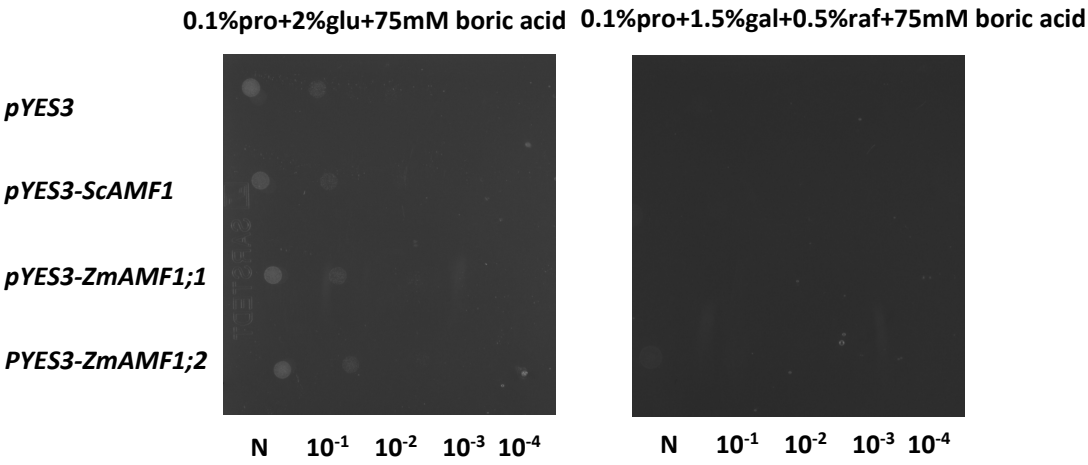
0.1%pro+2%glu+75mM boric acid
0.1%pro+1.5%gal+0.5%raf+75mM boric acid
pYES3
pYES3-ScAMF1
pYES3-ZmAMF1;1
PYES3-ZmAMF1;2
N 10-1 10-2 10-3 10-4
N 10-1 10-2 10-3 10-4

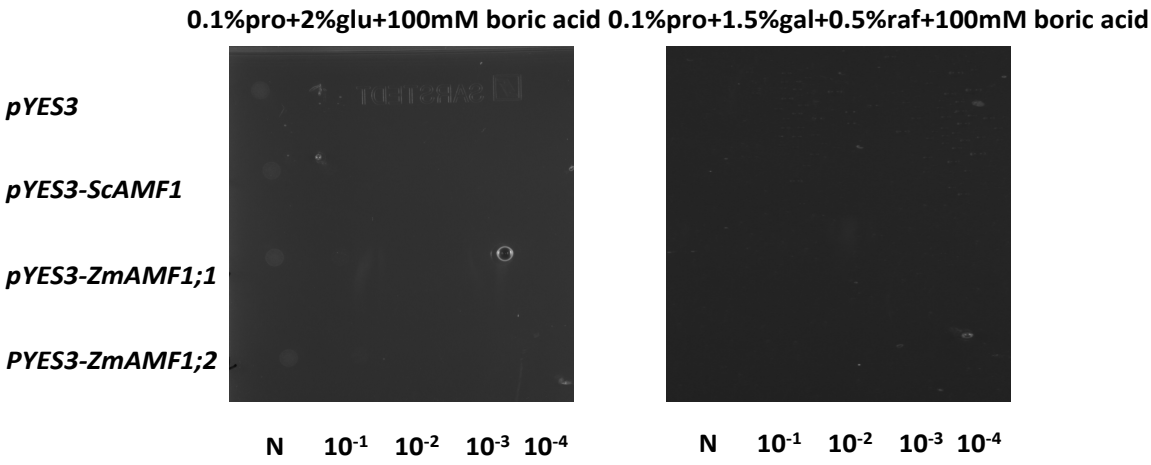

Figure 4.3 Boron tolerance test of ZmAMF1;1 and ZmAMF1;2 in 26972c

Yeast strain 26972c transformed with *pYES3-DEST*, *pYES3-ScAMF1*, *pYES3-ZmAMF1;1* or *pYES3-ZmAMF1;2*. All cells were diluted to a uniform OD_{600nm} of 0.1 and then diluted further using a 10-fold dilution series before spotting 5 μL aliquots onto solid media plates containing 0.17% YNB supplemented with 0.1% L-proline (pro) and 0, 50, 75 or 100 mM boric acid with 2% glucose (glu) or 1.5% galactose (gal) plus 0.5% raffinose (raf) as a carbon source, respectively. All the plates were incubated at 28°C for 5 d.

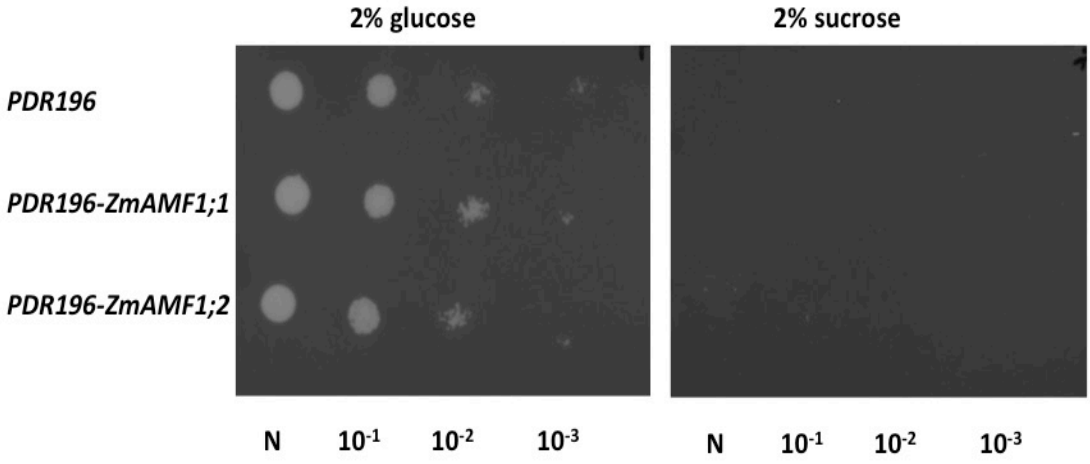

Figure 4.4 Sucrose transport test of ZmAMF1;1 and ZmAMF1;2 in SUSY7

Yeast strain SUSY7 was transformed with empty *PDR196* vector, *PDR196-ZmAMF1;1* and *PDR196-ZmAMF1;2*. All cells were diluted to a uniform OD_{600nm} of 0.1 and then diluted further using a 10-fold dilution series before spotting 5μL aliquots onto solid media plates containing 0.17% YNB with 5 g/L ammonium sulphate and 20 mg/L tryptophan and supplemented with 2% glucose or 2% sucrose as carbon source. The plates were incubated at 28°C for 5 d.

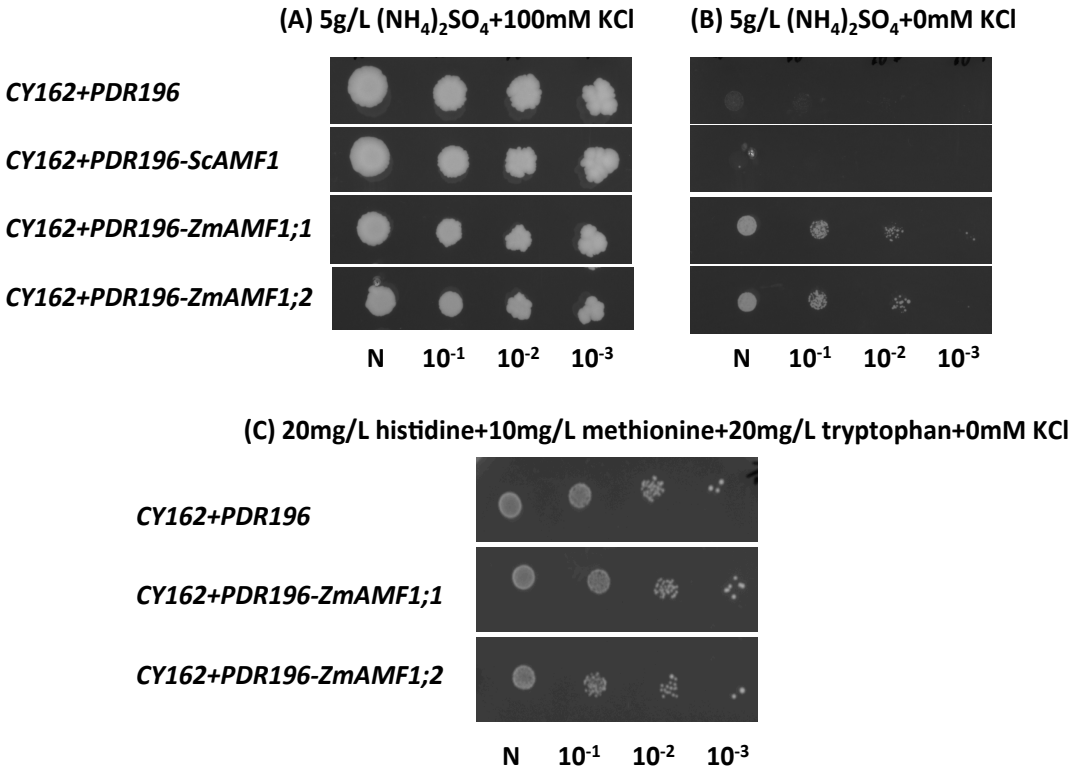

Figure 4.5 ZmAMF1;1 and ZmAMF1;2 reduced ammonium toxicity in yeast CY162

Yeast strain CY162 was transformed with empty *PDR196* vector, *PDR196-ScAMF1*, *PDR196-ZmAMF1;1* and *PDR196-ZmAMF1;2*. All cells were diluted to a uniform OD_{600nm} of 0.1 and then diluted further using a 10-fold dilution series before spotting 5 µL aliquots onto solid media plates containing 0.17% YNB with 5 g/L ammonium sulphate, 1.92 g/L SD-uracil and 2% glucose supplemented with 0 mM (A) or 100 mM KCl (B). In C, plate media consisted of 0.17% (w/v) YNB with 10 mg/L histidine, 20 mg/L methionine, 20 mg/L tryptophan, and 2% glucose. Plates with medium (A) and (B) were incubated at 28°C for 8 days, while plates with medium (C) were incubated at 28°C for 9 days.

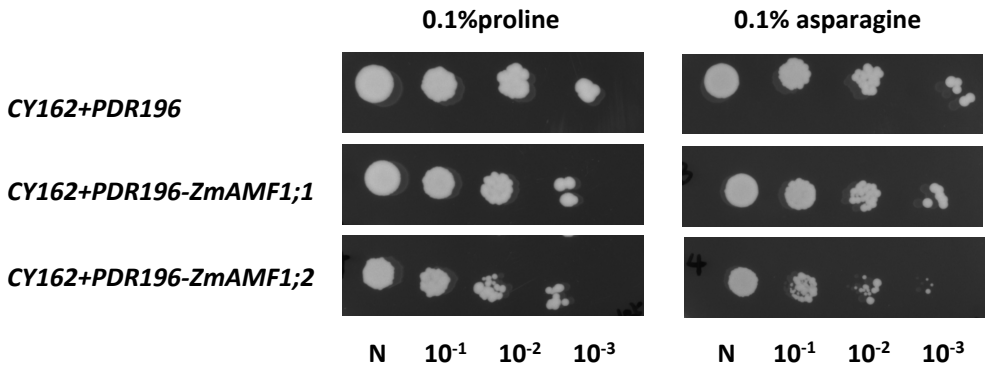

Figure 4.6 Ammonium toxicity was eliminated when using different nitrogen source in CY162

Yeast strain CY162 was transformed with empty *PDR196* vector, *PDR196-ZmAMF1;1* and *PDR196-ZmAMF1;2*. All cells were diluted to a uniform OD_{600nm} of 0.1 and then diluted further using a 10-fold dilution series before spotting 5μL aliquots onto solid media plates containing YNB with 1.92 g/L SD-uracil and 2% glucose supplemented with 0.1% (w/v) L-proline and 0.1% (w/v) L-asparagine as a nitrogen source. The plates were incubated at 28°C for 5 d.

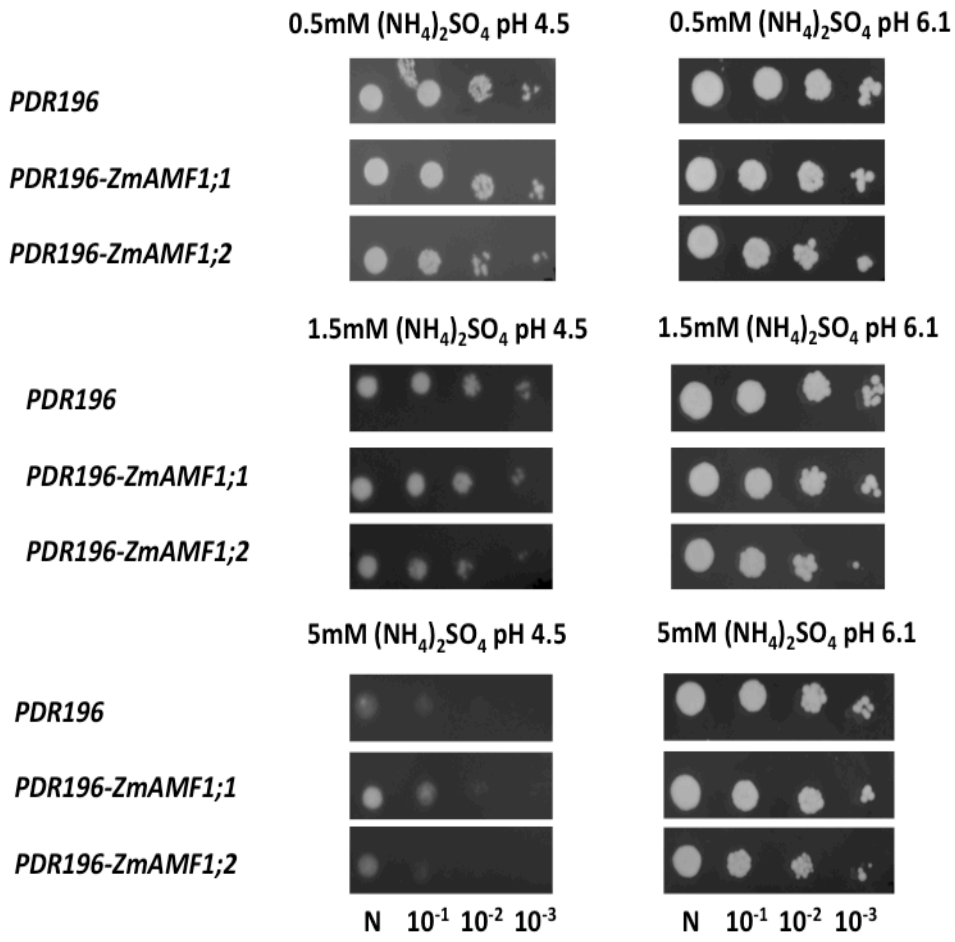

Figure 4.7 The effects of ammonium concentration and pH level on ammonium toxicity in CY162

Yeast strain CY162 was transformed with empty *PDR196* vector, *PDR196-ZmAMF1;1* and *PDR196-ZmAMF1;2*. All cells were diluted to a uniform OD_{600nm} of 0.1 and then diluted further using a 10-fold dilution series before spotting 5µL aliquots onto solid media plates containing YNB with 1.92 g/L SD-uracil, 2% glucose and increasing (0.5, 1.5, 5 mM) ammonium sulphate. The medium was buffered with 50 mM MES/Tris to reach pH 4.5 or 6.1. The plates were incubated at 28°C for 4 days.

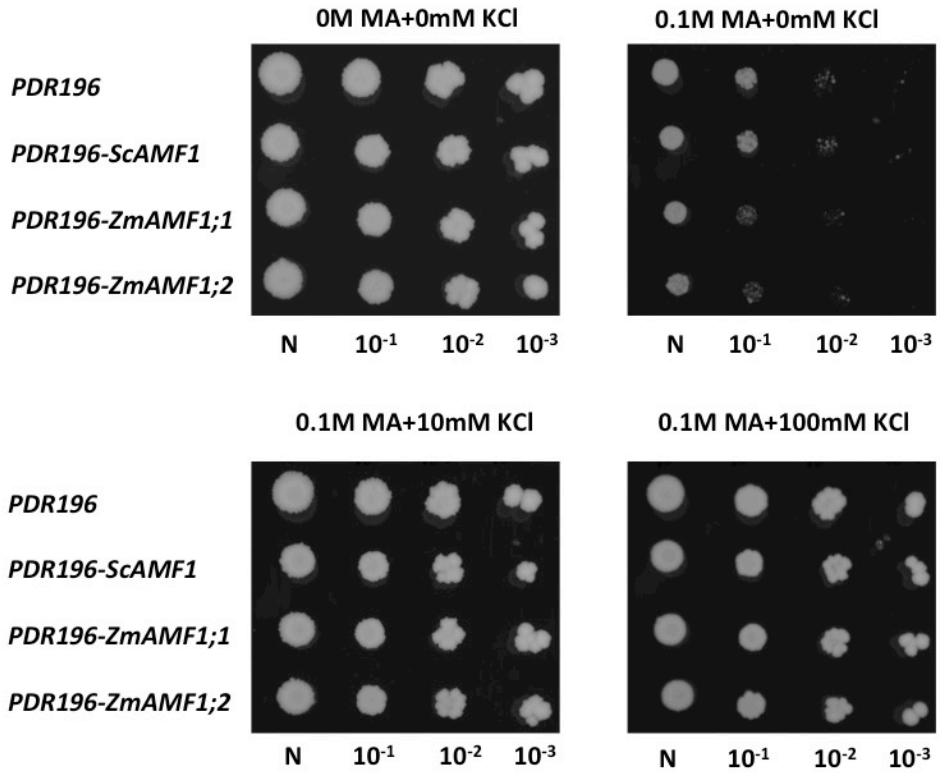

Figure 4.8 CY162 transformed with ZmAMF1;1 and ZmAMF1;2 were more susceptible to MA when potassium concentration was low

Yeast strain CY162 transformed with empty *PDR196* vector, *PDR196-ScAMF1, PDR196-ZmAMF1;1* and *PDR196-ZmAMF1;2* were incubated with shaking overnight and then diluted a uniform OD_{600nm} of 0.1. Cells were then diluted by a 10-fold dilution series, and each dilution spotted onto plates at 5 µl aliquots. The experiment was carried on YNB medium without ammonium sulphate and amino acids supplemented with 1.92g/L SD-uracil, 0.1% proline and 2% glucose, ± 0.1M MA with either 0, 10 or 100 mM KCl. The medium was buffered with MES/Tris to pH 6.1. The plates were incubated at 28°C for 5 days.

4.4 Discussion

The membrane bound transcription factor GmbHLHm1 had previously identified a new form of low affinity ammonium transport protein family, AMF1 in both yeast and plants (Chiasson et al., 2014). In this chapter, we utilized yeast expression systems to help elucidate the function of two members of the maize AMF1 family, ZmAMF1;1 and ZmAMF1;2. We first examined the complementation of ZmAMF1;1 and ZmAMF1;2 in an ammonium uptake deficient yeast strain, 26972c. Unlike ScAMF1 and GmAMF3, which showed signs of toxicity when supplied 0.1M MA (Mazurkiewicz, 2013), ZmAMF1;1 and ZmAMF1;2 displayed no sensitivity to MA at either 0.1 or 0.15 M MA containing media prepared at pH 4.5 or 6.1 (Figure 4.1). To eliminate background ScAMF1 effects in yeast, a yeast strain where ScAMF1 was deleted, 26972c:*Δamf1* was also tested. The elimination of ScAMF1 in 26972c did not affect the sensitivity to MA with either ZmAMF1;1 or ZmAMF1;2 (Figure 4.2). We also ruled out that ZmAMF1;1 and ZmAMF1;2 were not involved in boron tolerance and sucrose transport (Figure 4.3 and 4.4). However, when *ZmAMF1;1* and *ZmAMF1;2* were transformed in the potassium uptake deficient strain CY162, the overexpression of *ZmAMF1;1* and *ZmAMF1;2* under the *PMA1* promoter was able to rescue the growth of yeast under high ammonium concentrations (37.8 mM) and at low potassium supply (~7.3 mM), whereas the empty *PDR196* control and *ScAMF1* were not able to grow (Figure 4.5A, B). When ammonium was removed from the medium and amino acids supplied, all yeast transformations grew even though there was only 7.3 mM K^+ supplied in the YNB medium (Figure 4.5C, 4.6).

The relationship between ammonium toxicity and potassium limitation has been reported previously in yeast (Hess et al., 2006). Yeast have been found to suffer from ammonium toxicity when low levels of potassium are supplied or genes responsible for ammonium transport are overexpressed (Hess et al., 2006). It was proposed that as external potassium decreased, ammonium could leak into the cells via potassium channels following concentration gradients. Detoxification of excess cellular ammonium occurred through the excretion of amino acids (Hess et al., 2006). TRK1 has previously been found to be involved in ammonium tolerance in yeast by facilitating potassium influx at the expense of ammonium (Reisser et al., 2013). In the *trk1*Δ *trk2*Δ yeast strain, a non-selective cation channel activity (NSC1) was found to conduct low affinity potassium transport, but it has also been found that ammonium can pass through this channel (Bihler et al., 2002). In addition, when external ammonium concentration is high, more NH_3 can diffuse into the cell directly via plasma membrane, and then diffuse into the vacuole across the vacuole membrane. As the vacuole is more acidic than the cytoplasm, NH_3 diffused into the vacuole will be protonated to NH_4^+. Ammonium accumulation in the vacuole could collapse the pH gradient between the vacuole and cytoplasm, which may then affect the accumulation of other substrates in the vacuole and potentially cause toxicity in the cell cytoplasm.

ZmAMF1;1 and ZmAMF1;2 were found to be localized on the tonoplast in tobacco epidermal cells, and AtAMF2 was found to be localized on the tonoplast in both yeast and tobacco (Apriadi Situmorang unpublished results). We hypothesise that ZmAMF1;1 and ZmAMF1;2 are functioning as an NH_4^+/H^+

anitporter on the tonoplast in yeast to facilitate ammonium efflux from the vacuole in the exchange of proton. The exchange of proton into the vacuole can recover the pH gradient between vacuole and cytoplasm. We think that the detoxification of ammonium toxicity in yeast by excreting amino acids will potentially cause nitrogen starvation of the yeast, continued release of ammonium from the vacuole to the cytoplasm by ZmAMF1;1 and ZmAMF1;2 may overcome cellular nitrogen starvation.

The hypothesis that ZmAMF1;1 and ZmAMF1;2 facilitate ammonium efflux from the vacuole to cytoplasm can also be verified with experiments using methylammonium (MA) in CY162. CY162 transformed with ZmAMF1;1 and ZmAMF1;2 were found to be more susceptible to MA when grown under low potassium concentrations (Figure 4.8). This could be due to the export of MA from the vacuole to the cytoplasm by ZmAMF1;1 and ZmAMF1;2 inducing cellular toxicity. In addition, the lack of sensitivity to MA in the ammonium transport deficient strain 26972c, also supported the fact that ZmAMF1;1 and ZmAMF1;2 are localized to the tonoplast limiting MA uptake into the cell. We tested for ammonium sensitivity by adding increasing amounts of ammonium sulfate into the medium at pH 4.5 and 6.1. We found that yeast cells always grew better at pH 6.1 and became sensitive to ammonium when the ammonium sulfate concentration increased to 5 mM at low pH (4.5) (Figure 4.7). This could be that *trk1* Δ *trk2* Δ yeast cells are sensitive to low pH, and cannot transport sufficient potassium efficiently under low pH (Ko and Gaber, 1991). However the reasons why external pH influenced ZmAMF1;1 and ZmAMF1;2 activity remains unclear.

Ammonium and potassium competition has also been studied in plants. Plants suffer from ammonium toxicity when using ammonium as sole nitrogen source a problem compounded with low amounts of potassium are available (Hoopen et al., 2010). The functional analysis of ZmAMF1;1 and ZmAMF1;2 needs to be further studied in maize plants to test whether their activities are able to overcome ammonium toxicities.

Chapter 5 Functional analysis of *ZmAMF1;1* and *ZmAMF1;2* in TUSC lines

5.1 Introduction

Over the course of this PhD program, each of the AMF TUSC lines were transitioned to a uniform GASPE background with repetitive backcrosses and continued selection for the TUSC alleles. After the third backcross the lines were self-pollinated and genotyped to identify homozygous lines for ADL 112 and 114 (*ZmAMF1;1* TUSC line mutants) and ADL 119 (*ZmAMF1;2* TUSC line mutant). A double mutant was then generated by crossing ADL 112 with ADL 119 (chapter 3). With each of these transitions, seed numbers were often the limiting factor in the speed by which the crossing program advanced. For the double mutant, two rounds of self-pollination and seed collection were required to generate a small sample of seed to conduct physiological analysis of the lines.

As ScAMF1 and GmAMF3 have been identified as low affinity ammonium transporters (Chiasson et al., 2014), ammonium is the main focus to study for the function of *ZmAMF1;1* and *ZmAMF1;2*. In this chapter, both mutants (single or double) and the wild-type GASPE were examined for changes in plant growth at low and adequate nitrogen provision and an analysis of nitrogen transport changes evaluated using stable isotopes. With these experiments, we wanted to investigate:

1) The effects that loss of *ZmAMF1;1* or *ZmAMF1;2*, or both have on ammonium uptake.
2) Whether loss of *ZmAMF1;1* or *ZmAMF1;2*, or both affect plant growth and nitrogen content inside plants.

5.2 Materials and Methods

5.2.1 Plant growth

TUSC seeds for ADL 112, 114, 119, the double mutant and the wild-type GASPE were surface sterilized with 70% (v/v) ethanol for 1 min, then submerged in 0.5% (v/v) sodium hypochlorite (Chem-supply) for 20min. Seeds were rinsed with RO water 5 times, and then soaked in RO water with aeration for 4 h. Seeds were placed into prewashed vermiculite to germinate in a temperature-controlled growth chamber for 4 days. Germinated seedlings (~1 cm tall shoots) were transferred to a recirculating hydroponics system. The hydroponics system was same as described in 3.2.5.1. Plants were grown with two nitrogen levels: 0.5 and 5 mM NH_4NO_3, supplemented with basal nutrients, including $MgSO_4 \cdot 7H_2O$ 0.5 mM, KH_2PO_4 0.5 mM, H_3BO_3 25 µM, $MnSO_4 \cdot H_2O$ 2 µM, $ZnSO_4 \cdot 7H_2O$ 2 µM, $CuSO_4 \cdot 5H_2O$ 0.5 µM, $Na_2MoO_4 \cdot 2H_2O$ 0.5 µM, KCl 1.05 mM, Fe-EDTA 0.1 mM, Fe-EDDHA 0.1 mM, K_2SO_4 1.25 mM, $CaCl_2 \cdot 2H_2O$ 0.25 mM, $CaSO_4 \cdot 2H_2O$ 1.75 mM (pH 5.5). Nutrient solutions were changed weekly.

5.2.2 flux measurement

Ammonium uptake (flux) measurements were conducted using ^{15}N-labelled NH_4^+ between 11:00 am and 1:00 pm. Each experiment was conducted on

seedlings 15 days after the radical emerged from germinating seeds. For each flux experiment, plants were first immersed in complete nutrient solution containing either 50 μM or 2.5 mM $(NH_4)_2SO_4$ for 10 min. After the pre-incubation the plants roots were transferred to same nutrient solutions but supplemented with labelled ^{15}N-labelled $(NH_4)_2SO_4$ (10% ^{15}N) at a final concentration of 50 μM or 2.5 mM of $(NH_4)_2SO_4$. After 10 minutes, plants transferred to unlabelled 50 μM or 2.5 mM $(NH_4)_2SO_4$ nutrient solutions for 5 min. Shoot and roots were harvested separately, and quickly weighed and then frozen individually in liquid nitrogen and stored at -80°C. Frozen shoot and root samples were ground frozen using a Genogrinder (SPEX SamplePrep). An aliquot of the frozen powder was used for RNA extraction, with the remainder lyophilized using a -50°C freeze drier. The dried samples (around 1.3 mg) were used to determine total N and ^{15}N content using an isotope ratio mass spectrometer as described by Garnett *et al.* (2013).

5.3 Results

5.3.1 The impact of a single mutation in *Zmamf1;1* and *Zmamf1;2* on plant growth and ammonium uptake.

Preliminary growth responses of the two *ZmAMF1;1* mutants (ADL 112 and ADL 114) was calculated through measurements of shoot and root fresh weights from plants grown hydroponically in complete nutrient solutions containing either 0.5 or 5 mM NH_4NO_3. In ADL 112, shoot fresh weights increased significantly (~ 1.3-fold) but with significant lower (~ 1.3-fold) root fresh weight when plants were grown on 5 mM NH_4NO_3 compared to the GASPE control (Table 5.1). In ADL 114,

both the shoot and root fresh weights were considerably higher (~ 1.2-fold) than GASPE under 5 mM NH_4NO_3 growth environment, and these differences were more remarkable on the 26th day after emergence, where ADL 114 had significantly higher (1.7 to 2.2-fold) shoot and root fresh weight compared to GASPE plants grown on both NH_4NO_3 nutrient solutions (Table 5.2). Root nitrogen content was also measured across the mutants and GASPE. ADL 112 had a drop of root nitrogen content compared to the GASPE control under both 0.5 and 5 mM NH_4NO_3 supply (12% and 4% respectively, Table 5.1). Similarly, ADL 114 showed a decrease in root nitrogen content on both 15th day and 26th day (8% and 20% respectively) compared to GASPE but only in plants grown in 0.5 mM NH_4NO_3 (Table 5.3).

Changes to ammonium uptake was investigated in ADL 112 and ADL 114 lines at external concentration of 50 µM or 2.5 mM $(NH_4)_2SO_4$ (100 µM or 5 mM NH_4^+, 10% ^{15}N) when plants were grown in nutrient solutions containing either 0.5 or 5mM NH_4NO_3. In ADL 112, there was nearly 10% reduction in low-affinity (5 mM NH_4^+) uptake compared to GASPE when grown with 5mM NH_4NO_3 (Figure 5.1). There were no differences in the high-affinity range or when plants were grown at low external nitrogen concentrations. In contrast, ADL 114 showed a reduction (20-26%) in high-affinity ammonium uptake only on plants grown at elevated nitrogen concentrations (Figure 5.2).

The impact of the *ZmAMF1;2* mutation was also determined in line ADL 119 relative to the control line GASPE. ADL 119 showed significantly higher shoot fresh weights (1.5 to 1.9-fold) compared to GASPE when grown with 0.5 or 5mM NH_4NO_3 (Table 5.4). ADL 119 showed an increased rate (around 2-fold) of

ammonium uptake in the high-affinity range when plants were grown at low external nitrogen (1.0 mM N) (Figure 5.3). All other ammonium flux rates were similar to GASPE. There were no differences in root nitrogen content relative to GASPE across all of the growth treatments (Table 5.4).

A second study was initiated to re-evaluate the changes in high-affinity ammonium uptake in ADL 119. Plants were grown in a similar manner with 0.5 or 5 mM NH_4NO_3 until 11 d after emergence. Half amount of the plants grown in 5 mM NH_4NO_3 were then grown 4 days starved of nitrogen, while the others continued a further 4 d with the same nitrogen provision. On 15 d, ammonium uptake was measured in the high-affinity range (100 μM) across all three nitrogen treatments. With each treatment, ADL 119 continued to have a higher (~ 1.5 to 2.2-fold) ammonium uptake rate in the high-affinity range than the control, GASPE (Figure 5.4). Analysis of the plant growth showed that ADL 119 when starved of nitrogen retained its shoot growth rate while GASPE plants appeared to stop growing (Table 5.5). Root nitrogen content in ADL 119 was significantly higher (5%) than GASPE under 0.5mM NH_4NO_3 supply (Table 5.5).

5.3.2 The impact of mutation of both *Zmamf1;1* or *Zmamf1;2* on plant growth and ammonium uptake.

To further understand the role of ZmAMF1;1 and ZmAMF1;2 on maize ammonium transport, plant growth and root nitrogen content, a double AMF1 mutant was generated by crossing ADL 112 and ADL 119. Remarkably, the double mutant performed considerably better than the GASPE control on many fronts. The double mutant displayed much higher high and low affinity

ammonium transport (around 1.4 to 3.3-fold) than the GASPE controls when grown either on 0.5 or 5 mM NH_4NO_3 nutrient solution (Figure 5.5). The double mutant also had significantly higher (~1.4-fold) shoot fresh weights and an elevated (~ 4% to 8% increase) root nitrogen content relative to GASPE (Table 5.6).

Table 5.1 ADL 112 and GASPE fresh weight and total root nitrogen content

Growth condition	ADL 112			GASPE		
	Fresh weight (g)		Root total N (%)	Fresh weight		Root total N (%)
	Shoot	Root		Shoot	Root	
0.5 mM NH_4NO_3	3.47±0.22	1.30±0.09	4.22±0.04	3.03±0.27	1.65±0.15	4.78±0.09***
5 mM NH_4NO_3	4.82±0.24**	1.28±0.07	5.74±0.08	3.70±0.21	1.60±0.07*	6.00±0.03*

ADL 112 and GASPE were grown in nutrient solution containing either 0.5 mM NH_4NO_3 or 5 mM NH_4NO_3. Values= mean ± SEM (n = 10). Plants were harvested on the 15th day after seeds showed an emerged radical. The significant difference of shoot and root fresh weight, and total root nitrogen (N) content between ADL 112 and GASPE are represented by star (unpaired t test with Welch's correction, $p< 0.05$).

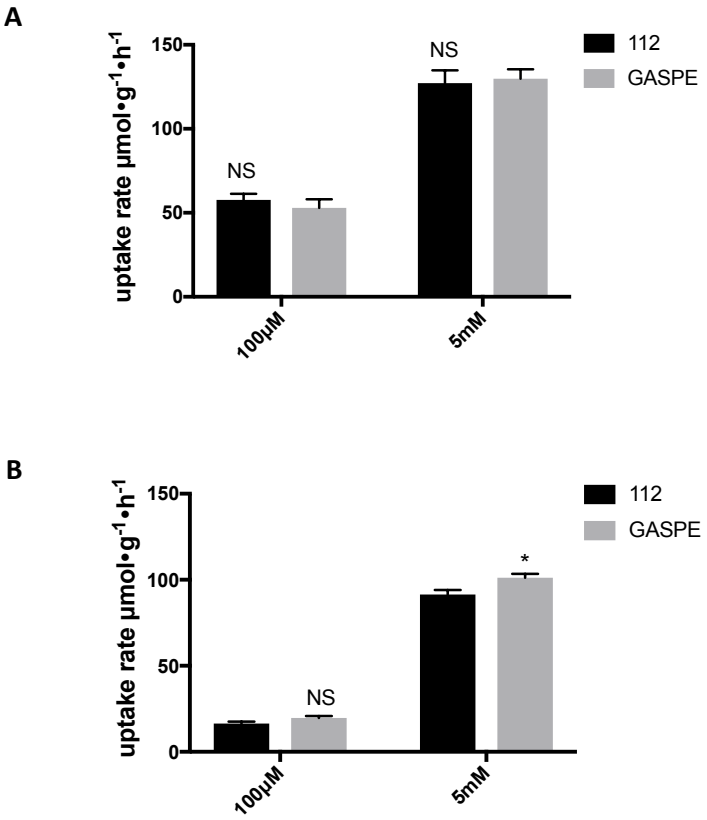

Figure 5.1 $^{15}NH_4^+$ uptake rate in TUSC line ADL 112 and GASPE

ADL 112 and GASPE plants were grown in nutrient solution with either 0.5 mM NH_4NO_3 (A) or 5 mM NH_4NO_3 (B). Ammonium flux was measured using ^{15}N labeled $(NH_4)_2SO_4$ (10% ^{15}N) at either 100 µM NH_4^+ or 5 mM NH_4^+ for 10 min on the 15th day after radical emergence. Values = mean ± SEM (n= 5 plants). The significant difference was represented by star (unpaired t test with Welch's correction, $p< 0.05$), NS = no significant difference.

Table 5.2 Fresh weight comparison between ADL 114 and GASPE

Harvest time	Growth condition NH_4NO_3	ADL 114		GASPE	
		Fresh weight (g)		Fresh weight (g)	
		Shoot	Root	Shoot	Root
15th day	0.5 mM	11.17±0.37	7.89±0.13	10.78±0.32	7.79±0.18
	5 mM	11.47±0.32 ****	7.85±0.11****	9.19±0.28	6.97±0.10
26th day	0.5 mM	37.16±2.11****	13.29±1.76**	17.99±2.25	6.25±0.80
	5 mM	35.97±2.80**	11.57±0.93****	20.81±2.52	5.16±0.16

ADL 114 and GASPE values = mean ± SEM (n = 10 plants). Plants were harvested on the 15th and 26th day after radical emergence. The significant differences of shoot and root fresh weight between ADL 114 and GASPE were represented by star (unpaired t test with Welch's correction, $p< 0.05$).

Table 5.3 Root total nitrogen content of ADL 114 and GASPE

Harvest time	Growth condition	Root total N (%)	
		114	GASPE
15th day	0.5 mM NH_4NO_3	4.12±0.04	4.50±0.09**
	5 mM NH_4NO_3	5.60±0.13	5.74±0.05
26th day	0.5 mM NH_4NO_3	2.26±0.11	2.85±0.17*
	5 mM NH_4NO_3	4.94±0.06	5.06±0.09

ADL 114 and GASPE were grown in nutrient solution in either 0.5 mM NH_4NO_3 or 5 mM NH_4NO_3. Values= mean ± SEM (n = 10 plants). Plants were harvested on the 15th and 26th day after radical emergence. The significant difference of root total nitrogen (N) content between ADL 114 and GASPE were represented by star (unpaired t test with Welch's correction, $p < 0.05$).

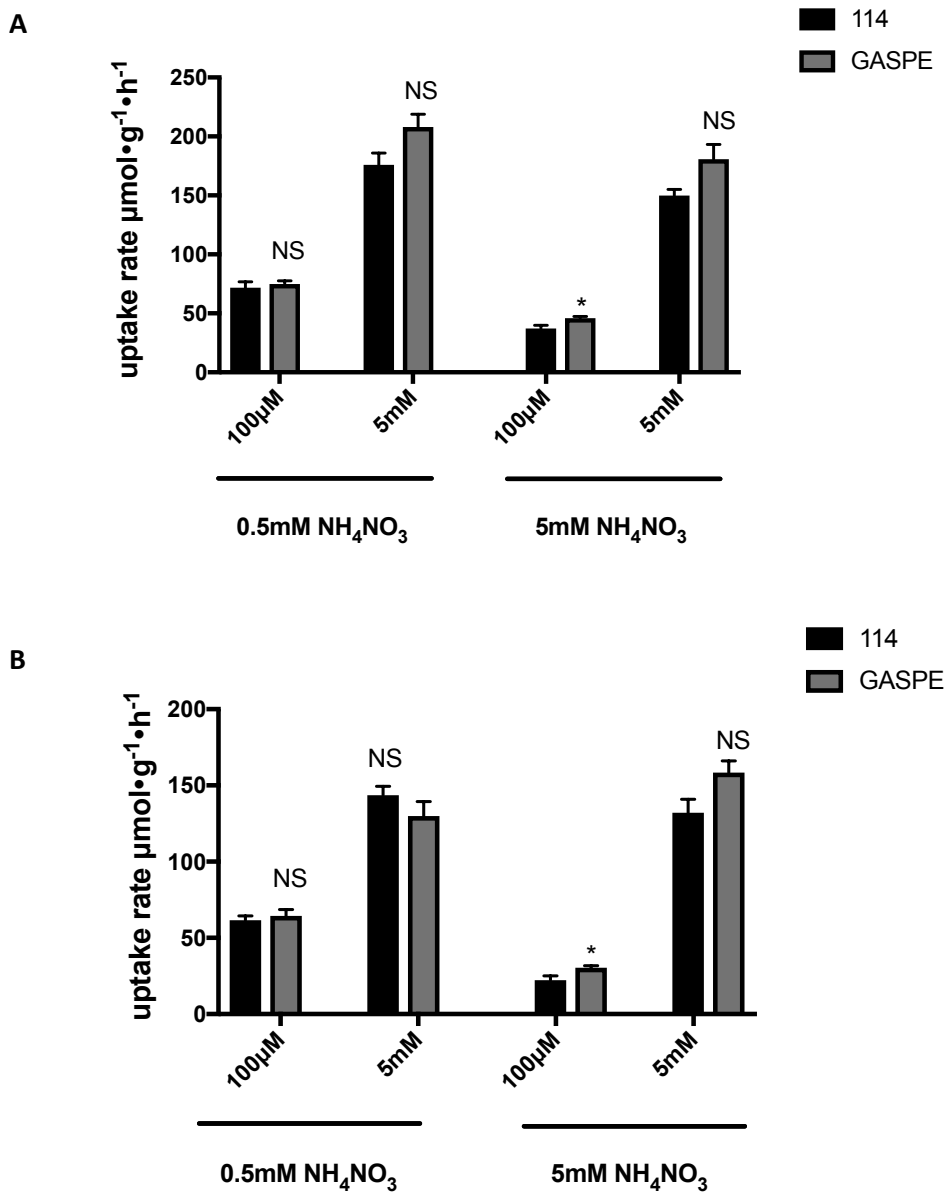

Figure 5.2 $^{15}NH_4^+$ uptake rate in TUSC line ADL 114 and GASPE

ADL 114 and GASPE plants were grown in nutrient solution in either 0.5 mM NH_4NO_3 or 5 mM NH_4NO_3. Ammonium flux was measured using ^{15}N labeled $(NH_4)_2SO_4$ (10% ^{15}N) at either 100 µM NH_4^+ or 5 mM NH_4^+ for 10 min on the 15th (A) and 26th (B) day after root emergence. Values = mean ± SEM (n= 3 to 5 plants). The significant difference was represented by star (unpaired t test with Welch's correction, $p< 0.05$), NS= no significant difference.

Table 5.4 ADL 119 and GASPE fresh weight and root total nitrogen content comparison

Growth condition	ADL 119			GASPE		
	Fresh weight (g)		Root total N (%)	Fresh weight		Root total N (%)
	Shoot	Root		Shoot	Root	
0.5 mM NH_4NO_3	3.68±0.30***	1.22±0.09*	4.29±0.19	1.94±0.22	0.93±0.07	4.50±0.09
5 mM NH_4NO_3	5.01±0.28***	1.18±0.08	6.03±0.07	3.43±0.25	1.13±0.09	5.82±0.07

ADL 119 and GASPE were grown in nutrient solution in either 0.5 mM NH_4NO_3 or 5 mM NH_4NO_3. Values = mean ± SEM (n= 7 to 10 plants). Plants were harvested on the 15th day after emergence. The significant difference of shoot and root fresh weight, and total root nitrogen (N) content between ADL 119 and GASPE were represented by a star (unpaired t test with Welch's correction, $p< 0.05$).

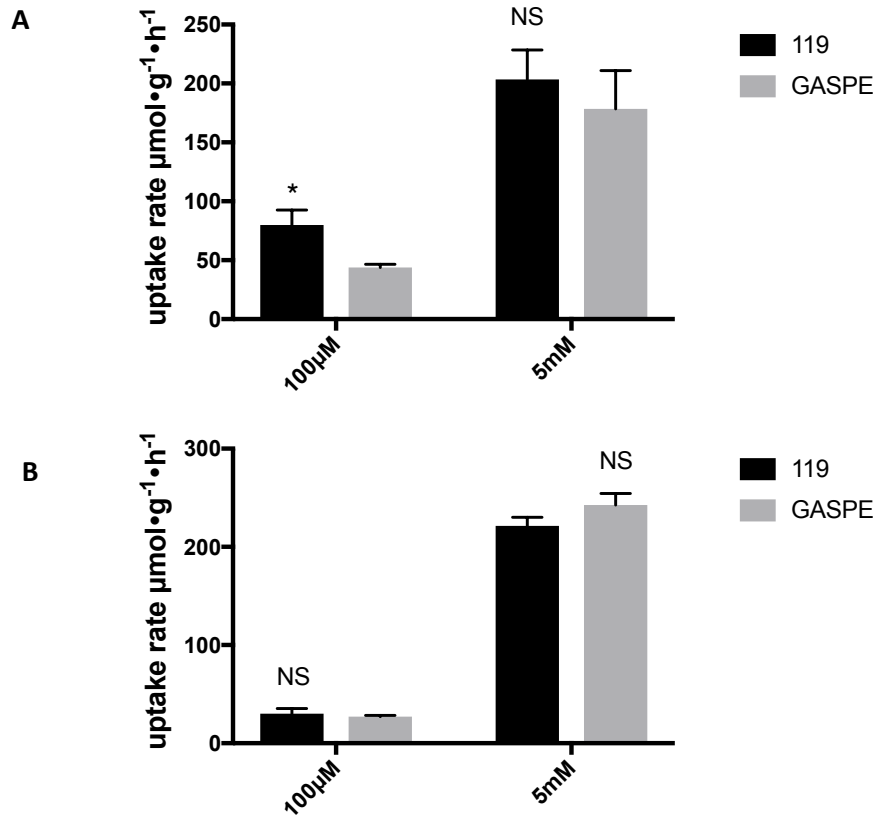

Figure 5.3 $^{15}NH_4^+$ uptake rate in TUSC line ADL 119 and GASPE

ADL 119 and GASPE plants were grown in nutrient solution in either 0.5 mM NH_4NO_3 (A) or 5 mM NH_4NO_3 (B). Ammonium flux was measured using ^{15}N labeled $(NH_4)_2SO_4$ (10% ^{15}N) at either 100 µM NH_4^+ or 5 mM NH_4^+ for 10 min on the 15th day after radical emergence. Values = mean ± SEM (n= 2 to 5 plants). The significant difference was represented by a star (unpaired t test with Welch's correction, $p< 0.05$), NS = no significant difference.

Table 5.5 ADL 119 and GASPE fresh weight and root total nitrogen content comparison under different nitrogen supply

Growth condition	ADL 119			GASPE		
	Fresh weight (g)		Root total N (%)	Fresh weight		Root total N (%)
	Shoot	Root		Shoot	Root	
0.5 mM NH_4NO_3	2.46±0.19	1.07±0.09	4.65±0.07*	1.82±0.22	0.90±0.11	4.42±0.07
5 mM NH_4NO_3	2.54±0.15	0.83±0.03	5.82±0.07	1.81±0.27	0.64±0.13	5.58±0.10
N starvation	2.24±0.15**	1.13±0.07*	2.85±0.06	1.52±0.10	0.84±0.06	2.68±0.04

ADL 119 and GASPE plants were grown in nutrient solution in either 0.5 mM NH_4NO_3 or 5 mM NH_4NO_3 until the 11th day after root emergence, and on the 11th day kept in solution or transferred to a nitrogen free nutrient solution for 4 days. Values = mean ± SEM (n= 6 to 10 plants). The significant difference between GASPE and ADL 119 under same growth condition in shoot or root fresh weight and root total N content were represented by a star (unpaired t test with Welch's correction, $p< 0.05$), NS = no significant difference.

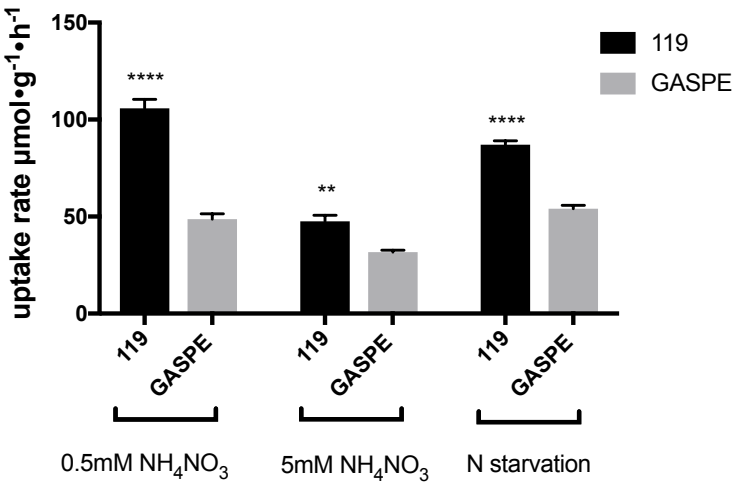

Figure 5.4 $^{15}NH_4^+$ uptake rate in TUSC line ADL 119 and GASPE under different nitrogen condition

ADL 119 and GASPE plants were grown in nutrient solution in either 0.5 mM NH_4NO_3 or 5 mM NH_4NO_3 until the 11th day after root emergence, and on the 11th day kept in solution or transferred to a nitrogen free nutrient solution. Ammonium flux was measured using ^{15}N labeled $(NH_4)_2SO_4$ (10% ^{15}N) at 100 µM NH_4^+ on the 15th day after radical emergence. Values = mean ± SEM (n= 6 to 10 plants). The significant difference was represented by star (unpaired t test with Welch's correction, $p< 0.05$), NS = no significant difference.

Table 5.6 Double mutant and GASPE fresh weight and root total nitrogen content

Growth condition	Double mutant			GASPE		
	Fresh weight (g)		Root total N (%)	Fresh weight (g)		Root total N (%)
	Shoot	Root		Shoot	Root	
0.5 mM NH_4NO_3	3.27±0.19 ***	1.18±0.08	5.11±0.06 ****	2.23±0.12	1.09±0.06	4.72±0.05
5 mM NH_4NO_3	2.05±0.12 **	0.59±0.03	5.69±0.06 **	1.50±0.13	0.55±0.04	5.46±0.05

Double mutant and GASPE were grown in nutrient solution in either 0.5 mM NH_4NO_3 or 5 mM NH_4NO_3. Values = mean ± SEM (n = 12 to 16 plants). Plants were harvested on the 15th day after root emergence. Significant differences in shoot and root fresh weight, and total root nitrogen (N) content between double mutant and GASPE are represented by star (unpaired t test with Welch's correction, $p < 0.05$).

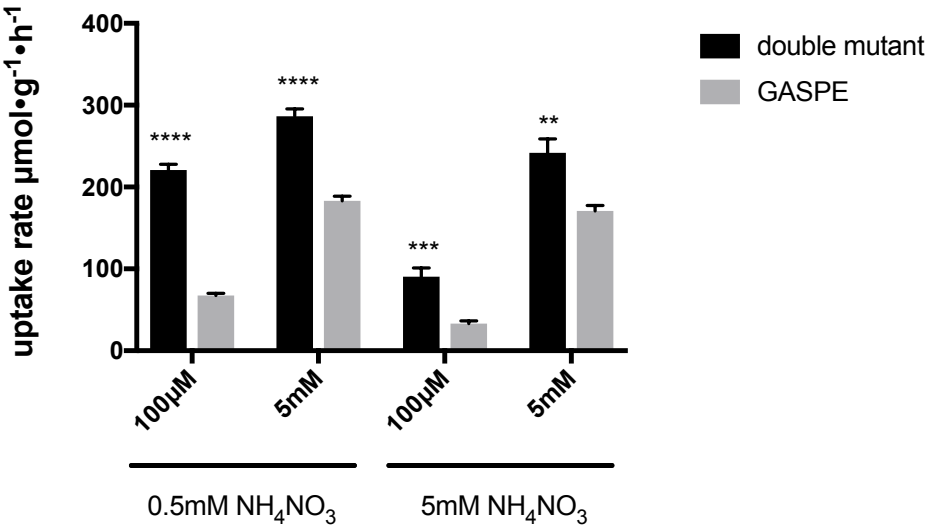

Figure 5.5 $^{15}NH_4^+$ uptake rate in TUSC line double mutant and GASPE

Double mutant and GASPE plants were grown in nutrient solution in either 0.5 mM NH_4NO_3 or 5 mM NH_4NO_3. Ammonium flux was measured using ^{15}N labeled $(NH_4)_2SO_4$ (10% ^{15}N) at either 100 µM NH_4^+ or 5 mM NH_4^+ for 10 min on the 15th day after radical emergence. Values = mean ± SEM (n = 6 to 8 plants). The significant difference was represented by star (unpaired t test with Welch's correction, $p < 0.05$), NS = no significant difference.

5.4 Discussion

The development of the AMF1 TUSC lines was initiated to provide tools to help better understand how the loss of ZmAMF1;1 and ZmAMF1;2 alone or together would influence maize growth and specifically root ammonium transport activities. Homozygous TUSC lines (ADL 114, 119, 112) backcrossed to GASPE (BC3) were grown using a hydroponic system previously used to demonstrate ammonium and nitrate transport in GASPE and other maize lines (Garnett et al., 2013). Ammonium transport was measured in young seedlings using ^{15}N-labelled $(NH_4)_2SO_4$ (10% ^{15}N) at 50 μM or 2.5 mM for 10 min. In both the single TUSC mutants (ADL 112 and ADL 114) the loss of *ZmAMF1;1* revealed small changes in ammonium uptake (Figure 5.1 and 5.2). In contrast, ADL 119 (*Zmamf1;2*) displayed a consistently greater (~1.5 to 2.2-fold) high-affinity ammonium uptake rate in plants grown in 0.5 or 5 mM NH_4NO_3 or when starved of nitrogen for 4 days (Figure 5.4). A double mutant line developed from a cross between ADL 112 and ADL 119, showed much higher ammonium uptake at both high affinity (around 3-fold) and low affinity (around 1.5-fold) concentrations regardless of the preliminary nitrogen treatment compare to GASPE (Figure 5.5). These changes to ammonium transport, particularly that observed with the double mutant was unexpected. As ScAMF1 and GmAMF3 have been both characterized as ammonium influx channels, we assumed there would be less uptake in the ZmAMF1 mutants not more. However, if these classes of AMF1 proteins in maize have a different functional role that differs from primary influx into root epidermal or cortical cells, possibly efflux or export to the shoot, then a

loss of AMF1 function could still influence short-term transient accumulation of ammonium when tested by unidirectional ^{15}N-ammonium influx assays.

Recently, ZmAMF1;1 and ZmAMF1;2 were both found to be localized on the tonoplast in tobacco (Apriadi Situmorang unpublished results). In this study, we observed enhanced growth when both AMF1 proteins were disrupted. This may be due to the loss of ZmAMF1;1 and ZmAMF1;2 resulting in a potential change in the transport of ammonium into or out of the vacuole. The yeast studies (Chapter 4) have suggested AMF1 involvement in vacuolar NH_4^+ homeostasis, possibly acting as a H^+-dependent NH_4^+ efflux channel. If AMF1 is involved in regulating vacuolar ammonium sequestration then a disruption of this process could result in a preferential increase in vacuole ammonium acquisition at the tissue level (roots versus shoots), and decrease the vacuolar sequestration ability (VSA) in roots. The vacuolar sequestration ability has been found to be related to the long distance transport of the nutrient from root to shoot (Peng and Gong, 2014). The decrease of VSA due to the loss of ZmAMF1;1 and ZmAMF1;2 may promote the translocation of nitrogen from root to shoot, and improve the shoot growth which we observed in the mutants. The apparent increase in root nitrogen content and ammonium influx in the ZmAMF1 mutant lines could be a response to the loss of vacuolar ammonium efflux control and ultimately increased nitrogen accumulation in the root. We can now hypothesise that ZmAMF1;1 and ZmAMF1;2 may act as putative ammonium efflux protein localized on the tonoplast potentially as an NH_4^+/ H^+ antiporter as suggested when expressed in CY162 yeast cells.

Plants suffer from ammonium toxicity when grown with potassium deficiencies

(Barker et al., 1967; Cao et al., 1993; Santa-Marıa et al., 2000; Szczerba et al., 2008; Hoopen et al., 2010). High ammonium supply under potassium deficiency inhibits plant growth, however this inhibition can be reversed when potassium is provided to the plants. This response is accompanied with a decrease in soluble ammonium concentrations and an increase of tissue potassium content resulting from an increase in potassium influx and translocation of potassium to the shoot (Cao et al., 1993; Santa-Marıa et al., 2000; Szczerba et al., 2008). The negative correlation between potassium and ammonium flux has been found in both ammonium sensitive (barley) and tolerant plants (rice) (Santa-Marıa et al., 2000; Szczerba et al., 2008; Hoopen et al., 2010). In rice, the low affinity potassium uptake pathway was linked to the efflux of ammonium, where the efflux:influx ratio decreases from ~90% to <70% when potassium supply increased from 0.02 to 5 mM and with 10 mM NH_4^+ being present (Szczerba et al., 2008). In barley, when external ammonium concentrations are high, an energy dependent ammonium efflux mechanism is activated, where as much as 80% of the primary influx of ammonium is rapidly effluxed from the cytoplasm into the root apoplast, a process accompanied by a decline of plant growth (Britto et al., 2001). This energy consuming process has been proposed as a central syndrome of ammonium toxicity in barley and other species that are susceptible to ammonium toxicity (Britto et al., 2001). The molecular identity of this transport activity has yet to be identified.

The results from the yeast study (Chapter 4) showed that ZmAMF1;1 and ZmAMF1;2 rescued growth in the presence of high ammonium concentrations under low potassium supply and a depleted high and low affinity potassium

transport capacity. Further studies will be required to test whether this recovery is linked to enhanced potassium uptake. Other studies that look at ammonium toxicity-linked respirational costs with the loss of AMF1 will be required.

Chapter 6 *ZmAMF1;1* and *ZmAMF1;2* gene expression

6.1 Introduction

6.1.1 Plant ammonium transporter expression in response to nitrogen and shows tissue specific expression

High-affinity ammonium transport in biological systems is mediated by members of the transport superfamily, AMT/MEP/Rh (Ammonium Transporter/ Methylammonium Permease / Rhesus) (Nacry et al., 2013). In plants, members of the *AMT1* and *AMT2* family have been identified and functionally characterized (Sohlenkamp et al., 2002; Ludewig et al., 2007; De Michele et al., 2012). The expression patterns of *AMT* genes vary within families, including those showing constitutive expression to ones that respond to the presence or absence of nitrogen. Arabidopsis roots increase their ammonium uptake after nitrogen starvation a process which is accompanied with the upregulation of *AtAMT1;1* expression (5-fold). However when resupplied nitrogen, *AtAMT1;1* expression is quickly repressed. *AtAMT1;3* shows a smaller increase in expression under nitrogen starvation while *AtAMT1;2* showing a stable expression (Gazzarrini et al., 1999; Shelden et al., 2001). Since *AtAMT1;1* expression increases under nitrogen starvation and correspondingly decreases with the resupply of nitrogen, it was proposed that AtAMT1;1 was the primary ammonium transport pathway under nitrogen starvation conditions (Gazzarrini

et al., 1999), and its quick repression by nitrogen resupply has been proposed to be a mechanism to avoid ammonium toxicity (Yuan et al., 2007a). *AtAMT1;1* is expressed in both shoots and roots, while *AtAMT1;3* shows exclusively expression in roots. *AtAMT1;2* expression is primarily in the roots with weak expression in stem and leaves (Gazzarrini et al., 1999). At the cellular level, *AtAMT1;1* and *AtAMT1;3* are expressed in rhizodermal cells and root hairs, while AtAMT1;2 is expressed in the endodermis and root cortex. The outer root cell localized AtAMT1;1 and AtAMT1;3 have a higher affinity to ammonium (50 and 61μM respectively) compared to AtAMT1;2 (the affinity is 234 μM) (Yuan et al., 2007b). The AtAMT2;1 homolog is closer to the MEP/ AmtB subfamily found in yeast and bacteria and also functions as high affinity ammonium transporter (Sohlenkamp et al., 2002; Loque et al., 2007), although it has not been shown to contribute to overall ammonium uptake in Arabidopsis (Yuan et al., 2007b). *AtAMT2;1* expression occurs in both shoot and root, increasing in roots under nitrogen starvation and decreasing with nitrate resupply. *AtAMT2;1* expression occurs in the vascular tissues of roots, leaves and flowers (Sohlenkamp et al., 2002).

In maize, the AMT response to nitrogen is slightly different to that of Arabidopsis. AMT genes show substrate-inducible expression where transcription of *ZmAMT1;1a* and *ZmAMT1;3* decreases under nitrogen deficiency but transiently increases with the resupply of ammonium. After 24h resupply of ammonium, the expression level of *ZmAMT1;1a* and *ZmAMT1;3* started to decline, and this repression of *ZmAMT1;1a* and *ZmAMT1;3* expression in maize is thought to occur as a result of a negative feedback inhibition caused by the increased availability

of reduced nitrogen metabolites, such as glutamine. This has been explained as a process to avoid ammonium toxicity during periods of excessive ammonium uptake (Glass et al., 2002). In tomato (*LeAMT1;2)* and rice (*OsAMT1;2*) *AMT1* genes show increased expression with a re-supply of ammonium, while other *AMT1* genes have shown a reduction in expression and a corresponding induction with extended nitrogen starvation (Von Wirén et al., 2000; Sonoda et al., 2003). At the tissue level, maize *AMT1* expression can vary between roots, shoots and flowering tissues. In maize seedlings, *ZmAMT1;1a* is expressed in both roots and shoots, while *ZmAMT1;3* is mainly expressed in roots. *ZmAMT1;1b* shows weak expression in shoots (Gu et al., 2013). *ZmAMT1;1* is highly expressed in both root and shoot tissues at levels well in excess of both *ZmAMT1;1b* and *ZmAMT1;3*. At the silking stage, *ZmAMT1;1* shows high expression in the tassel, while *ZmAMT1;1b* is more expressed in immature ears, while *ZmAMT1;3* less expressed. At the post pollination stage, *ZmAMT1;1a* has the highest expression in the ear leaf, whereas *ZmAMT1;3* is more expressed in both young and ear leaves (Gu et al., 2013). At the cellular level, *ZmAMT1;1* and *ZmAMT1;3* are expressed in the epidermal cells of roots while *ZmAMT1;3* is also expressed in the root stele especially in the pericycle cell layer.

Currently, the response of AMF1 to nitrogen status and their tissue level expression pattern remains to be discovered. In this chapter, the effects of different nitrogen treatments on the expression of *ZmAMF1;1* and *ZmAMF1;2* was studied, and the expression of *ZmAMF1;1* and *ZmAMF1;2* were also studied in GASPE across different shoot parts and different growth stages.

6.1.2 AMF1 expression and cellular localization

AMF1 has been suggested to be a low-affinity ammonium transport system. Unfortunately, little is known about the genetic response of *AMF1* to internal or external nitrogen status. Currently, the localization of an AMF1 protein has been studied in yeast and soybean. In soybean, using the *GmAMF3* promoter fused to a GUS reporter, GUS activity was detected in both nodules and roots. In nodules, GUS staining was found in cells surrounding the vascular bundles and also in the nodule parenchyma cell layer (Chiasson et al., 2014). In root tissues, *GmAMF3* expression was predominantly in the stele and more specifically the cell layer located between the xylem and phloem (Chiasson, 2012). In yeast, when ScAMF1 was fused with a N terminal GFP tag it was found localized on the plasma membrane (Mazurkiewicz, 2013; Chiasson et al., 2014). When GmAMF3 was expressed with a YFP tag in onion epidermal cells, the expression was also found on plasma membrane (Chiasson et al., 2014).

Previous findings in Chapter 5 described the possibility that ZmAMF1;1 and ZmAMF1;2 are putative NH_4^+/H^+ antiporter on the tonoplast and facilitate ammonium efflux from the vacuole to cytoplasm in maize. To further understand the function of these two proteins, their expression patterns were examined in maize plants exposed to variable nitrogen treatments, and the cellular localization of ZmAMF1;1 and ZmAMF1;2 in maize root was investigated by *in situ* PCR.

6.2 Materials and methods

6.2.1 *ZmAMF1;1* and *ZmAMF1;2* gene expression in response to nitrogen supply

6.2.1.1 Plant growth condition

B73 seeds were submerged in Reverse Osmosis (RO) water aerated by air stone and pump for 4h, and then placed into wet diatomite to germinate in a temperature controlled growth chamber for 4 days. The growth chamber had a day and night temperature of 28°C/25°C. The plants were provided a 12h light cycle with 1000 W metal halide lamps providing at pot level 400 µmol m^{-2} s^{-1} light intensity. The chambers were maintained with a relative humidity of 80% in the day and 50% at night. A small hydroponics system was set up to germinate and grow the plants. The hydroponic system consisted of a low profile base tank (12L) covered by a plant support structure consisting of removable 5 cm ×5 cm square cut-outs containing a glued on mesh support collar. Germinated B73 seed were placed on the mesh collar with the emerged root penetrating the mesh and the filled tank below. Diatomite was used to cover the rest of the space of the mesh to stabilize plants as well as stop light getting into the nutrient solution. The nutrient solution was continually aerated with an air pump. Plants were initially grown in nutrient solution containing NH_4NO_3 2.5 mM, $MgSO_4 \cdot 7H_2O$ 0.5 mM, KH_2PO_4 0.5 mM, H_3BO_3 25 µM, $MnSO_4 \cdot H_2O$ 2 µM, $ZnSO_4 \cdot 7H_2O$ 2 µM, $CuSO_4 \cdot 5H_2O$ 0.5 µM, $Na_2MoO_4 \cdot 2H_2O$ 0.5 µM, KCl 1.05 mM, Fe-EDTA 0.1 mM, Fe-EDDHA 0.1 mM, K_2SO_4 1.25 mM, $CaCl_2 \cdot 2H_2O$ 0.25 mM, $CaSO_4 \cdot 2H_2O$ 1.75 mM (pH 5.5). After one week, plants were transferred to a nitrogen free nutrient solution for 4 days and then transferred to the same nutrient solution containing

either 2.5 mM $(NH_4)_2SO_4$, 5 mM KNO_3 or 2.5 mM NH_4NO_3 for 4h. Plants were harvested and root and shoots separated, weighed and then frozen in liquid nitrogen and stored at -80°C.

6.2.1.2 Real-time quantitative PCR

Total RNA was extracted from root and shoot tissues using Trizol reagent (Invitrogen) following the manufacturer's instructions. cDNA was synthesized using 1 µg of total RNA with SuperScript™ III Reverse Transcriptase (Invitrogen), according to the manufacturer's instructions. Primers (EF1A F1 and EF1A R1) were designed against the maize elongation factor gene *ZmElF1* (GRMZM2G154218) across an intron to check for genomic DNA contamination in all cDNA samples. To help minimise genomic DNA contamination, all RNA samples were treated with DNase I (RNase free) kit (New England Biolabs). Q-PCR primers were designed against the 3'UTR of *ZmAMF1;1* (primer ZmAMF1;1 qPCR F and R) and *ZmAMF1;2* (primer ZmAMF1;2 qPCR F and R). Three reference genes *ZmActin*, *ZmELF1* and *ZmGaPDh* were used, and the primers used for these genes were identical to those used by Garnett *et al.*(2013). With each Q-PCR assay, primer efficiencies were tested against a 10-fold dilution series developed from 1µl of the purified template cDNA. Each cDNA sample was then subjected to a 5-fold dilution series for Q-PCR reactions using SsoAdvanced™ Universal SYBR® Green Supermix (BioRad). PCR amplification was on a Mx3005p PCR machine (Agilent Technologies) with the following program setting: i) 30s at 95°C, ii) 40 cycles of 95°C for 10s, 60°C for 30s, iii) melt curve analysis of 95°C for 20s, 55°C for 30s and then 0.5°C temperature increase from 55°C to 95°C followed by final step at 95°C for 30s. The Ct values of 2 technical

replicates were averaged, and the efficiency was calculated from the standard curve using the $E = (10^{(-1/slope)})-1$ equation (Peirson et al., 2003). Primers with efficiencies between 90% and 110% were acceptable and used in subsequent qPCR analysis. The expression of *ZmAMF1;1* and *ZmAMF1;2* was calculated by mean Ct value of 5 biological replicates relative to the geometric average Ct of *ZmActin*, *ZmELF1* and *ZmGaPDh* (Vandesompele et al., 2002) with the equation of $2^{-\Delta Ct}$.

6.2.2 *ZmAMF1;1* and *ZmAMF1;2* expression pattern across GASPE different growth stages

6.2.2.1 Plant growth condition

GASPE seeds were surface sterilized with 70% ethanol for 1min, and then submerged in 0.5% sodium hypochlorite (Chem-supply) for 20 min and then rinsed several times in RQ water, before soaking in RO water with aeration for 4h. Imbibed seeds were placed onto a piece of moist filter paper in a clean petri dish to germinate at 28°C. After 3 days, germinated seeds were planted into deep pots (183mm square × 240mm deep) containing Osmocote Premium Potting Mix (Scotts). Plants were watered daily. At the third leaf stage, a soluble fertilizer (Aquasol, total nitrogen 23% (w/w), total phosphorus 3.95%, total potassium 14%) was applied. The plants were grown in a growth chamber with a day (14 h) and night (10 h) temperature of 28°C/25°C. The plants were provided light with 1000 W metal halide lamps providing at pot level 400 μmol m^{-2} s^{-1}light intensity. The chambers were maintained with a relative humidity of 80% in the day and 50% at night.

6.2.2.2 Tissue sampling and preparation

Plant samples were collected on day 15, 20, 26, 37, 53 after planting. The tip, middle and base of 3rd leaf, stem and top most leaf was sampled from 15-53 days. Tassel and silks were sampled on day 26 and 37 respectively. Husks were sampled on day 37 and 53. Seeds were sampled on day 53. Plants developed tassels around day 20, pollen around day 32, and silks around day 34. Samples were frozen in liquid nitrogen and ground frozen to powder in a Genogrinder (SPEX SamplePrep).

6.2.2.3 Q-PCR

Total RNA extraction and Q-PCR analysis of *ZmAMF* gene expression was completed as previously described in section 6.2.1.2. For *ZmAMF1;1* and *ZmAMF1;2*, new qPCR primers (*ZmAMF1;1 qPCR F1*, *R1* and *ZmAMF1;2 qPCR F1, R1*) were designed at 3'CDS intron spanning regions. The expression of *ZmAMF1;1* and *ZmAMF1;2* was calculated by mean Ct value of 4 biological replicates relative to the geometric average Ct of *ZmELF1* and *ZmGaPDh* (Vandesompele et al., 2002) with the equation of $2^{-\Delta Ct}$.

6.2.3 *In situ* PCR of *ZmAMF1;1* and *ZmAMF1;2*

6.2.3.1 Plant growth condition

B73 maize seeds surface sterilization was done as described in 6.2.2.1. Seeds were then germinated in vermiculite for 3 days. Germinated seeds were transferred to a hydroponic system (described in 6.2.1.1) and grown on nutrient solution containing NH_4NO_3 2.5 mM, $MgSO_4 \cdot 7H_2O$ 0.5 mM, KH_2PO_4 0.5 mM, H_3BO_3 25 µM, $MnSO_4 \cdot H_2O$ 2 µM, $ZnSO_4 \cdot 7H_2O$ 2 µM, $CuSO_4 \cdot 5H_2O$ 0.5 µM,

$Na_2MoO_4 \cdot 2H_2O$ 0.5 µM, KCl 1.05 mM, Fe-EDTA 0.1 mM, Fe-EDDHA 0.1 mM, K_2SO_4 1.25 mM, $CaCl_2 \cdot 2H_2O$ 0.25 mM, $CaSO_4 \cdot 2H_2O$ 1.75 mM (pH 5.5) for 5 days before transferring to nitrogen-free nutrient solution for 4 days. Plant growth conditions were identical to those previously described (Section 6.2.2.1).

6.2.3.2 Tissue fixation for *in situ* PCR analysis

In situ PCR was performed by the method described by Athman *et al.* (2014) with some modifications. Maize B73 was harvested between 11:00 am – 12:00 pm. Crown roots and young primary roots (without lateral root emerge) were chosen (n= 5 plants) and cut into 5mm long pieces, and then put into fixative solution (63% ethanol, 5% acetic acid, 2% formalin). The samples were vacuum infiltrated twice with 5min each and then incubated on ice for 4h. After fixation, the tissues were rinsed three times in washing buffer (63% ethanol, 5% acetic acid), and then once in 1X PBS (10 mM Na phosphate, 130mM NaCl, pH 7.5). Root fragments were then imbedded in 5% (w/v) low gelling molten agarose (Sigma) dissolved in 1×PBS.

6.2.3.3 Tissue preparation and gene amplification

The imbedded samples were sectioned using a vibratome (Leica). Sections were cut at a thickness of 50µm, amplitude 0.6 mm and speed 0.4 mm/s. The sections were put into a 100 µL solution containing 1U/µL RNAseOUT (Invitrogen) mixed with 10 µl of 10X Turbo DNase buffer (Invitrogen) and 2.5 µL DNase (Qiagen). The sections were incubated for 45 min at 37°C. The reaction was stopped by adding 0.1 M EDTA to a final concentration of 15 mM and by heating at 70°C for 15 min and then washed once with DEPC-water. The reverse transcriptase reaction was done using SuperScript® IV Reverse Transcriptase (Invitrogen)

according to the manufacturer's instructions with gene specific reverse primers. For *ZmAMF1;1* and *ZmAMF1;2*, the primers *ZmAMF1;1 qPCR R1* and *ZmAMF1;2 qPCR R1* were used. Background amplification (positive control) was tested against the maize 18s ribosomal RNA gene (GRMZM2G114613) using the primer*18s R1* for the positive RT reaction. For the negative control, tissues were kept in DEPC-water without a RT reaction step. Following the RT reactions, the sections of *ZmAMF1;1*, *ZmAMF1;2* and 18s were washed twice with DEPC-water, and then immersed in 50µl PCR reaction mix containing 10 µl of 5X Phusion HF buffer, 1 µl of 10 mM mixed dNTPs (10 mM of each), 0.2 µl of digoxigenin-11-dUTP (Roche), 2.5 µl of 10 µM forward primer and reverse primer, 0.5µl of Phusion polymerase (New England Biolabs) and 33.3 µl of sterile water. For *ZmAMF1;1*, primer *ZmAMF1;1 in situ F* and *ZmAMF1;1 qPCR R1* were used, while for *ZmAMF1;2*, primer *ZmAMF1;2 in situ F* and *ZmAMF1;2 qPCR R1* was added. For 18s gene, primer *18s F1* and *R1* were used. The PCR programme for *ZmAMF1;1* and *ZmAMF1;2* involved an initial denaturation at 98°C for 30s and then 28 cycles of (98°C for 10s, 61°C for 25s, 72°C for 3s) followed by a final extension at 72°C for 3 min. For the 18s gene, the PCR programme used an annealing temperature of 58°C, and extension time was extended to 5min.

6.2.3.6 Staining and detection of DIG-labelled PCR products

After the PCR reaction, sections were washed twice for 5mins in 100 µl of 1X PBS, blocked for 30 min in 100 µl of 1 X block solution (1 mg of BSA dissolved in 1 ml of 1 X PBS) at room temperature. Then sections were incubated with 1.5 units of AP-conjugated anti-DIG Fab fragments (Roche) at room temperature for 1 h. Sections were then washed 2 x 15 min in 100 uL of 1 X washing buffer (0.1M

Tris-Cl; 0.15M NaCl, pH 9.5). After washing, sections were transferred onto a silane-coated microscope slide (ProSciTech) and 50 µl of BM purple (Roche) was added to each slide. After 1h, the BM purple was refreshed. All slides were kept in dark to stain. The staining was stopped at 1h, 2h and 3h by washing 2 times with 100 uL of 1 X washing buffer. The sections were mounted in 100 uL of 40% glycerol. A Leica DM 2500M optical microscope was used to observe the slides with bright field, 10 × objective, and all images were processed by software LAS V3.8.

6.3 Results

6.3.1 *ZmAMF1;1* and *ZmAMF1;2* expression responded to different nitrogen treatments

To understand whether *ZmAMF1;1* and *ZmAMF1;2* expression responds to nitrogen supply, B73 maize seedlings were grown on 2.5mM NH_4NO_3 for one week and then transferred to nitrogen free diet for 4 d. After starvation, plants were resupplied with 2.5 mM $(NH_4)_2SO_4$, 5 mM KNO_3 or 2.5 mM NH_4NO_3 respectively for 4 h. *ZmAMF1;1* showed nearly equal expression levels in shoots and roots when grown in 2.5 mM NH_4NO_3. However, when seedlings were under nitrogen starvation, *ZmAMF1;1* expression increased nearly 4-fold in the shoot while the expression in the root displayed no significant difference (Figure 6.1 A and B). Nevertheless, *ZmAMF1;1* expression in N starved roots exhibited a significant decreased (~ 2-fold compare to the original value under 2.5 mM NH_4NO_3) when resupplied with 2.5 mM $(NH_4)_2SO_4$ or 2.5 mM NH_4NO_3, but there were no significant changes in expression in the shoots (Figure 6.1 A and B).

With *ZmAMF1;2*, basal expression was higher in the roots than in the shoots (> 2-fold) when grown on 2.5mM NH_4NO_3 (Figure 6.2 A and B). After a period of nitrogen starvation, *ZmAMF1;2* expression increased significantly (~3-fold) in the shoots, while the root tissues remained the same (Figure 6.2 A and B). After a 4 h resupply of nitrogen, *ZmAMF1;2* expression in both shoot and root tissues remained unchanged (Figure 6.2 A and B). Between *ZmAMF1;1* and *ZmAMF1;2*, *ZmAMF1;2* always showed about 2-fold higher levels of expression than *ZmAMF1;1* in root tissues, while the expression in the shoot was similar (Figure 6.3 A and B).

6.3.2 *ZmAMF1;1* and *ZmAMF1;2* expression pattern across different GASPE growth stages

To better understand the function of *ZmAMF1;1* and *ZmAMF1;2*, their expression patterns were tracked in the third leaf, stem, top most leaf, tassel, silks, husk and seeds across GASPE developmental growth period. In the third leaf, the leaf was separated into three parts, leaf tip, middle and base sections. In the leaf tip, Z*mAMF1;1* expression increased as the leaf aged, peaked on 37 d (increased around 2-fold compare to 15 d), then decreased about 25% on 53 d compare to 37 d (Figure 6.4 A). In contrast, *ZmAMF1;2* expression remained stable in the leaf tip, only having roughly 2-fold increase on day 53 from the original value on 15 d (Figure 6.4 A). *ZmAMF1;1* expression was always significantly higher (1.5 to 3-fold) than *ZmAMF1;2* in 3rd leaf tip across the developmental stages (Figure 6.4 A).

In the middle and base sections of the third leaf, *ZmAMF1;1* expression was higher (~ 2 to 4-fold) than *ZmAMF1;2* but there was no developmental change with either gene between days 15-53, except a drop *ZmAMF1;2* expression on day 37 (Figure 6.4 B and C).

ZmAMF1;1 and *ZmAMF1;2* expression in the stem did not change until day 53 where they increased 2.5-fold and 1.8-fold respectively (Figure 6.4 D). In the top leaf, *ZmAMF1;1* expression increased from day 15-26, then decreased slightly thereafter, while *ZmAMF1;2* expression was stable (Figure 6.4 E). *ZmAMF1;1* always expressed significantly higher (2 to 4- fold) than *ZmAMF1;2* in both the stem and the top most leaf across developmental stages (Figure 6.4 D and E).

The expression pattern of *ZmAMF1;1* and *ZmAMF1;2* were also compared in the reproductive organs. In the tassel, both genes were expressed equally. In the silk, *ZmAMF1;1* was strongly induced (p=0.0027) while in the seed, *ZmAMF1;2* expression was the most dominant (p= 0.0008) (Figure 6.4 F). The husk tissue of the maize cob had about 2.5-fold higher levels of expression of *ZmAMF1;1* than *ZmAMF1;2* between days 37 and 53, and the expression of both *ZmAMF1;1* and *ZmAMF1;2* increased more than 1.5-fold from days 37 to days 53 (Figure 6.4 G).

6.3.3 *ZmAMF1;1* and *ZmAMF1;2* cellular localization in maize root

To understand the cellular localization of *ZmAMF1;1* and *ZmAMF1;2* gene activity, *in situ* PCR was conducted in nitrogen starved B73 maize roots. After 1h of staining, both *ZmAMF1;1* and *ZmAMF1;2* sections developed increased blue staining in the vascular tissue, which indicated their expression in the vascular cylinder (Figure 6.5 A). With the staining time increased to 2 and 3 h, the staining

became stronger, where *ZmAMF1;2* staining was stronger than that of *ZmAMF1;1*(Figure 6.5 B and C). This is consistent with the gene expression pattern of *ZmAMF1;1* and *ZmAMF1;2* in roots under nitrogen starvation (Figure 6.3 B). The 18s positive control showed the strongest blue staining from 1h to 3h (Figure 6.5).

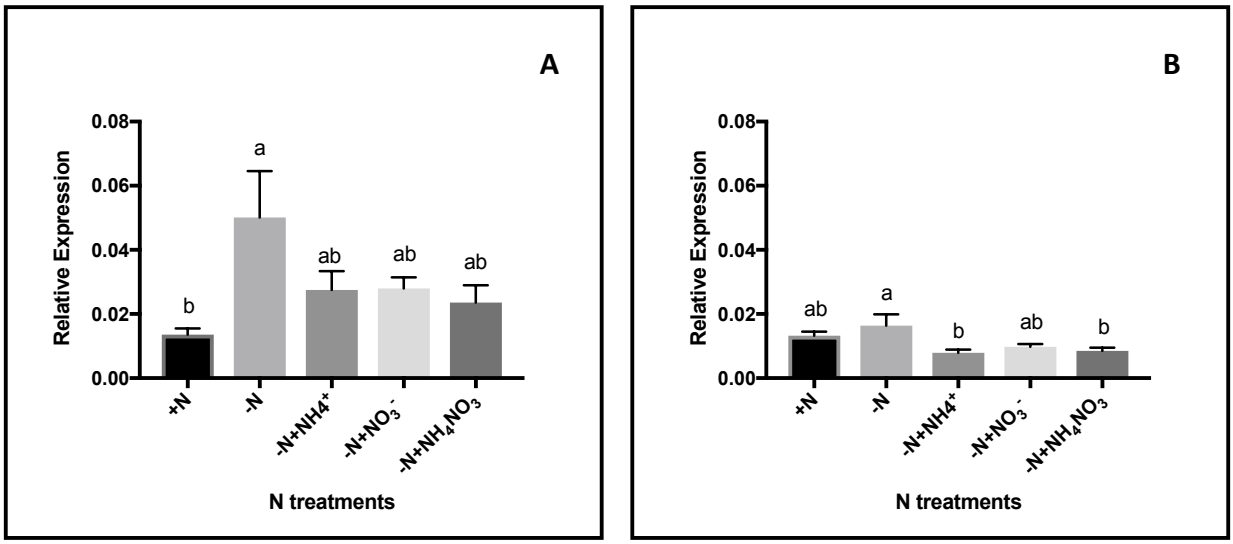

Figure 6.1 *ZmAMF1; 1* expression under different nitrogen treatments.

Seedlings were grown hydroponically in 2.5 mM NH_4NO_3 nutrient solution for 7d, then transferred to a -N (nitrogen starvation) solution for 4d before resupplying with NH_4^+, NO_3^- or NH_4NO_3 for 4h. Total RNA was extracted from root and shoot tissues. Data represents the mean ± SEM (n=5). A) *ZmAMF1;1* shoot expression pattern under different nitrogen treatments. B) *ZmAMF1;1* root expression pattern under different nitrogen treatments. Significant differences between the different nitrogen treatments are indicated by different letters (one way ANOVA, $p< 0.05$).

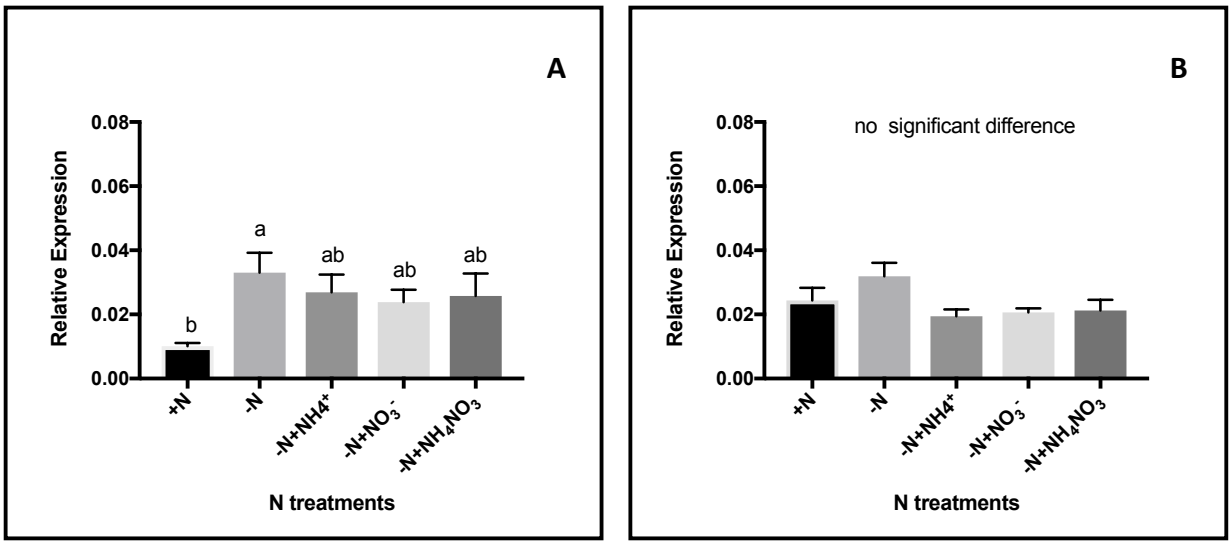

Figure 6.2 *ZmAMF1; 2* expression under different nitrogen treatments.

Seedlings were grown hydroponically in 2.5 mM NH_4NO_3 nutrient solution for 7d, then transferred to a -N (nitrogen starvation) solution for 4d before resupplying with NH_4^+, NO_3^- or NH_4NO_3 for 4h. Total RNA was extracted from root and shoot tissues. Data represents the mean ± SEM (n=5). A) *ZmAMF1;2* shoot expression pattern under different nitrogen treatments. B) *ZmAMF1;2* root expression pattern under different nitrogen treatments. Significant differences between the different nitrogen treatments are indicated by different letters (one way ANOVA, $p< 0.05$).

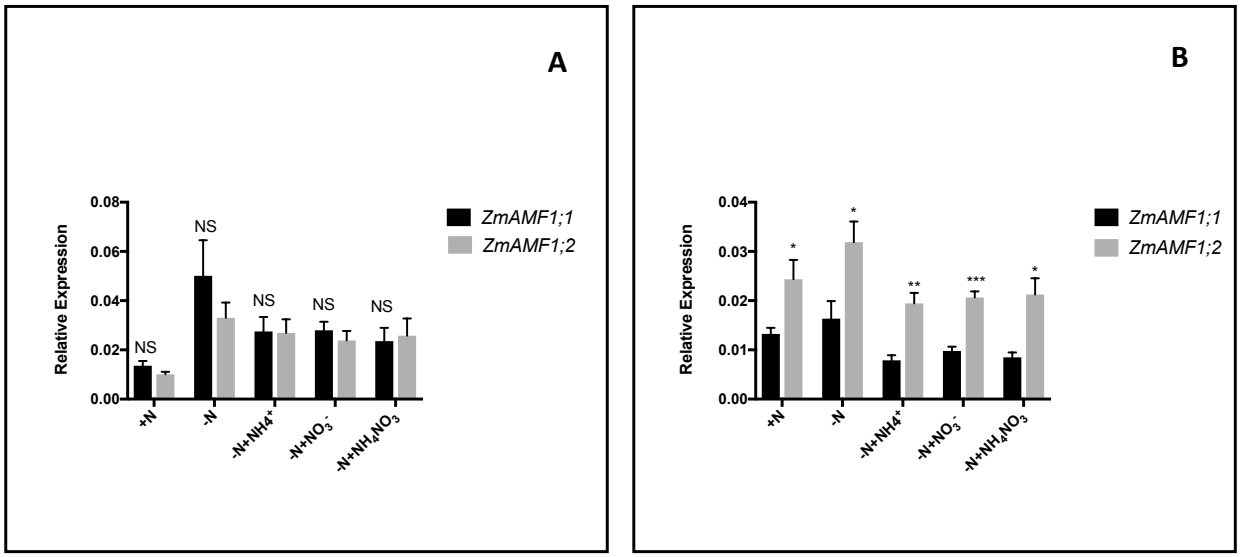

Figure 6.3 Gene expression comparison between *ZmAMF1;1* and *ZmAMF1;2* under different nitrogen treatments

This data is the same as presented in Figures 6.1 and 6.2 but has been combined to directly compare ZmAMF1;1 and ZmAMF1;2 gene expression in shoot and root tissues. A) *ZmAMF1;1* and *ZmAMF1;2* expression in shoot under different nitrogen treatments. B) *ZmAMF1;1* and *ZmAMF1;2* expression in root under different nitrogen treatments. Significant differences between *ZmAMF1;1* and *ZmAMF1;2* were shown by star (unpaired t test with Welch's correction , $p < 0.05$, NS= no significant difference).

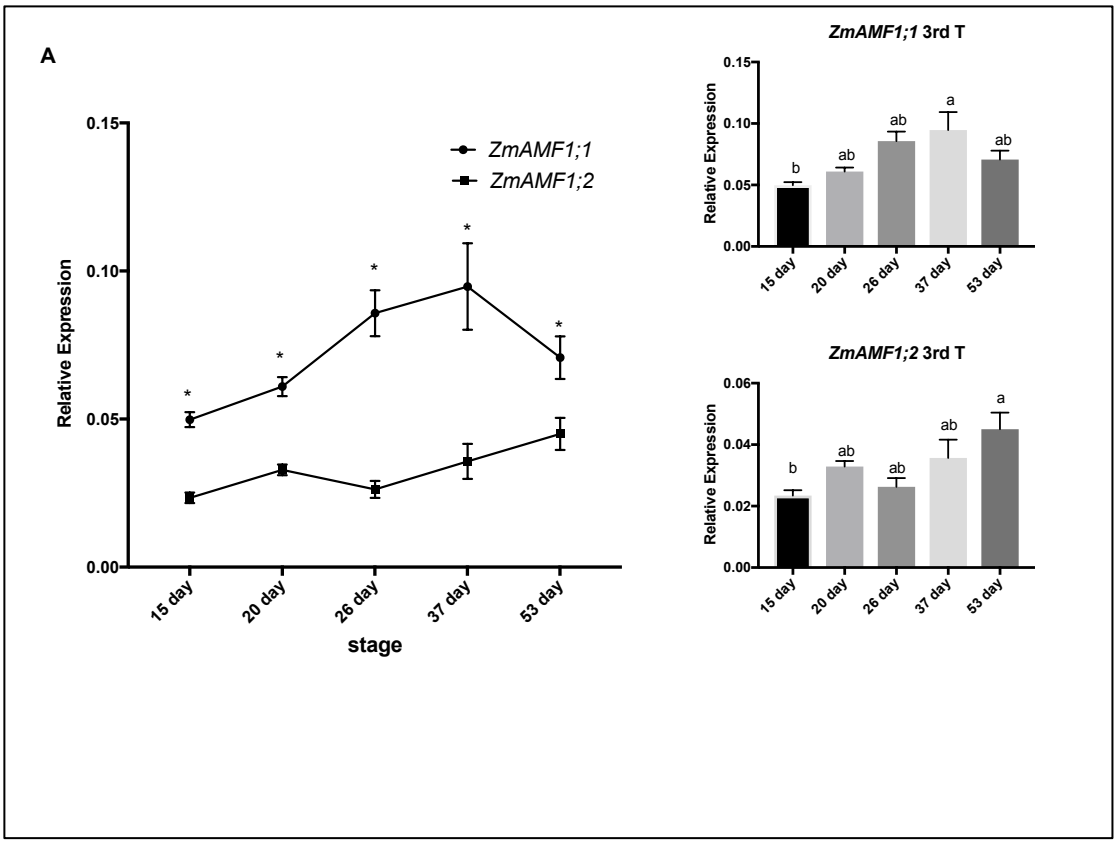
A
ZmAMF1;1
ZmAMF1;2
Relative Expression
0.15
0.10
0.05
0.00
15 day
20 day
26 day
37 day
53 day
stage
ZmAMF1;1 3rd T
b
ab
ab
a
ab
ZmAMF1;2 3rd T
0.06
0.04
0.02
a

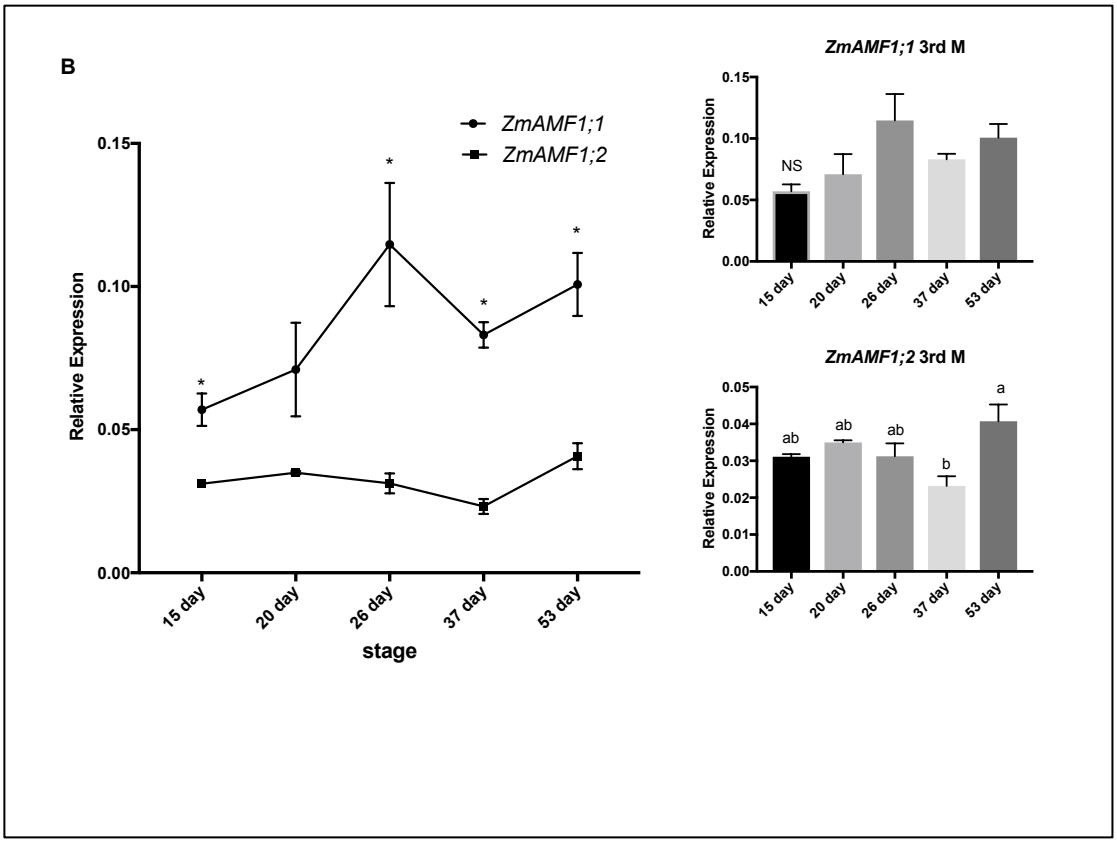
B
ZmAMF1;1
ZmAMF1;2
Relative Expression
0.15
0.10
0.05
0.00
15 day
20 day
26 day
37 day
53 day
stage
ZmAMF1;1 3rd M
NS
ZmAMF1;2 3rd M
ab
ab
ab
b
a
0.04
0.03
0.02
0.01

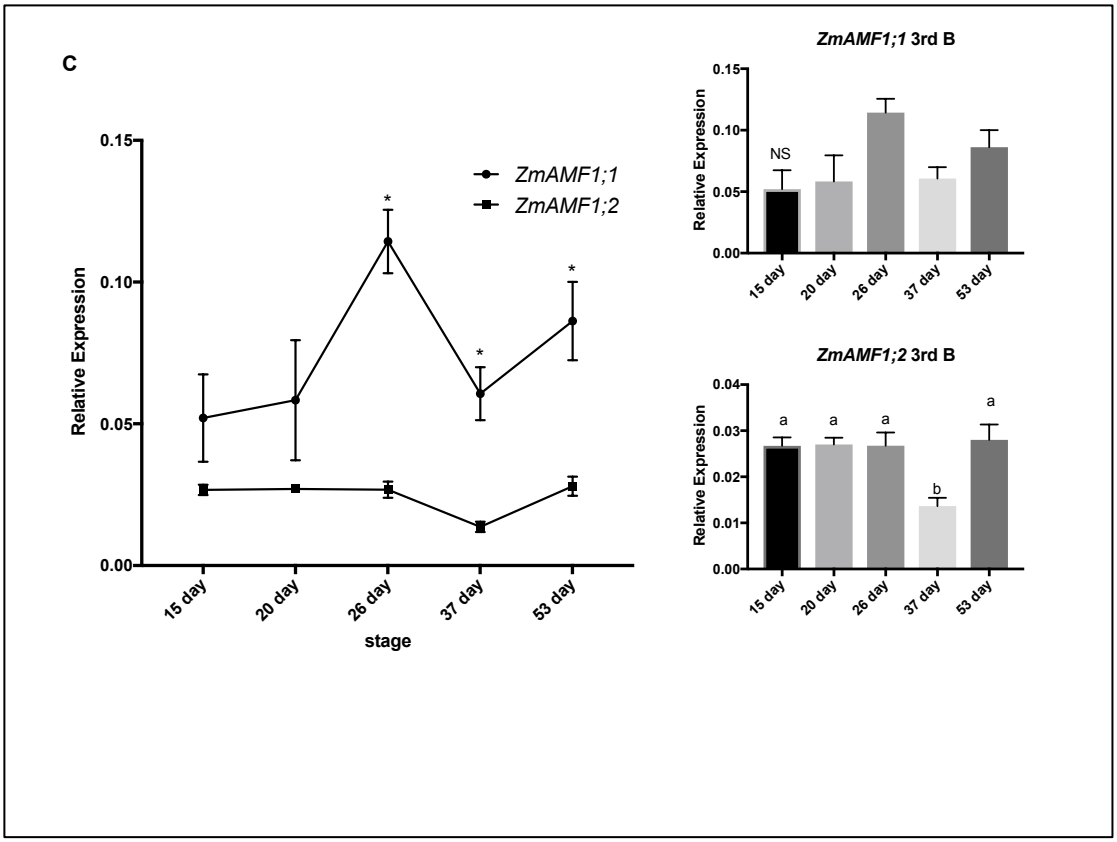
C
ZmAMF1;1
ZmAMF1;2
Relative Expression
0.15
0.10
0.05
0.00
15 day
20 day
26 day
37 day
53 day
stage
*
ZmAMF1;1 3rd B
NS
ZmAMF1;2 3rd B
a
a
a
b
a

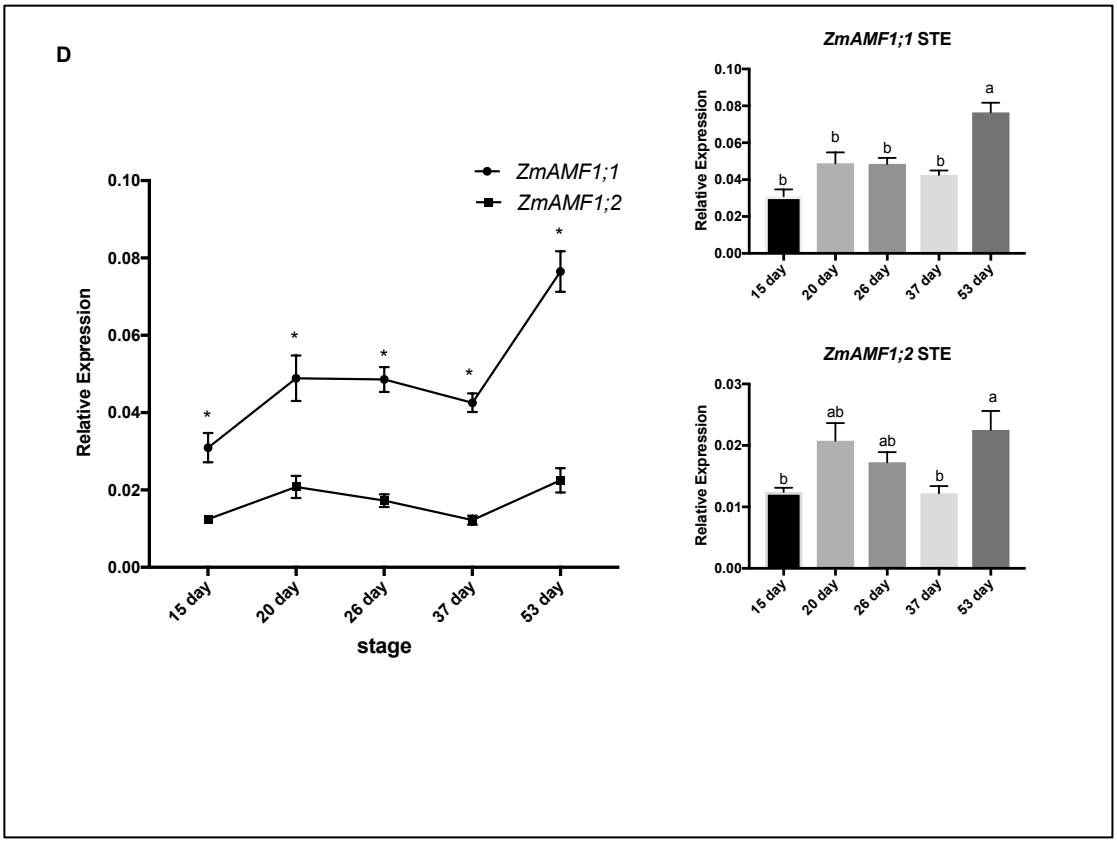
D
ZmAMF1;1
ZmAMF1;2
Relative Expression
0.10
0.08
0.06
0.04
0.02
0.00
15 day
20 day
26 day
37 day
53 day
stage
*
ZmAMF1;1 STE
b
b
b
b
a
ZmAMF1;2 STE
b
ab
ab
b
a

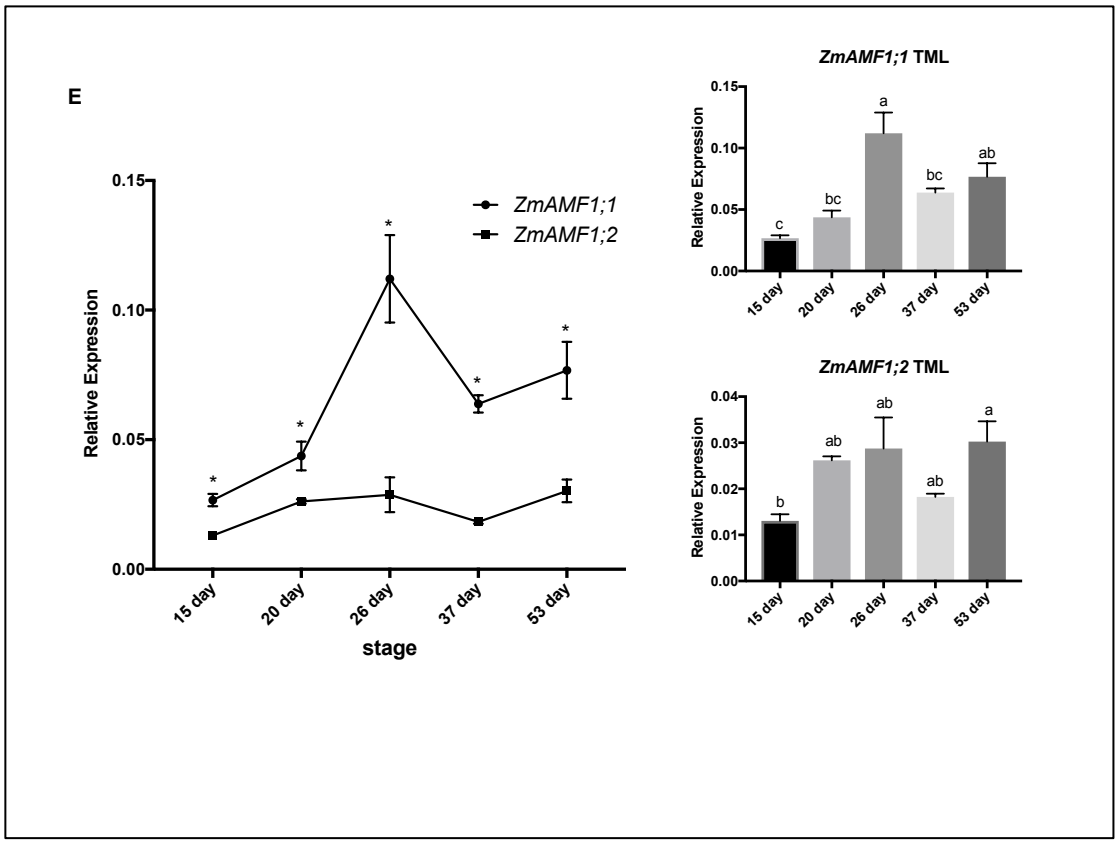
E
ZmAMF1;1
ZmAMF1;2
Relative Expression
0.15
0.10
0.05
0.00
15 day
20 day
26 day
37 day
53 day
stage
ZmAMF1;1 TML
ZmAMF1;2 TML
c
bc
a
bc
ab
b
ab
ab
ab
a

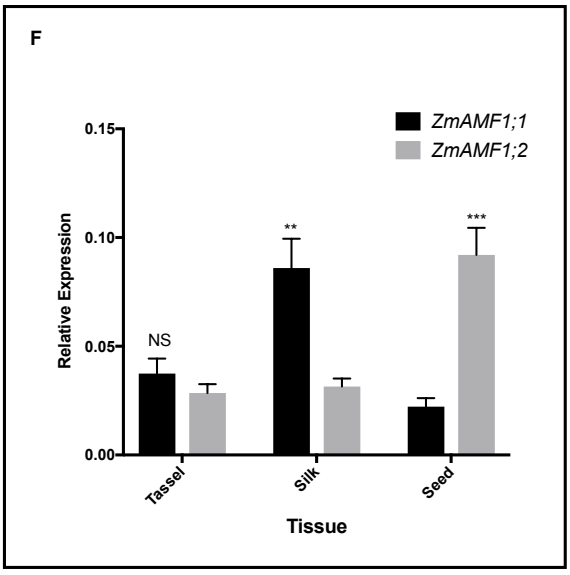
F
ZmAMF1;1
ZmAMF1;2
Relative Expression
NS
**
***
Tassel
Silk
Seed
Tissue

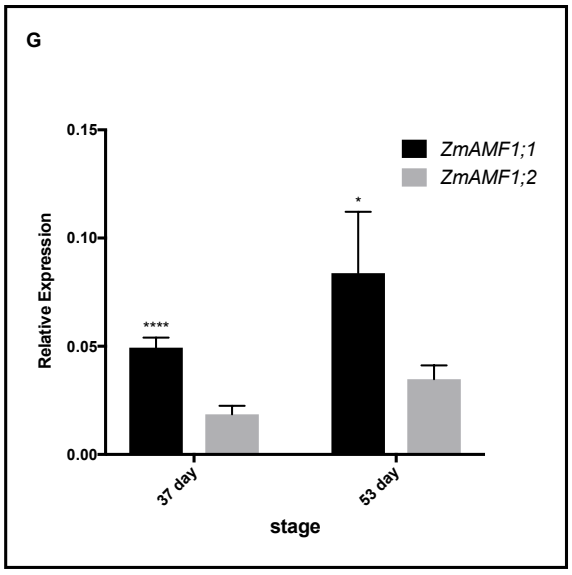
G
ZmAMF1;1
ZmAMF1;2
Relative Expression
****
*
37 day
53 day
stage

Figure 6.4 *ZmAMF1;1* and *ZmAMF1;2* expression across GASPE different growth stages and different tissue.

Growth stages represent days after planting. Gene expression was calculated relative to the control genes *ZmELF1* and *ZmGaPDh*. Values represent mean ± SEM (n=4). Samples were collected on the 15, 20, 26, 37, 53 days after planting from 3rd leaf tip (T), middle (M), base (B), stem (STE), top most leaf (TML), and tassel (collected on day 26), silk (collected on day 37), seed(collected on day 53) and husk (collected on day 37 and 53). A) to G) *ZmAMF1;1* and *ZmAMF1;2* expression in 3rd leaf tip, middle, base and stem, top most leaf, tassel, silk, seed, husk. Significant differences between different growth stages within each gene were represented by different letters (one way ANOVA, $P<0.05$). Significant difference between *ZmAMF1;1* and *ZmAMF1;2* in same tissue was represented by star (t test, $P<0.05$), NS= no significant difference.

A

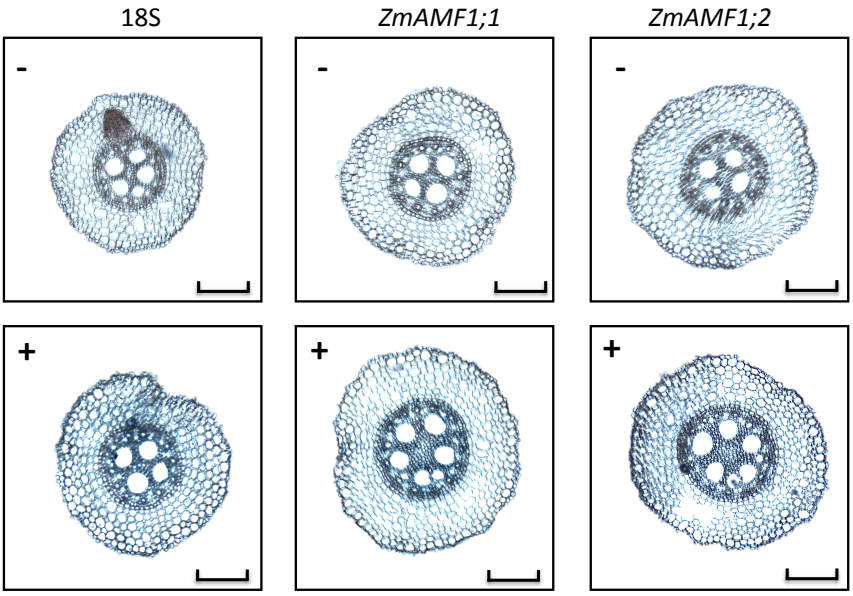

B

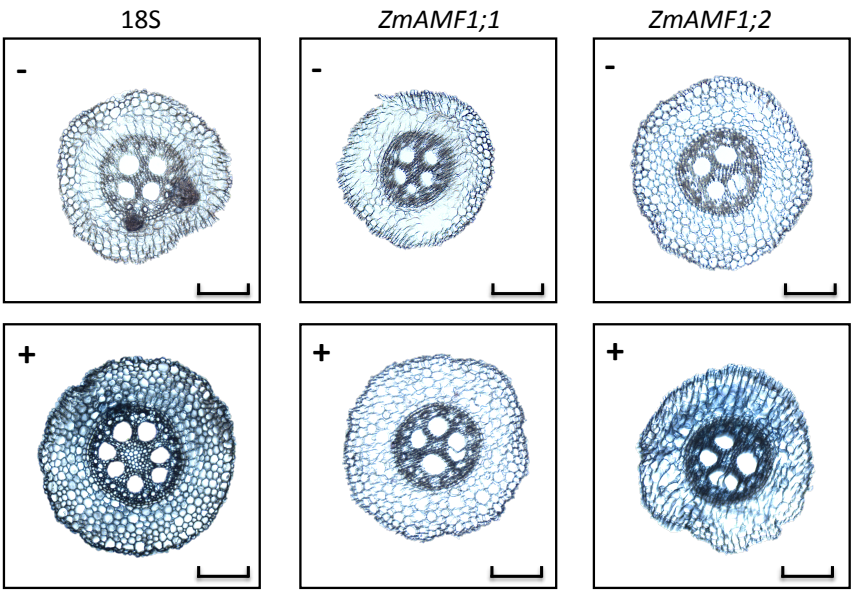

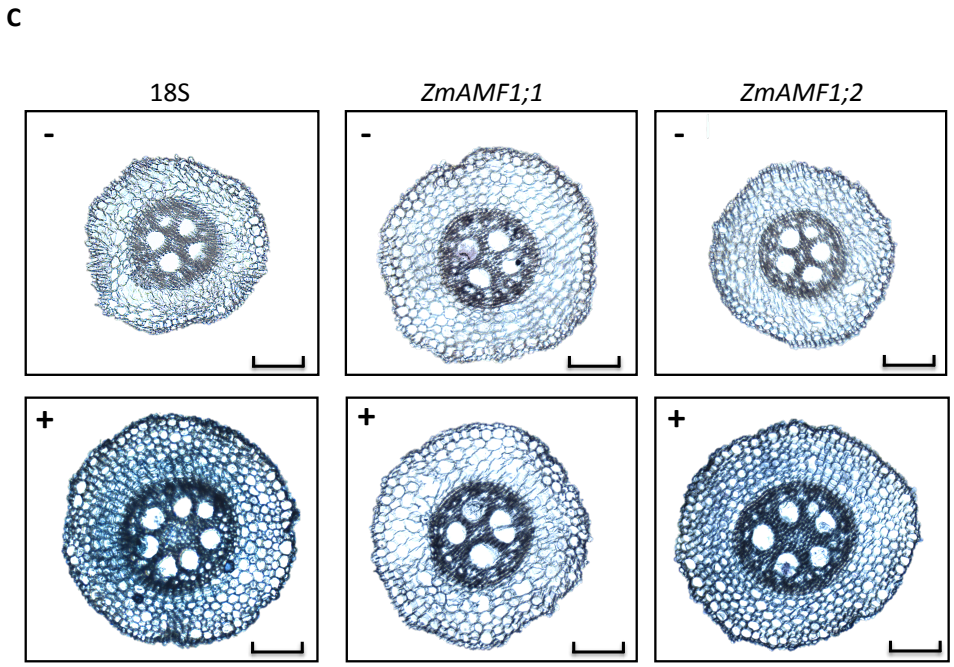

Figure 6.5 *In situ* PCR of *ZmAMF1;1* and *ZmAMF1;2* in B73 maize root under nitrogen starvation.

Five independent B73 seedlings were first grown in nutrient solution with 2.5 mM NH_4NO_3 for 5 days, and then transferred to nutrient solution without nitrogen for 4 days before harvesting. Blue staining represents the presence of target cDNA, while the brown colour shows the absence of target cDNA. 18s ribosomal RNA gene was used as positive control. Minus (-) means negative control (without reverse transcription step), while plus (+) means a reverse transcription step was completed. Scale bar=200μm. A) 18s, *ZmAMF1;1* and *ZmAMF1;2* 1h staining. B) 18s, *ZmAMF1;1* and *ZmAMF1;2* 2h staining. C) 18s, *ZmAMF1;1* and *ZmAMF1;2* 3h staining. Both *ZmAMF1;1* and *ZmAMF1;2* show staining in root vascular tissues, and the staining in *ZmAMF1;2* was stronger than *ZmAMF1;1*.

6.4 Discussion

To better understand the function of ZmAMF1;1 and ZmAMF1;2, their expression patterns were studied in this chapter. Both *ZmAMF1;1* and *ZmAMF1;2* had similar responses to nitrogen supply, where the expression of *ZmAMF1;1* and *ZmAMF1;2* were both induced by a period of nitrogen starvation in shoots. Resupply of nitrogen for 4 hours failed to decrease expression. The nitrogen deficiency response is similar to a number of *AMT1* genes including, *AtAMT1;1* and *OsAMT1;3* (Gazzarrini et al., 1999; Sonoda et al., 2003). Unlike these genes, *AMF1* expression wasn't quickly repressed when nitrogen was returned to the growth system. Interestingly, the response to nitrogen starvation occurred predominantly in the shoots (Figure 6.1 and 6.2). This may indicate a role in shoot-based ammonium transport, possibly in ammonium export as plants respond to nitrogen limiting conditions and remobilize ammonium from proteins breaking down during senescence, photorespiration or other processes producing ammonium (Masclaux‐Daubresse et al., 2008; Bieker and Zentgraf, 2013).

This putative function in nitrogen remobilization is supported by their subcellular localization. Both ZmAMF1;1 and ZmAMF1;2 were found to be localized on the tonoplast (Apriadi Situmorang unpublished results). Moreover in Chapter 4, we found ZmAMF1;1 and ZmAMF1;2 may facilitate ammonium efflux from the vacuole to the cytoplasm. The vacuole plays an important role in plant senescence and nutrient remobilization (Carrión et al., 2014). ZmAMF1;1 and ZmAMF1;2 may be involved in the export of ammonium from protein

degradation in the vacuole which is an important process in remobilizing reduced nitrogen in the plant.

Between the two genes, *ZmAMF1;2* consistently showed around 2-fold higher levels of expression than *ZmAMF1;1* in root tissues under each nitrogen treatment (5 mM nitrogen supply, nitrogen starvation and nitrogen resupply) (Figure 6.3 B). This indicates there may be different roles for *ZmAMF1;1* and *ZmAMF1;2* in root ammonium transport. The higher expression of *ZmAMF1;2* over that of *ZmAMF1;1* was also observed in the *in situ* PCR experiments in nitrogen starved roots (Figure 6.5).

The expression of *ZmAMF1;1* and *ZmAMF1;2* was also tracked across different growth stages and different tissues in GASPE. *ZmAMF1;1* showed continuously higher expression levels than *ZmAMF1;2* in shoot tissues. *ZmAMF1;1* showed strong expression in the third leaf tip (15-37 days) and the top most leaf (26 and 53 d) (Figure 6.4 A and E). At these stages, GASPE plants are starting to shed pollen and begin the kernel filling period. The elevated expression of *ZmAMF1;1* may indicate an initiation of leaf senescence linked to the transition to reproductive growth. This period has been linked with nitrogen remobilization from senescing tissues (Bieker and Zentgraf, 2013). There were interesting differences in the expression of *ZmAMF1;1* and *ZmAMF1;2* in seeds and silk tissues (Figure 6.4 F). Interestingly, *ZmAMF1;2* showed exclusively higher levels of expression (p= 0.0008) in the developing seeds, which may indicate its role in seed filling while *ZmAMF1;1* was more localized to the silks (Figure 6.4 F and G). At the cellular level in root tissues, both *ZmAMF1;1* and *ZmAMF1;2* were found

expressed in root vascular tissues using *in situ* PCR (Figure 6.5). This may relate to a role in ammonium transport in the root.

Chapter 7 General Discussion

In plants, ammonium transport is mediated by two systems, the high affinity transport pathway operating at low ammonium concentrations, and the low affinity transport pathway functioning at high ammonium concentrations (Nacry et al., 2013). The high affinity transport system has been examined in many plant species and shown to involve members of the AMT transport family. AMTs belong to the large super family of ammonium transporters commonly called AMT/MEP/Rh and found in both eukaryotic and prokaryotic organisms (Sonoda et al., 2003; Ludewig et al., 2007; Yuan et al., 2007b; Masclaux-Daubresse et al., 2010; Gu et al., 2013). In contrast, information on the molecular identities of low-affinity transport pathways remains less clear. A number of potassium channels and non-selective cation channels have be suggested to transport ammonium into plants at high concentrations (Schachtman et al., 1992; White, 1996; Hoopen et al., 2010). The discovery of the putative low affinity transporter in yeast (ScAMF1) and a paralog in soybean (GmAMF3) has provided a molecular identity of a low affinity ammonium transport protein in yeast and plants (Chiasson et al., 2014). AMF1 proteins share sequence homology to the DHA2 family of H^+/drug antiporters (Chiasson et al., 2014). Whether AMF proteins operate as antiporters is currently unknown.

Maize possesses two AMF paralogs, ZmAMF1;1 and ZmAMF1;2. The focus of this study was to understand the function of ZmAMF1;1 and ZmAMF1;2 including

their role in low affinity ammonium transport in maize plants, their contribution to growth and their potential role in nitrogen remobilization.

7.1 ZmAMF1;1 and ZmAMF1;2 are putative tonoplast localized NH_4^+/H^+ antiporters to facilitate vacuole ammonium efflux

Through functional complementation studies using the ammonium uptake deficient yeast strains, 26972c and its derivate strain 26972c:Δ*amf1*, both ZmAMF1;1 and ZmAMF1;2 displayed contrasting activities to the previously characterized, ScAMF1 and GmAMF3. Both were not able to mimic a methyl ammonium toxicity response when plated on media containing 0.1 M or 0.15 M MA at either pH 4.5 or 6.1. Cells continued to grow on the high methylammonium concentrations while cells expressing either *ScAMF1* or *GmAMF1;3* would die (Figure 4.1 and 4.2). In a set of parallel investigations, the role of ZmAMF1;1 and ZmAMF1;2 in boron or sucrose transport was also ruled out (Figure 4.3 and 4.4). Nevertheless, when using a potassium transport deficient yeast strain, CY162, which has both high and low affinity potassium transport pathways knocked out, both ZmAMF1;1 and ZmAMF1;2 were able to compliment growth on media containing high concentrations of ammonium (37.8 mM) and low potassium (~7.3 mM). Neither the empty vector control or ScAMF1 was able to rescue growth (Figure 4.5). However, when ammonium was replaced by an alternative nitrogen source or supplied at a lower concentration (< 5 mM) the mutant grew without ZmAMF1;1 or ZmAMF1;2 (Figure 4.6 and 4.7).

The knockout of both the high and low affinity potassium transporters in yeast strain CY162 results in a limited capacity to accumulate potassium when

external K concentrations are low (<15 mM) (Bihler et al., 2002). This most likely creates an imbalance between K and ammonium, where ammonium entry, possibly through MEP proteins (Marini et al., 1997), ScAMF1 (Chiasson et al., 2014) and non selective cation channels, such as NSC1 (Bihler et al., 2002) collectively contribute to the accumulation of ammonium inside the cell. High concentrations of internal ammonium in yeast cells is toxic especially when potassium is limiting. It has been proposed that yeast detoxify ammonium by excreting amino acids through the SPS system induced amino acid transporters (Hess et al., 2006).

ZmAMF1;1 and ZmAMF1;2 were found to be localized on the tonoplast in tobacco cells, and AtAMF2 was found to be localized on the tonoplast in both yeast and tobacco cells (Apriadi Situmorang unpublished results). The vacuole plays an important role in regulating cell volume, pH and ion homeostasis, therefore it is also important in regulating ammonium in cells. When extracellular ammonium concentrations are high, ammonia diffuses or is transported as ammonium into the cell across the plasma membrane, and then diffuses as ammonia into the vacuole across the tonoplast membrane, most likely through aquaporin proteins such as TIPs. Entry into the vacuole results in the acid-trapping of ammonium in the vacuole (Roberts and Pang, 1992; Wood et al., 2006). The vacuole is normally more acidic than the cytoplasm. A large accumulation of ammonium in the vacuole could collapse the pH gradient between the vacuole and cytoplasm, potentially affecting the accumulation of other substrates and resulting in toxicity issues inside the cell (Roberts and Pang, 1992). Moreover, yeast excrete amino acids possibly to reduce nitrogen in the

cell when experiencing high concentrations of ammonium (Hess et al., 2006). This process will potentially result in the starvation of nitrogen of yeast. We propose that ZmAMF1;1 and ZmAMF1;2 function as an NH_4^+/H^+ antiporter on the tonoplast. The exchange of the proton into the vacuole can recover the pH gradient between cytoplasm and vacuole, and in addition the export of ammonium can offer nitrogen source for the yeast to utilize, which would overcome the ammonium toxicity and rescue growth. The experiment of CY162 with MA also verified our hypothesis. CY162 transformed with ZmAMF1;1 and ZmAMF1;2 were more susceptible to 0.1mM MA compared to empty vector and ScAMF1 control when no KCl was supplied (Figure 4.8). This is because ZmAMF1;1 and ZmAMF1;2 could release MA into the cytoplasm, which induced the toxicity. In the MA test in 26972c which is an ammonium uptake deficient yeast mutant, ZmAMF1;1 and ZmAMF1;2 didn't show MA toxicity, which verified their tonoplast location and their inability to take ammonium up from the external medium.

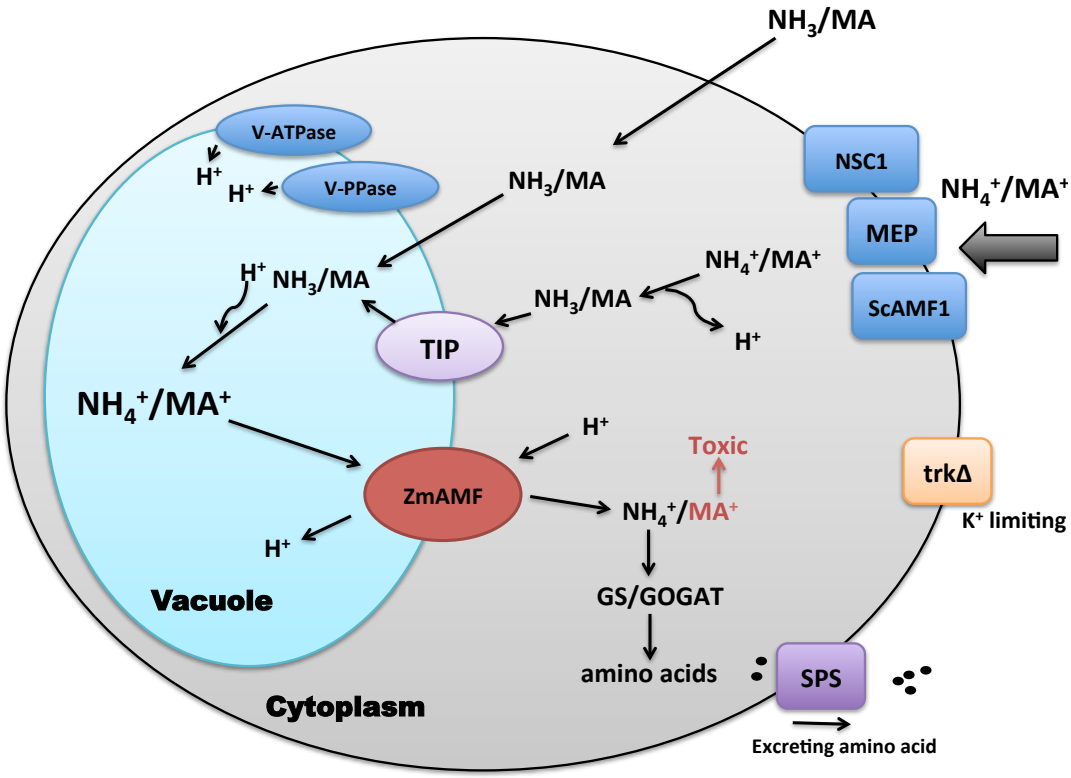

Figure 7.1 Proposed mechanism of ZmAMF1;1 and ZmAMF1;2 to reduce ammonium toxicity in CY162 yeast mutant.

When high concentration of ammonium is accumulated in the cytoplasm, yeast suffers from ammonium toxicity. Vacuole will store the ammonium to reduce the cytoplasmic ammonium, which decreases the pH gradient between vacuole and cytoplasm and affect the accumulation of other substrates. Meanwhile SPS induced amino acid transporters were upregulated to export amino acids to detoxify ammonium toxicity, which will potentially lead yeast cells to be starved of nitrogen. ZmAMF1;1 and ZmAMF1;2 are putative tonoplast localized NH_4^+/H^+ antiporter which can facilitate ammonium export from vacuole to cytoplasm to offer nitrogen source for the yeast cells as well as recover the pH gradient between vacuole and cytoplasm.

7.2 Loss of both ZmAMF1;1 and ZmAMF1;2 enhanced root ammonium uptake, root nitrogen content and plant growth

In this study, TUSC mutants were used to help understand the functional properties of *ZmAMF1;1* and *ZmAMF1;2*. The genetic background of each individual TUSC mutant was normalized through three backcross events with the maize inbred GASPE. Homozygous TUSC lines were then selected after self-pollinating and genotype selection of the segregating seed population. A double AMF mutant was generated by crossing individual *ZmAMF1;1* and *ZmAMF1;2* mutants.

In general, TUSC events for *ZmAMF1;1* (ADL 112, ADL 114) or *ZmAMF1;2* (ADL119) consistently displayed larger shoots compared to the GASPE controls. This trend was also evident in the double mutant (ADL119 x ADL 112). A more detailed look at the double mutant revealed plants to be taller, producing more leaves and had increased stem thickness prior to the onset of its reproductive stage (Table 3.2). Unfortunately, limited seed for experimental use restricted full characterization of the TUSC lines. The lack of seed was exacerbated by the general poor state of the reproductive phase of development for each line. Pollen from developed tassels was often compromised limiting cob and seed development. Future experiments will require the generation of significantly more seed so that a detailed analysis of the reproductive phase can be captured.

Apart from the changes in growth there were noticeable differences in the unidirectional transport of ammonium into the *ZmAMF1;2* TUSC lines, ADL 119 and the double mutant (ADL 112 x ADL 119). Both lines displayed significantly higher NH_4^+ uptake rates at the high affinity ranges compared to the control

GASPE (Figure 5.4 and 5.5). In the double mutant, ammonium uptake increased at both concentration ranges (1.4 to 3.3-fold, HATS and LATS) (Figure 5.5). The increase in the transport rate of ammonium was accompanied by higher %N levels (up to 8% higher) in harvested roots (Table 5.5 and 5.6). If AMF proteins in plants behave as an ammonium efflux channel on the tonoplast this may lead to a decrease in ammonium efflux and an increase in root ammonium concentrations. Meanwhile the reduced efflux of ammonium in the vacuole would also decrease the vacuolar sequestration capacity (VSC). VSC has been reported to the linked with long distance translocation of nutrients from root to shoot. When VSC decreases, more nutrients will prefer to translocate into the shoot (Peng and Gong, 2014). This is consistent with our experiment results, where we found that the double mutant performed dramatically better in its vegetative growth than GASPE (Table 3.2 and 5.6). This is possibly because the double mutant which lacks ZmAMF1;1 and ZmAMF1;2 reduced the level of ammonium efflux from the vacuole which decreased the VSC and promote the translocation of ammonium from root to the shoot. This result may help improve shoot growth. However, one thing that should be considered is that the double mutant had higher ammonium uptake rates compared to GASPE. A detailed examination of the ammonium transport activities in the TUSC mutant lines is still required to confirm if higher rates of uptake are linked to a drop in ammonium efflux to the shoot or an increase in the uptake through other AMT activities.

7.3 ZmAMF1;1 and ZmAMF1;2 respond to different nitrogen supply and play different roles in maize

We found that both *ZmAMF1;1* and *ZmAMF1;2* expression was induced by nitrogen starvation in the shoots but not in roots (Figure 6.1 and 6.2). This expression pattern was not tempered by a resupply of nitrogen (4 h) after the starvation period. This response contrasts many *AMT1* genes which are upregulated under N starvation but quickly down regulated when N is resupplied (Rawat et al., 1999; Kaiser et al., 2002). ZmAMF1;1 and ZmAMF1;2 also appear to perform different roles in maize, where *ZmAMF1;1* was more active in the shoots, particularly during the reproductive stages, while *ZmAMF1;2* was more expressed in root tissues (whole tissue and using *in situ* analysis, Figure 6.3, 6.4 and 6.5). The tissue localized expression supports the apparent differences in ammonium uptake rates, where ALD 119 (*ZmAMF1;2* mutant) influenced root NH_4^+ uptake while there were little impact on root ammonium transport in the *ZmAMF1;1* mutants (ADL 112 and ADL 114) (Figure 5.1, 5.2, 5,3 and 5.4).

In summary, the data suggest both ZmAMF1;1 and ZmAMF1;2 are putative NH_4^+/H^+ antiporters on the tonoplast in yeast and potentially in maize which facilitate ammonium efflux from vacuole to the cytoplasm. The loss of both increases unidirectional (10 min-influx) ammonium uptake as well as enhances plant growth and root nitrogen content. Their broad localization across the root, albeit with increased expression in the stele, indicates a potential role in ammonium transport. The high expression of *ZmAMF1;1* but not *ZmAMF1;2* in

the shoots of plants across seedling and reproductive stages indicate an alternative role of ZmAMF1;1 in ammonium redistribution.

7.4 Future works in this research

Ammonium toxicity in plants, especially under potassium deficiency has been reported in different plant species, and also in yeast (Hess et al., 2006; Hoopen et al., 2010). This preliminary study on ZmAMF1;1 and ZmAMF1;2 in yeast and maize, displayed their potential roles in exporting ammonium from the vacuole to the cytoplasm in yeast and potentially and in maize. To confirm whether ZmAMF1;1 and ZmAMF1;2 are NH_4^+/ H^+ antiporters, detailed electrophysiological analysis in *Xenopus* oocytes will be required to study the mechanism. Besides, it is also necessary to explore the subcellular localization in maize to confirm their function.

Unfortunately, the tenure of a PhD degree has limited the genetic progression of the TUSC population. Three backcrosses with GASPE were achieved and homozygous lines selected. However, this process needs to continue to strengthen the genetic background in both GASPE and a second test cross such as B73. Furthermore, the data showed that the *Mu* insertion did not disrupt gene transcription but most-likely created a dysfunctional mRNA transcript. It is still to be determined whether the proteins are still translated and if translated, are they still functional. Alternative mutants will also be required possibly through gene editing approaches or analysis of other plant species with disruptions in *AMF* genes. On that note, a parallel study in Arabidopsis within the research group has revealed that a loss of AMF activity enhances plant growth and

ammonium uptake, while yeast functional complementation experiments also show a K-dependent mitigation of ammonium toxicity by AtAMF1 in the CY162 strain (Apriadi Situmorang, unpublished results).

Chapter 8 Bibliography

Athman A, Tanz SK, Conn VM, Jordans C, Mayo GM, Ng WW, Burton RA, Conn SJ, Gilliham M (2014) Protocol: a fast and simple in situ PCR method for localising gene expression in plant tissue. Plant methods **10:** 29

BaAueIos MA, Sychrová H, Bleykasten-Grosshans C, Souciet J-L, Potier S (1998) The Nhal antiporter of *Saccharomyces cerevisiae* mediates sodium and potassium efflux. Microbiology **144:** 2749-2758

Balkos KD, Britto DT, Kronzucker HJ (2010) Optimization of ammonium acquisition and metabolism by potassium in rice (*Oryza sativa L*. cv. IR‐72). Plant, Cell & Environment **33:** 23-34

Bañuelos MaA, Rodríguez-Navarro A (1998) P-type ATPases mediate sodium and potassium effluxes in *Schwanniomyces occidentalis*. Journal of Biological Chemistry **273:** 1640-1646

Barker AV, Maynard DN, Lachman WH (1967) Induction of tomato stem and leaf lesions, and potassium deficiency, by excessuve ammonium nutrition. Soil Science **103:** 319-327

Bauwe H, Hagemann M, Fernie AR (2010) Photorespiration: players, partners and origin. Trends in plant science **15:** 330-336

Bennetzen J (1996) The Mutator transposable element system of maize. *In* Transposable elements. Springer, pp 195-229

Bennetzen J, Springer P (1994) The generation of Mutator transposable element subfamilies in maize. Theoretical and Applied Genetics **87:** 657-667

Bernard SM, Habash DZ (2009) The importance of cytosolic glutamine synthetase in nitrogen assimilation and recycling. New Phytologist **182:** 608-620

Bieker S, Zentgraf U (2013) Plant senescence and nitrogen mobilization and signaling. *In* Senescence and Senescence-Related Disorders. InTech

Bihler H, Slayman CL, Bertl A (2002) Low-affinity potassium uptake by *Saccharomyces cerevisiae* is mediated by NSC1, a calcium-blocked non-specific cation channel. Biochimica et Biophysica Acta (BBA)-Biomembranes **1558:** 109-118

Bittsánszky A, Pilinszky K, Gyulai G, Komives T (2015) Overcoming ammonium toxicity. Plant Science **231:** 184-190

Bozdag GO, Uluisik I, Gulculer GS, Karakaya HC, Koc A (2011) Roles of ATR1 paralogs YMR279c and YOR378w in boron stress tolerance. Biochemical and biophysical research communications **409:** 748-751

Britto DT, Kronzucker HJ (2002) NH_4^+ toxicity in higher plants: a critical review. Journal of Plant Physiology **159:** 567-584

Britto DT, Kronzucker HJ (2006) Futile cycling at the plasma membrane: a hallmark of low-affinity nutrient transport. Trends in plant science **11:** 529-534

Britto DT, Siddiqi MY, Glass AD, Kronzucker HJ (2001) Futile transmembrane NH_4^+ cycling: a cellular hypothesis to explain ammonium toxicity in plants. Proceedings of the National Academy of Sciences **98:** 4255-4258

Bu Y, Takano T, Nemoto K, Liu S (2011) Research Progress of Ammonium Transporter in Rice Plants. Genomics and Applied Biology **2**

Cantón FR, Suárez MF, Cánovas FM (2005) Molecular aspects of nitrogen mobilization and recycling in trees. Photosynthesis Research **83:** 265-278

Cao Y, Glass AD, Crawford NM (1993) Ammonium inhibition of Arabidopsis root growth can be reversed by potassium and by auxin resistance mutations aux1, axr1, and axr2. Plant Physiology **102:** 983-989

Carrión CA, Martínez DE, Costa ML, Guiamet JJ (2014) Senescence-Associated Vacuoles, a Specific Lytic Compartment for Degradation of Chloroplast Proteins? Plants **3:** 498-512

Chiasson DM (2012) Characterization of GmSAT1 and related proteins from legume nodules. The University of Adelaide

Chiasson DM, Loughlin PC, Mazurkiewicz D, Mohammadidehcheshmeh M, Fedorova EE, Okamoto M, McLean E, Glass ADM, Smith SE, Bisseling T, Tyerman SD, Day DA, Kaiser BN (2014) Soybean SAT1 (Symbiotic Ammonium Transporter 1) encodes a bHLH transcription factor involved in nodule growth and NH_4^+ transport. Proceedings of the National Academy of Sciences **111:** 4814-4819

Chuck G, Meeley RB, Hake S (1998) The control of maize spikelet meristem fate by the APETALA2-like gene indeterminate spikelet1. Genes & Development **12:** 1145-1154

Couturier J, Montanini B, Martin F, Brun A, Blaudez D, Chalot M (2007) The expanded family of ammonium transporters in the perennial poplar plant. New Phytologist **174:** 137-150

De Michele R, Loqué D, Lalonde S, Frommer WB (2012) Ammonium and urea transporter inventory of the Selaginella and Physcomitrella genomes. Frontiers in plant science **3**

Demidchik V, Davenport RJ, Tester M (2002) Nonselective cation channels in plants. Annual review of plant biology **53:** 67-107

Deol KK, Mukherjee S, Gao F, Brûlé-Babel A, Stasolla C, Ayele BT (2013) Identification and characterization of the three homeologues of a new sucrose transporter in hexaploid wheat (*Triticum aestivum L.*). BMC plant biology **13:** 181

Dietrich CR, Cui F, Packila ML, Li J, Ashlock DA, Nikolau BJ, Schnable PS (2002) Maize *Mu* transposons are targeted to the 5' untranslated region of the gl8 gene and sequences flanking *Mu* target-site duplications exhibit nonrandom nucleotide composition throughout the genome. Genetics **160:** 697-716

Diouf D (2004) Genetic transformation of forest trees. African Journal of Biotechnology **2:** 328-333

Du C, Hoffman A, He L, Caronna J, Dooner HK (2011) The complete Ac/Ds transposon family of maize. BMC Genomics **12:** 588

Edwards JW, Coruzzi GM (1989) Photorespiration and light act in concert to regulate the expression of the nuclear gene for chloroplast glutamine synthetase. The Plant Cell Online **1:** 241-248

Edwards JW, Walker EL, Coruzzi GM (1990) Cell-specific expression in transgenic plants reveals nonoverlapping roles for chloroplast and cytosolic glutamine synthetase. Proceedings of the National Academy of Sciences **87:** 3459-3463

Edwards K, Johnstone C, Thompson C (1991) A simple and rapid method for the preparation of plant genomic DNA for PCR analysis. Nucleic acids research **19:** 1349

Engels C, Marschner H (1993) Influence of the form of nitrogen supply on root uptake and translocation of cations in the xylem exudate of maize (*Zea mays L*). Journal of experimental botany **44:** 1695-1701

Fried M, Zsoldos F, Vose P, Shatokhin I (1965) Characterizing the NO_3^- and NH_4^+ uptake process of rice roots by use of ^{15}N labelled NH_4NO_3. Physiologia Plantarum **18:** 313-320

Gaber RF, Styles CA, Fink GR (1988) TRK1 encodes a plasma membrane protein required for high-affinity potassium transport in *Saccharomyces cerevisiae*. Molecular and Cellular Biology **8:** 2848-2859

Gallavotti A, Zhao Q, Kyozuka J, Meeley RB, Ritter MK, Doebley JF, Pe ME, Schmidt RJ (2004) The role of barren stalk1 in the architecture of maize. Nature **432:** 630-635

Garnett T, Conn V, Kaiser BN (2009) Root based approaches to improving nitrogen use efficiency in plants. Plant, cell & environment **32:** 1272-1283

Garnett T, Conn V, Plett D, Conn S, Zanghellini J, Mackenzie N, Enju A, Francis K, Holtham L, Roessner U (2013) The response of the maize nitrate transport system to nitrogen demand and supply across the lifecycle. New Phytologist **198:** 82-94

Gaufichon L, Reisdorf-Cren M, Rothstein SJ, Chardon F, Suzuki A (2010) Biological functions of asparagine synthetase in plants. Plant Science **179:** 141-153

Gazzarrini S, Lejay L, Gojon A, Ninnemann O, Frommer WB, von Wirén N (1999) Three functional transporters for constitutive, diurnally regulated, and starvation-induced uptake of ammonium into Arabidopsis roots. The Plant Cell Online **11:** 937-947

Gietz RD, Schiestl RH (2007) High-efficiency yeast transformation using the LiAc/SS carrier DNA/PEG method. Nature protocols **2:** 31-34

Glass AD (2003) Nitrogen use efficiency of crop plants: physiological constraints upon nitrogen absorption. Critical Reviews in Plant Sciences **22:** 453-470

Glass AD, Britto DT, Kaiser BN, Kinghorn JR, Kronzucker HJ, Kumar A, Okamoto M, Rawat S, Siddiqi M, Unkles SE (2002) The regulation of nitrate and ammonium transport systems in plants. Journal of Experimental Botany **53:** 855-864

Graff L, Obrdlik P, Yuan L, Loqué D, Frommer WB, von Wirén N (2011) N-terminal cysteines affect oligomer stability of the allosterically regulated ammonium transporter LeAMT1; 1. Journal of experimental botany **62:** 1361-1373

Gregersen P, Holm P, Krupinska K (2008) Leaf senescence and nutrient remobilisation in barley and wheat. Plant Biology **10:** 37-49

Gu R, Duan F, An X, Zhang F, von Wirén N, Yuan L (2013) Characterization of AMT-Mediated High-Affinity Ammonium Uptake in Roots of Maize (*Zea mays L.*). Plant and Cell Physiology **54:** 1515-1524

Heim MA, Jakoby M, Werber M, Martin C, Weisshaar B, Bailey PC (2003) The basic helix–loop–helix transcription factor family in plants: a genome-wide study of protein structure and functional diversity. Molecular biology and evolution **20:** 735-747

Heldt H-W (2005) Nitrate assimilation is essential for the synthesis of organic matter. *In* Plant biochemistry, Ed 3rd Elsevier Academic Press, Amsterdam, pp 275-308

Hess DC, Lu W, Rabinowitz JD, Botstein D (2006) Ammonium toxicity and potassium limitation in yeast. PLoS biology **4:** e351

Hildebrand D (2013) Plant Biochemistry, BCH/PPA/PLS 609,Lecture Twenty-four. *In*, Vol 2013

Hoopen Ft, Cuin TA, Pedas P, Hegelund JN, Shabala S, Schjoerring JK, Jahn TP (2010) Competition between uptake of ammonium and potassium in barley and Arabidopsis roots: molecular mechanisms and physiological consequences. Journal of Experimental Botany **61:** 2303-2315

Husted S, Hebbern CA, Mattsson M, Schjoerring JK (2000) A critical experimental evaluation of methods for determination of NH_4^+ in plant tissue, xylem sap and apoplastic fluid. Physiologia Plantarum **109:** 167-179

Jahn TP, Møller AL, Zeuthen T, Holm LM, Klærke DA, Mohsin B, Kühlbrandt W, Schjoerring JK (2004) Aquaporin homologues in plants and mammals transport ammonia. FEBS letters **574:** 31-36

Jeschke WD, Hartung W (2000) Root-shoot interactions in mineral nutrition. Plant and Soil **226:** 57-69

Kaiser BN, Finnegan PM, Tyerman SD, Whitehead LF, Bergersen FJ, Day DA, Udvardi MK (1998) Characterization of an ammonium transport protein from the peribacteroid membrane of soybean nodules. Science **281:** 1202-1206

Kaiser BN, Rawat SR, Siddiqi MY, Masle J, Glass AD (2002) Functional analysis of an Arabidopsis T-DNA "Knockout" of the high-affinity NH_4^+ transporter AtAMT1; 1. Plant Physiology **130:** 1263-1275

Kaya A, Karakaya HC, Fomenko DE, Gladyshev VN, Koc A (2009) Identification of a novel system for boron transport: Atr1 is a main boron exporter in yeast. Molecular and cellular biology **29:** 3665-3674

Ketchum KA, Joiner WJ, Sellers AJ, Kaczmarek LK, Goldstein SA (1995) A new family of outwardly rectifying potassium channel proteins with two pore domains in tandem. Nature **376:** 690-695

Ko CH, Buckley AM, Gaber RF (1990) TRK2 is required for low affinity K^+ transport in *Saccharomyces cerevisiae*. Genetics **125:** 305-312

Ko CH, Gaber RF (1991) TRK1 and TRK2 encode structurally related K^+ transporters in *Saccharomyces cerevisiae*. Molecular and Cellular Biology **11:** 4266-4273

Kronzucker HJ, Schjoerring JK, Erner Y, Kirk GJ, Siddiqi MY, Glass AD (1998) Dynamic interactions between root NH_4^+ influx and long-distance N translocation in rice: Insights into feedback processes. Plant and Cell Physiology **39:** 1287-1293

Lam H-M, Coschigano K, Oliveira I, Melo-Oliveira R, Coruzzi G (1996) The molecular-genetics of nitrogen assimilation into amino acids in higher plants. Annual review of plant biology **47:** 569-593

Lanquar V, Frommer WB (2010) Adjusting ammonium uptake via phosphorylation. Plant Signaling & Behavior **5:** 735-738

Lea P, Miflin B (1974) Alternative route for nitrogen assimilation in higher plants. Nature **251:** 614-616

Lea P, Thurman D (1972) Intracellular location and properties of plant L-glutamate dehydrogenases. Journal of Experimental Botany **23:** 440-449

Lea PJ, Sodek L, Parry MA, Shewry PR, Halford NG (2007) Asparagine in plants. Annals of Applied Biology **150:** 1-26

Leonard A, Holloway B, Guo M, Rupe M, Yu G, Beatty M, Zastrow-Hayes G, Meeley R, Llaca V, Butler K (2014) tassel-less1 encodes a boron channel protein required for inflorescence development in maize. Plant and Cell Physiology**:** pcu036

Li B-Z, Merrick M, Li S-M, Li H-Y, Zhu S-W, Shi W-M, Su Y-H (2009) Molecular basis and regulation of ammonium transporter in rice. Rice Science **16:** 314-322

Lillis M, Freeling M (1986) *Mu* transposons in maize. Trends in Genetics **2:** 183-188

Lisch D (2002) Mutator transposons. Trends in plant science **7:** 498-504

Liu J, Wu YH, Yang JJ, Liu YD, Shen FF (2008) Protein degradation and nitrogen remobilization during leaf senescence. Journal of Plant Biology **51:** 11-19

Loque D, Lalonde S, Looger L, Von Wiren N, Frommer W (2007) A cytosolic trans-activation domain essential for ammonium uptake. Nature **446:** 195-198

Loqué D, Yuan L, Kojima S, Gojon A, Wirth J, Gazzarrini S, Ishiyama K, Takahashi H, Von Wirén N (2006) Additive contribution of AMT1; 1 and AMT1; 3 to high-affinity ammonium uptake across the plasma membrane of nitrogen-deficient Arabidopsis roots. The Plant Journal **48:** 522-534

Ludewig U, Neuhäuser B, Dynowski M (2007) Molecular mechanisms of ammonium transport and accumulation in plants. FEBS letters **581:** 2301-2308

Ludewig U, von Wirén N, Frommer WB (2002) Uniport of NH_4^+ by the root hair plasma membrane ammonium transporter LeAMT1; 1. Journal of Biological Chemistry **277:** 13548-13555

Marini A-M, Soussi-Boudekou S, Vissers S, André B (1997) A family of ammonium transporters in *Saccharomyces cerevisiae*. Molecular and cellular biology **17:** 4282-4293

Marini AM, Springael JY, Frommer WB, André B (2000) Cross-talk between ammonium transporters in yeast and interference by the soybean SAT1 protein. Molecular microbiology **35:** 378-385

Masclaux C, Valadier M-H, Brugière N, Morot-Gaudry J-F, Hirel B (2000) Characterization of the sink/source transition in tobacco (*Nicotiana tabacum L.*) shoots in relation to nitrogen management and leaf senescence. Planta **211:** 510-518

Masclaux-Daubresse C, Daniel-Vedele F, Dechorgnat J, Chardon F, Gaufichon L, Suzuki A (2010) Nitrogen uptake, assimilation and remobilization in plants: challenges for sustainable and productive agriculture. Annals of Botany **105:** 1141-1157

Masclaux-Daubresse C, Reisdorf-Cren M, Orsel M (2008) Leaf nitrogen remobilisation for plant development and grain filling. Plant Biology **10:** 23-36

Mayer M, Schaaf G, Mouro I, Lopez C, Colin Y, Neumann P, Cartron J-P, Ludewig U (2006) Different transport mechanisms in plant and human

AMT/Rh-type ammonium transporters. The Journal of general physiology **127:** 133-144

Mazurkiewicz D (2013) Characterisation of a novel family of eukaryotic ammonium transport proteins. The University of Adelaide

McCarty DR, Meeley RB (2009) Transposon resources for forward and reverse genetics in maize. *In* Handbook of Maize. Springer, pp 561-584

McClintock B (1950) The origin and behavior of mutable loci in maize. Proceedings of the National Academy of Sciences **36:** 344-355

Miflin BJ, Habash DZ (2002) The role of glutamine synthetase and glutamate dehydrogenase in nitrogen assimilation and possibilities for improvement in the nitrogen utilization of crops. Journal of Experimental Botany **53:** 979-987

Miflin BJ, Lea PJ (1976) The pathway of nitrogen assimilation in plants. Phytochemistry **15:** 873-885

Nacry P, Bouguyon E, Gojon A (2013) Nitrogen acquisition by roots: physiological and developmental mechanisms ensuring plant adaptation to a fluctuating resource. Plant and Soil**:** 1-29

Neuhäuser B, Dynowski M, Ludewig U (2009) Channel-like NH_3 flux by ammonium transporter AtAMT2. FEBS letters **583:** 2833-2838

Neuhäuser B, Dynowski M, Mayer M, Ludewig U (2007) Regulation of NH_4^+ transport by essential cross talk between AMT monomers through the carboxyl tails. Plant physiology **143:** 1651-1659

Oaks A (1994) Primary nitrogen assimilation in higher plants and its regulation. Canadian Journal of Botany **72:** 739-750

Oaks A, Ross D (1984) Asparagine synthetase in *Zea mays*. Canadian journal of botany **62:** 68-73

Oliveira IC, Brears T, Knight TJ, Clark A, Coruzzi GM (2002) Overexpression of cytosolic glutamine synthetase. Relation to nitrogen, light, and photorespiration. Plant Physiology **129:** 1170-1180

Peirson SN, Butler JN, Foster RG (2003) Experimental validation of novel and conventional approaches to quantitative real-time PCR data analysis. Nucleic acids research **31:** e73-e73

Peng J, Gong J (2014) Vacuolar sequestration capacity and long-distance metal transport in plants. Frontiers in plant science **5:** 19

Peterman TK, Goodman HM (1991) The glutamine synthetase gene family of *Arabidopsis thaliana* light-regulation and differential expression in leaves, roots and seeds. Molecular and General Genetics MGG **230:** 145-154

Peuke AD, Jeschke WD, Hartung W (1994) The uptake and flow of C, N and ions between roots and shoots in *Ricinus communis L*. III. Long-distance transport of abscisic acid depending on nitrogen nutrition and salt stress. Journal of Experimental Botany **45:** 741-747

Rachmilevitch S, Cousins AB, Bloom AJ (2004) Nitrate assimilation in plant shoots depends on photorespiration. Proceedings of the National Academy of Sciences of the United States of America **101:** 11506-11510

Raun WR, Johnson GV (1999) Improving nitrogen use efficiency for cereal production. Agronomy Journal **91:** 357-363

Rawat SR, Silim SN, Kronzucker HJ, Siddiqi MY, Glass AD (1999) AtAMT1 gene expression and NH_4^+ uptake in roots of *Arabidopsis thaliana*:

evidence for regulation by root glutamine levels. The Plant Journal **19:** 143-152

Reisser C, Dick C, Kruglyak L, Botstein D, Schacherer J, Hess DC (2013) Genetic basis of ammonium toxicity resistance in a sake strain of yeast: a Mendelian case. G3: Genes, Genomes, Genetics **3:** 733-740

Riesmeier JW, Willmitzer L, Frommer WB (1992) Isolation and characterization of a sucrose carrier cDNA from spinach by functional expression in yeast. The EMBO Journal **11:** 4705

Roberts JK, Pang MK (1992) Estimation of ammonium ion distribution between cytoplasm and vacuole using nuclear magnetic resonance spectroscopy. Plant Physiology **100:** 1571-1574

Robertson DS (1978) Characterization of a mutator system in maize. Mutation Research/Fundamental and Molecular Mechanisms of Mutagenesis **51:** 21-28

Rodríguez-Navarro A, Ramos J (1984) Dual system for potassium transport in *Saccharomyces cerevisiae*. Journal of bacteriology **159:** 940-945

Santa-Marıa GE, Danna CH, Czibener C (2000) High-affinity potassium transport in barley roots. Ammonium-sensitive and-insensitive pathways. Plant Physiology **123:** 297-306

Schachtman DP, Schroeder JI, Lucas WJ, Anderson JA, Gaber RF (1992) Expression of an inward-rectifying potassium channel by the Arabidopsis KAT1 cDNA. Science **258:** 1654-1659

Schjoerring JK, Husted S, Mäck G, Mattsson M (2002) The regulation of ammonium translocation in plants. Journal of Experimental Botany **53:** 883-890

Shelden MC, Dong B, Guy L, Trevaskis B, Whelan J, Ryan PR, Howitt SM, Udvardi MK (2001) Arabidopsis ammonium transporters, AtAMT1;1 and AtAMT1;2, have different biochemical properties and functional roles. Plant and Soil **231:** 151-160

Slewinski TL, Meeley R, Braun DM (2009) Sucrose transporter1 functions in phloem loading in maize leaves. Journal of Experimental Botany **60:** 881-892

Sohlenkamp C, Shelden M, Howitt S, Udvardi M (2000) Characterization of Arabidopsis AtAMT2, a novel ammonium transporter in plants. FEBS letters **467:** 273-278

Sohlenkamp C, Wood CC, Roeb GW, Udvardi MK (2002) Characterization of Arabidopsis AtAMT2, a high-affinity ammonium transporter of the plasma membrane. Plant Physiology **130:** 1788-1796

Sonoda Y, Ikeda A, Saiki S, von Wirén N, Yamaya T, Yamaguchi J (2003) Distinct expression and function of three ammonium transporter genes (OsAMT1;1–1;3) in rice. Plant and Cell Physiology **44:** 726-734

Suárez MF, Avila C, Gallardo F, Cantón FR, García‐Gutiérrez A, Claros MG, Cánovas FM (2002) Molecular and enzymatic analysis of ammonium assimilation in woody plants. Journal of Experimental Botany **53:** 891-904

Suzuki A, Knaff DB (2005) Glutamate synthase: structural, mechanistic and regulatory properties, and role in the amino acid metabolism. Photosynthesis Research **83:** 191-217

Szczerba MW, Britto DT, Ali SA, Balkos KD, Kronzucker HJ (2008) NH_4^+-stimulated and-inhibited components of K^+ transport in rice (*Oryza sativa L.*). Journal of Experimental Botany **59:** 3415-3423

Taiz L, Zeiger E (2002) Assimilation of Mineral Nutrients. *In* Plant Physiology, Ed 3rd. Sinauer Associates, Sunderland, Massachusetts, pp 260-282

Talbert L, Patterson G, Chandler V (1989) *Mu* transposable elements are structurally diverse and distributed throughout the genus *Zea*. Journal of molecular evolution **29:** 28-39

Tan B-C, Chen Z, Shen Y, Zhang Y, Lai J, Sun SS (2011) Identification of an active new mutator transposable element in maize. G3: Genes, Genomes, Genetics **1:** 293-302

Tilman D, Cassman KG, Matson PA, Naylor R, Polasky S (2002) Agricultural sustainability and intensive production practices. Nature **418:** 671-677

Vale FR, Volk RJ, Jackson WA (1988) Simultaneous influx of ammonium and potassium into maize roots: kinetics and interactions. Planta **173:** 424-431

Vandesompele J, De Preter K, Pattyn F, Poppe B, Van Roy N, De Paepe A, Speleman F (2002) Accurate normalization of real-time quantitative RT-PCR data by geometric averaging of multiple internal control genes. Genome biology **3:** research0034. 0031

von Wirén N, Gazzarrini S, Gojont A, Frommer WB (2000) The molecular physiology of ammonium uptake and retrieval. Current opinion in plant biology **3:** 254-261

Von Wirén N, Lauter FR, Ninnemann O, Gillissen B, Walch‐Liu P, Engels C, Jost W, Frommer WB (2000) Differential regulation of three functional

ammonium transporter genes by nitrogen in root hairs and by light in leaves of tomato. The Plant Journal **21:** 167-175

Wang MY, Siddiqi MY, Ruth TJ, Glass AD (1993) Ammonium uptake by rice roots (II. Kinetics of $^{13}NH_4^+$ influx across the plasmalemma). Plant physiology **103:** 1259-1267

Weise A, Barker L, Kühn C, Lalonde S, Buschmann H, Frommer WB, Ward JM (2000) A new subfamily of sucrose transporters, SUT4, with low affinity/high capacity localized in enucleate sieve elements of plants. The Plant Cell **12:** 1345-1355

Whetten R, Sederoff R (1995) Lignin biosynthesis. The Plant Cell **7:** 1001

White P (1996) The permeation of ammonium through a voltage-independent K^+ channel in the plasma membrane of rye roots. Journal of Membrane Biology **152:** 89-99

Wingler A, Lea PJ, Quick WP, Leegood RC (2000) Photorespiration: metabolic pathways and their role in stress protection. Philosophical Transactions of the Royal Society of London. Series B: Biological Sciences **355:** 1517-1529

Wood CC, Porée F, Dreyer I, Koehler GJ, Udvardi MK (2006) Mechanisms of ammonium transport, accumulation, and retention in ooyctes and yeast cells expressing Arabidopsis AtAMT1;1. FEBS letters **580:** 3931-3936

Yuan L, Graff L, Loqué D, Kojima S, Tsuchiya YN, Takahashi H, von Wirén N (2009) AtAMT1;4, a pollen-specific high-affinity ammonium transporter of the plasma membrane in Arabidopsis. Plant and cell physiology **50:** 13-25

Yuan L, Loqué D, Kojima S, Rauch S, Ishiyama K, Inoue E, Takahashi H, von Wirén N (2007b) The organization of high-affinity ammonium uptake in Arabidopsis roots depends on the spatial arrangement and biochemical properties of AMT1-type transporters. The Plant Cell Online **19:** 2636-2652

Yuan L, Loqué D, Ye F, Frommer WB, von Wirén N (2007a) Nitrogen-dependent posttranscriptional regulation of the ammonium transporter AtAMT1; 1. Plant Physiology **143:** 732-744

Appendix A

Table I List of primers used in the thesis

Primer name	Primer sequence 5' to 3'
9242	AGAGAAGCCAACGCCAWCGCCTCYATTTCGTC
157308	CTGTCTCCCTCGTTGCAATCACCAC
157309	TTAGGTGTGAACCAGGAAGGCTTGTCAC
ZmAMF1;1 F-g	ATGCCAGATAAGCGGCCGGT
ZmAMF1;1 R-g	GGGGCTCAAGAGAAGCAAAAAAAATCCTCAG
157313	GCCGTGGCCTTCTCATTCCGTTCAA
157316	AGATCAAGCCTACCACAGCCGAGTCT
ZmAMF1;1 F2	ATGGCGGTCACCGTAGTG
ZmAMF1;1 R2	GGCATAAGGGAAAAACTACGG
ZmAMF1;2 F2	GAGACAGAGGAGCCTAAGCA
ZmAMF1;2 R2	TACCCTAAGATTGCAACTGGC
ZmAMF1;2 F3	CATTCCGTTTGGACCCATGA
ZmAMF1;2 R3	CTCTTAGGTGTGAACCAGGAAGGGT
ZmAMF1;1 qPCR F1	TAATTGGAGGGCCACAGC
ZmAMF1;1 qPCR R1	GCTCGTCCTTTTCATCAAGG
ZmAMF1:2 qPCR F1	ACTGGAGGGAGACAGCTC
ZmAMF1;2 qPCR R1	CCAAGCAGTGGCCTGATACT
ZmAMF1;1 qPCR F	ATGCCCATTGGCTGTACCTG
ZmAMF1;1 qPCR R	AGTTATGCCATGTCACAATCCG
ZmAMF1;2 qPCR F	GGTCTGTTTGCCTTGCGTTT
ZmAMF1:2 qPCR R	GGGAGTAATATTGTAGCCAGTAAGT
ZmAMF1;1 restriction F	AAGTGAACTAGTATGGCGGTCACCGTAGTG
ZmAMF1;1 restriction R	TCACTTCTCGAGGGCATAAGGGAAAAACTACGG
ZmAMF1;2 restriction F	AAGAAGACTAGTGAGACAGAGGAGCCTAAGCA
ZmAMF1;2 restriction R	AAGAAGCTCGAGTACCCTAAGATTGCAACTGGC
ZmAMF1;1 in situ F	AATCCATATATTTGGCGATGTG
ZmAMF1;2 in situ F	GATCCATATATTTGGTGATGTCC
ScAMF1 Res-F	GCAAAACTGCAGATGTCAACTAGCTCCTCCGTA
ScAMF1 Res-R	GACAGCCTCGAGTTATTCTATAAAATGCTGCTT
EF1A F1	CGACCACCACAGGACACCTGA
EF1A R1	GCAGGGTTGGGCCTTTGTACC
ZmGaPDh F	GACAGCAGGTCGAGCATCTTC
ZmGaPDh R	GTCGACGACGCGGTTGCTGTA
ZmActin-F	CCAATTCCTGAAGATGAGTCT
ZmActin-R	TGGTAGCCAACCAAAAACAGT
ZmELF1 F	GCCGCCAAGAAGAAATGATGC
ZmELF1 R	CGCCAAAAGGAGAAATACAAG
18S-F1	TGGCTCGACTTATATGTGGT
18S-R1	ACAACAGTTACATTCCGCGGT

Appendix B

Abbreviations in the thesis

5'	Five prime of nucleic acid sequence
3'	Three prime of nucleic acid sequence
~	Approximately
±	Plus and minus
µg	Microgram
µM	Micromolar
Ac	Activator
ADL	Adelaide line in quarantine
ADP	Adenosine diphosphate
AMF1	Ammonium Major Facilitator 1
AMT	Ammonium Transporter
As	Asparagine synthetase
Asp-AT	Aspartate aminotransferase
ATP	Adenosine triphosphate
BC	Backcrossing
bp	Base pairs
bHLHm1	Basic helix-loop-helix transcription factor1
BLAST	Basic Local Alignment Search Tool
BSA	Bovine Serum Albumin
cDNA	Complementary deoxyribonucleic acid
CDS	Coding DNA sequence
Ct	Threshold cycle
C terminal	Carboxyl terminal
DEPC	Diethyl pyrocarbonate
DNA	Deoxyribonucleic acid
DNase	deoxyribonuclease
Ds	Dissociation
EDTA	Ethylene Diamine Tetracetic Acid
EMS	Ethyl methane sulphonate
FAD	Flavin adenine dinucleotide
Fd	ferredoxin
g	Grams
gal	Galactose
GAL1	Galactose inducible promoter 1
GAPDH	Glyceraldehyde 3-phosphate dehydrogenase
GDH	Glutamate dehydrogenase
GFP	Green Fluorescent Protein
glu	Glucose
GmSAT1	*Glycine max* Symbiotic Ammonium Transporter 1
GUS	β-Glucuronidase
h	Hour(s)

HATS	High affinity transporters
K	Potassium
kb	Kilo base pairs
LATS	Low affinity transporters
LB	Lysogeny broth
LiAc	Lithium acetate
MA	Methylammonium
MEP	Methylammonium permease
MES	2-(N-morpholino)ethanesulfonic acid
MFS	Major facilitator superfamily
mg	Milligram
Min	Minute(s)
mM	Millimolar
MoCo	Molybdenum cofactor
Mu	Mutators
NADH	Nicotinamide adenine dinucleotide
NADPH	Nicotinamide adenine dinucleotide phosphate
N	Nitrogen
NCBI	National Centre for Biotechnology Information
NiR	Nitrite reductase
NR	Nitrate reductase
NSC1	Non selective channel 1
NSCCs	Non-selective cation channels
NUE	Nitrogen use efficiency
OD	Optical Density
PAL	Phenylalanine ammonia-lyase
PCR	Polymerase chain reaction
PEG	Polyethylene Glycol
2PG or PG	2-phosphoglycolate
PGA	3-phosphoglycerate
pro	L-proline
qPCR	Quantitative PCR
Rh	Rhesus protein
RNA	Ribonucleic acid
Rnase	Ribonuclease
RO	Reverse osmosis
RT-PCR	Reverse transcription polymerase chain reaction
RuBP	Ribolose bis phosphate
s	Second(s)
SC	selfcrossing
SD-uracil	Yeast synthetic drop out medium without uracil
SDS	Sodium Dodecyl Sulfate
TF	Transcription factor
TIR	Terminal inverted repeat
Tris	Tris(hydroxymethyl)aminomethane
TUSC	Trait Utility System for Corn

UTR	Untranslated region
v/v	Volume/volume
w/v	Weight/volume
w/w	Weight/weight
YFP	Yellow Fluorescent Protein
YPD	Yeast extract peptone dextrose medium
YNB	Yeast Nitrogen Base without amino acid and ammonium sulphate